Chemical Aspects of Solution Routes to Perovskite-Phase Mixed-Metal Oxides from Metal–Organic Precursors

Clive D. Chandler, Christophe Roger, and Mark J. Hampden-Smith*

Department of Chemistry and Center for Micro-Engineered Ceramics, University of New Mexico, Albuquerque, New Mexico 87131

Contents

1. Introduction

In recent years there has been a great deal of interest in the use of molecular species as precursors for the formation of inorganic materials.[1-4] Techniques for the formation of such materials, including chemical vapor deposition (CVD), sol–gel processes, metal–organic decomposition, and molecular beam epitaxy, to name but a few, require metal–organic molecules as precursors which have specific physical and chemical properties. The primary characteristics are generally either a high vapor pressure and/or substantial solubility in particular solvents. With more effort devoted to research in this area, metal–organic precursor molecules are steadily becoming more sophisticated to include design aspects such as particular decomposition mechanisms, including β-hydride elimination,[5] or disproportionation for the CVD of metals[6] and the synthesis of heteromultimetallic precursors with a specific stoichiometry desired for the final material.[7-10] The preparation of inorganic materials from metal–organic precursors generally has the advantages over "traditional routes" of low temperatures of formation, low crystallization temperatures, better compositional uniformity at low temperatures, and conformal coverage in the case of films. Disadvantages of traditional routes often include incorporation of impurities, inhomogeneity and phase segregation and the need for high sintering temperatures.

There has been a resurgence in interest in the chemistry of metal alkoxide compounds due to the advantages of sol–gel techniques for the preparation of metal oxide ceramics.[10-21] This technique is based on the hydrolysis and condensation of metal alkoxide compounds according to eqs 1–4 below. Hydrolysis

$$MOR + H_2O \rightarrow MOH + ROH \quad \text{hydrolysis} \quad (1)$$

$$MOH + MOR \rightarrow MOM + ROH \quad \text{alkoxolation} \quad (2)$$

$$MOH + MOH \rightarrow MOM + H_2O \quad \text{oxolation} \quad (3)$$

$$MOH_2 + MOR \rightarrow M(OH)M + ROH \quad \text{olation} \quad (4)$$
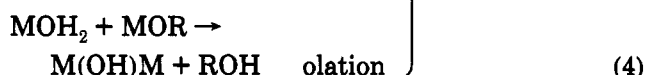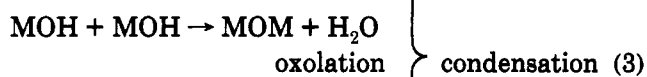
condensation

replaces the alkoxide groups with hydroxyl groups and subsequent condensation reactions involving the hydroxyl groups produce M–O–M or M(μ-OH)M bonds in addition to other byproducts such as water or alcohol.[12,22]

In this manner, inorganic polymers are constructed progressively, resulting ultimately (often after heating) in metal oxides. The advantages of sol–gel processing over conventional ceramic processing methods include the ability to make special shapes derived from the sol or the gel state (such as monoliths, films, fibers, and

* Author to whom correspondence should be addressed.
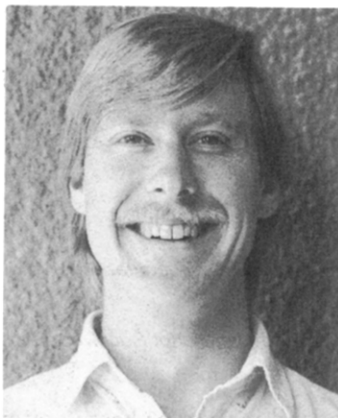
Clive Chandler was born in Melbourne, Australia in 1963. He studied chemistry at Monash University, obtaining a Bachelors Degree with honors in 1985. He returned in 1987 to complete a Ph.D. in Prof. Bruce West's group on sol–gel routes to cadmium stannate thin films in 1991. His research interest in materials chemistry led to a postdoctoral fellow at the University of New Mexico with Mark Hampden Smith investigating single component routes to perovskite-phase materials.

Christophe Roger was born on July 4, 1964, in Dijon, France. He received a M.S. in Chemical Engineering from the Ecole Nationale Supérieure de Chimie de Rennes (1986) and his Ph.D. in Organic Chemistry from the University of Rennes (1989), working under Claude Lapinte on electron-transfer activation and electrocatalysis of iron alkylidene complexes. He held a 2-year postdoctoral position with John A. Gladysz at the University of Utah (1989–1991) studying the synthesis and rearrangement mechanism of chiral rhenium complexes. He is now a Research Associate in Mark Hampden-Smith's group at the University of New Mexico investigating a general sol–gel route to porous metal oxides.

Mark Hampden-Smith is an Assistant Professor and Regents Lecturer in Chemistry at the University of New Mexico. He received his Ph.D. from London University, Queen Mary/Westfield College in 1984 and held post-doctoral fellowships at the University of Guelph, Ontario, Canada (1984–1986) and Indiana University (1986–1988), conducting research focusing on problems in synthetic and mechanistic inorganic and organometallic chemistry. His current research interests are in the areas of nanostructured inorganic materials, chemical vapor deposition and etching, and liquid-phase routes to metal oxides. He is a member of the American Chemical Society, the Royal Society of Chemistry, and the Materials Research Society.

mechanistic understanding is gradually being derived. This literature has been reviewed extensively and only the relevant chemistry of monometallic metal–organic systems will be discussed here.

The goal of this article is to review the reaction chemistry occurring in solution routes to *multicomponent* metal oxides (i.e. containing two or more metals) from metal–organic precursors. In this context, the metal–organic precursor is usually a metal alkoxide, metal β-diketonate or metal carboxylate compound. In the preparation of *multicomponent* metal oxide compounds, a number of key issues should be addressed which relate to the structure, properties, and performance of the final ceramic material. These issues pertain to control over the stoichiometry, homogeneity, phase, and crystallinity, which relate directly to the structure and reactivity of the metal–organic precursors in homogeneous solutions and their fate in subsequent processing steps. Control over these properties are often crucial to the performance of "advanced" mixed metal oxide materials such as optoelectronic ceramics. Furthermore, the necessity for control over these properties is likely to increase as applications become more demanding. The possible dependence of stoichiometry and homogeneity on the structure and reactivity of the precursor solution is illustrated schematically in Figure 1. Addition of two different metal–organic reagents, AX_n (*closed spheres*) and BY_m (*open spheres*), in equimolar ratios to a solvent can result in a number of different possibilities (assuming they dissolve!): (i) they may not react, (ii) they may react, especially with the addition of water, to form a single molecular species such as ABX_pY_q (*shaded spheres*), or (iii) a mixture of molecular species with *different* metal atom stoichiometries may be formed. Films or powders formed from this solution are likely to be quite different for each scenario. For i and ii, molecular level homogeneity is likely, but for iii regional inhomogeneity is possible, even though the overall stoichiometry is correct. Subsequent processing, usually thermal, results in forma-

monosized powders) combined with compositional and microstructural control and low processing temperatures. The mechanistic aspects of these reactions are quite well understood for M = Si, but there is now substantial interest in the preparation of non-silicate metal oxides by this method as a result of their interesting physical and chemical properties.[1,23,24] However, while the principles of these hydrolysis and condensation reactions are similar for the non-silicon systems, the kinetic and thermodynamic aspects are substantially different.[25] Other metals are more electropositive than silicon and generally exhibit a variety of coordination numbers and geometries leading to oligomerization unless special precautions are taken. The rapidity of the hydrolysis step has resulted in a paucity of data on the intermediates in the hydrolysis and condensation reactions of metal alkoxides. However, with careful studies in mononuclear systems, a

Figure 1. Dependence of stoichiometry and homogeneity of mixed metal oxides on the precursor solution.

Figure 2. Structure of ABO_3, emphasizing the coordination number of the A cation at the body center.

tion of the corresponding ABO_x phase. Clearly, it is important to ask the question, what effect do the possibilities i–iii have on the properties of the final ceramic? Presently, we propose that method ii is likely to be most valuable since the molecular level homogeneity proposed in route i is not likely to be achieved due to the different reactivities of the individual precursors toward themselves (i.e. hydrolysis to form different sized clusters). Perhaps a more important question is does it matter? Whatever the outcome it seems reasonable to suppose that the development of an understanding of the control over homogeneity and stoichiometry at the molecular level would be a useful attribute and might for example lead to low crystallization temperatures by circumventing diffusion-limited crystallization processes. A more suitable question relates to the polymorphism in crystalline metal oxide phases formed from metal–organic precursors. Where two crystalline polymorphs exist with identical stoichiometry but different metal ion coordination number or geometry, is it possible to control which phase is formed as a function of some property of the precursor? For example, the metal atom coordination environment in the precursor might influence the final structure formed.

Perovskite-phase multicomponent mixed-metal oxides have been chosen as the material to which these questions are addressed in this review. The rationale for the choice of these materials is that they exhibit a large variety of interesting chemical and physical properties; they have been studied in some detail and they are polymorphic, exhibiting a facile phase transformation to an alternate structure with identical stoichiometry (pyrochlore).[26] However, it is noteworthy that a change in stoichiometry may be necessary to cause a crystalline phase transformation.

The discussion is organized in the following manner. The relevant properties of perovskite-phase materials are reviewed and the requirements for the materials produced from metal–organic precursors are identified. The synthesis of perovskite-phase materials is reviewed with specific attention on those reports where mechanistic insight is presented. Recent advances in relevant structural and reaction chemistry of metal–organic precursors necessary to interpret these observations is
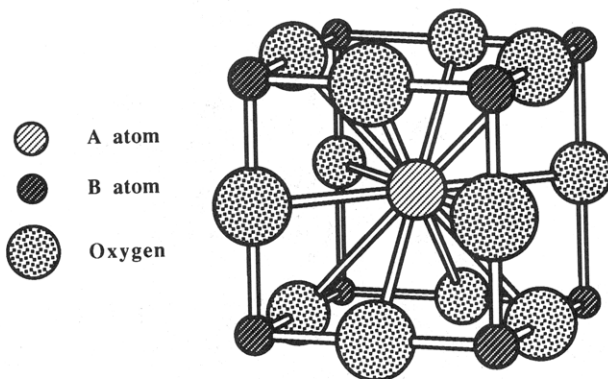
then presented, and finally, conclusions are drawn and directions for future work are discussed.

2. Perovskite-Phase Mixed-Metal Oxides

2.1. Introduction

Perovskite-phase mixed-metal oxide ceramics are interesting materials due to changes in their physical properties on application of an external electrical stimulus. These properties include ferroelectric, pyroelectric, piezoelectric, and dielectric behavior and have led to numerous applications in electromechanic transducers,[27] light modulation,[28] charge storage,[28] nonvolatile memory applications,[27] and infrared detection. Since these physical properties generally arise from the crystal chemistry of these materials, the formation of pure, stoichiometric, homogeneous, crystalline metal oxide materials with controlled crystalline size is crucial. In this section the crystal chemistry, properties, and potential applications of these materials are briefly reviewed.

2.2. Crystal Chemistry of Perovskite-Phase Metal Oxides

The perovskite structure is known for a range of compounds which include metal oxides, some complex metal halides, and a few metal carbides and nitrides.[29] The later three groups are not included in this review. The class of metal oxides, with the empirical formula ABO_3, derives its name from the rare mineral, $CaTiO_3$, commonly called perovskite. The structure of this mineral was first thought to be cubic and although it was later found to be orthorhombic, the name perovskite has been retained for this structure type. The truly cubic form of this material is referred to as "ideal perovskite", and has a unit cell edge of ~ 4 Å containing one ABO_3 unit. Few perovskite materials have this structure at room temperature, but many assume this structure at higher temperatures.[29]

In the perovskite structure the A cation is coordinated to 12 oxygen ions to form a cuboctahedral coordination environment while the B cation is coordinated to six oxygen ions in an octahedral array. Thus the A cation is normally larger than the B cation. The simple cubic structure emphasizing the coordination environment about the A cation is shown in Figure 2. In an alternate representation, the coordination environment about the B cation is emphasized in Figure 3. The oxygen ions form octahedra around the smaller B cation and it is
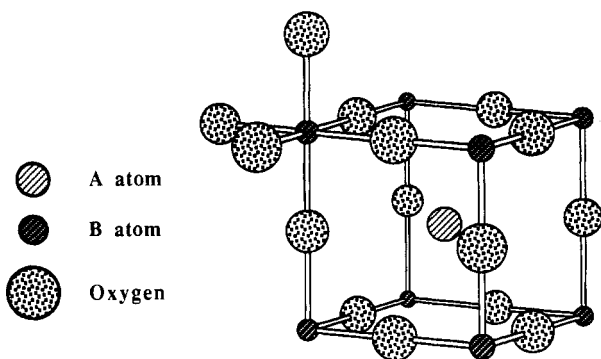
Figure 3. Structure of ABO_3 emphasizing the octahedral environment of the B cation.
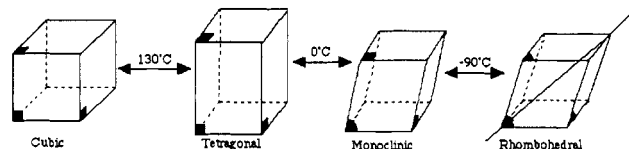

Figure 4. Schematic representation of the distortion of the unit cell of the cubic ideal perovskite structure with $BaTiO_3$ transition temperatures.

the corner shading of these octahedra which leads to the cubic structure with the large A cation situated in the interstices of the octahedral frame works. In order for there to be contact between the A, B, and O ions, $R_A + R_O$ should equal $2^{1/2}(R_B + R_O)$, where R_A, R_B, and R_O are the ionic radii. Goldschmit[30] defined a tolerance factor, t, to define the limits of stability of the perovskite structure: $t = (R_A + R_O)/2^{1/2}(R_B + R_O)$. The perovskite phase is stable within the range $0.75 < t < 1.0$ with t lying between 0.8 and 0.9 in most cases, and below this limit the stable structures are ilmenite and corundum.[31] The necessity for octahedral coordination of the B cation sets a lower limit of 0.51 Å to the ionic radius of this ion in oxide systems. The calculated minimum ionic radius of the A cation derived from the smallest B ion is 0.9 Å. Other ABO_3 structure types exist, including corundum and ilmenite, where the A and B cations are of similar size and both prefer to adopt a coordination number of six.[31]

In an alternate approach,[26] the structure adopted by perovskite-phase materials has been analyzed in terms of their coordination polyhedra. This analysis shows that the occurrence of ferroelectric behavior in a perovskite-phase material with empirical formula ABO_3 requires that the ratio of the volume of the oxide ion cuboctahedron about A to the volume of the oxide ion octahedron about B be five. There is also a minimum B-ion octahedral volume associated with ferroelectric behavior.

Distortion from the ideal ABO_3 cubic symmetry is common at room temperature, and structures with tetragonal, orthorhombic, rhombohedral, monoclinic, and triclinic symmetry are known. Some of these distortions of the unit cell and their relationships are shown in Figure 4. Many examples of orthorhombic and rhombohedral structures have been reported, but there are fewer reports of triclinic, monoclinic, and tetragonal systems, although the common phases Ba-TiO_3 and lead zirconate titanate (PZT) can exist as tetragonal phases. These distortions are readily observed by diffraction techniques, where lowering of the symmetry of the unit cell is manifest in the appearance
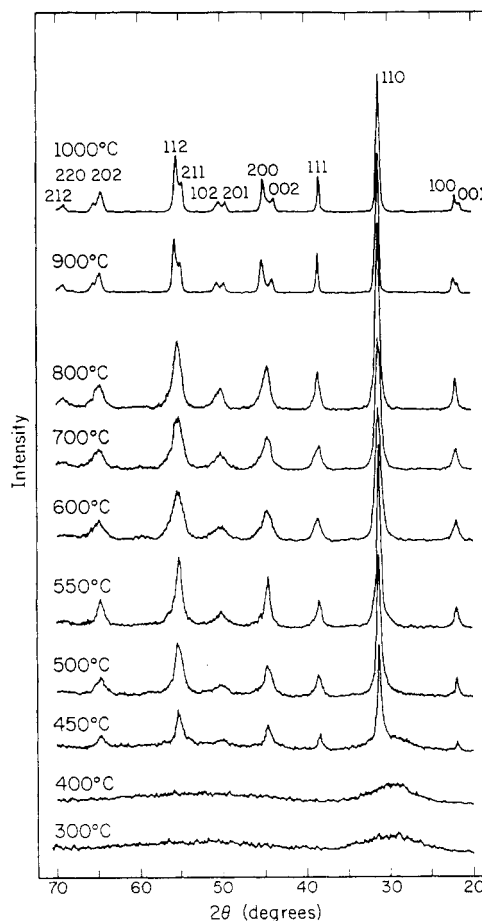

Figure 5. Effect of heat treatment temperature on the room temperature X-ray diffraction spectra for coprecipitated PZT (53:47) powder.[32]

of additional peaks. For example, Figure 5 shows the temperature dependent X-ray powder diffraction data for PZT, $PbZr_{0.53}Ti_{0.47}O_3$, formed via a coprecipitation technique.[32] Formation of crystalline pseudocubic perovskite-phase $PbZr_{0.53}Ti_{0.47}O_3$ is observed between 450 and 800 °C. At 900 °C and above, the splitting observed in some of the peaks reveals the presence of a tetragonal distortion.

The chemical composition of these perovskite-phase materials can vary depending on the valency of the cations and includes the following combinations, $A^{1+}B^{5+}O_3$, $A^{2+}B^{4+}O_3$ to $A^{3+}B^{3+}O_3$.[29] In addition, the substitution of A and B cations with A' and B' cations of the same valency can be used to form nonintegral stoichiometry species such as $(A_xA'_{1-x})(B_yB'_{1-y})O_3$, which also have interesting properties. This produces a wide range of compounds with the perovskite structure. In the $A^{1+}B^{5+}O_3$ system, the niobates are the most widely known, and $KNbO_3$ and $NaNbO_3$ have been studied extensively. Sodium and potassium tantalates are also known to have the perovskite structure.

Some of the best known perovskite-phase mixed-metal oxide compounds have the formula $A^{2+}B^{4+}O_3$. This is due to the interesting physical properties of certain members of this class, especially $PbTiO_3$ and $BaTiO_3$. As mentioned previously, $CaTiO_3$ has an orthorhombic structure, but $SrTiO_3$ is truly cubic while the atomic displacements from idealized lattice sites in $PbTiO_3$ and $BaTiO_3$ result in their ferroelectric properties. Both $PbTiO_3$ and $BaTiO_3$ become cubic at higher temperatures, $PbTiO_3$ changes from tetragonal to cubic

at 490 °C while $BaTiO_3$ undergoes three transformations: rhombohedral to orthorhombic at -90 °C, orthorhombic to tetragonal at 0 °C, and tetragonal to cubic at 130 °C, as shown in Figure 4.

The last group of oxides with the formula $A^{3+}B^{3+}O_3$ is usually found for the rare earth derivatives. None of these compounds have the ideal perovskite structure, but some of the rhombohedral perovskites are only slightly distorted from the ideal cubic perovskite structure. Complex oxides with the perovskite phase can be produced with substitutions occurring for either the A atom, the B atom, or both. For example, oxides with the formulations $A^{2+}(B^{3+}_{0.67}B'^{6+}_{0.33})O_3$, $A^{2+}(B^{2+}_{0.33}B'^{5+}_{0.67})O_3$, $A^{2+}(B^{3+}_{0.5}B'^{5+}_{0.5})O_3$, $A^{2+}(B^{2+}_{0.5}B'^{6+}_{0.5})O_3$, $A^{2+}(B^{4+}_{0.5}B'^{4+}_{0.5})O_3$, $A^{3+}(B^{2+}_{0.5}B'^{4+}_{0.5})O_3$ have been prepared[29] and many others involving A and B substitution are known. The ordering of the different B atoms in these substituted materials depends on the size and charge of the B ions themselves. Galasso has postulated that ordering of the B ions is likely when there is a large difference in the size or ionic radii of the B atoms.[29] If the B and B' atoms occupy the same set of atomic positions but in a regular way, this is called a superstructure. If the arrangement of the atoms is random then this is termed a solid solution.

2.3. Properties of Perovskite-Phase Materials

Perovskite-phase metal oxides exhibit a variety of interesting physical properties which include ferroelectric, dielectric, pyroelectric, and piezoelectric behavior. These properties are defined as follows.[33-37] Linear dielectric materials exhibit linear polarization behavior as a function of applied field.[23] Ferroelectric ceramics are a group of electronic materials consisting of dielectrics with a permanent electric dipole which can be oriented by the application of an electric field. Pyroelectric materials exhibit a spontaneous polarization, but the direction of the polarization cannot be reversed on application of an electric field. Piezoelectric materials exhibit an electrical charge when mechanically stressed or undergo mechanical deformation on the application of an electric field. These properties arise from the crystal symmetry adopted by these materials and its relationship to the symmetry of its physical properties. The equilibrium properties of a material can be described in tensor notation and can be transformed by symmetry operations. Neumann's principle states that the symmetry elements of any physical property of a crystalline material must include all the symmetry elements of the point group of the crystal. The physical properties may, and often do, possess more symmetry elements than the point group. As a result it is possible to predict the physical properties of a crystalline material based on crystal symmetry. The seven crystal systems (cubic, hexagonal, trigonal, tetragonal, orthorhombic, monoclinic, and triclinic) are comprised of 32 crystal classes according to their point group symmetry. Of the 32 crystal classes, 20 are piezoelectric (see Table I) and 10 of these (1, 2, m, $2mm$, 4, $4mm$, 3, $3m$, 6, and $6mm$ or C_1, C_2, C_{1h}, C_{2v}, C_4, C_{4v}, C_3, C_{3v}, C_6, and C_{6v}, respectively in the Schoenflies notation) possess spontaneous electrical polarization and are termed "polar". The polar axis of the crystal is a direction that is parallel to the spontaneous polarization vector. The internal or external electrical

Table I. Crystallographic Classes Allowing for Piezoelectricity

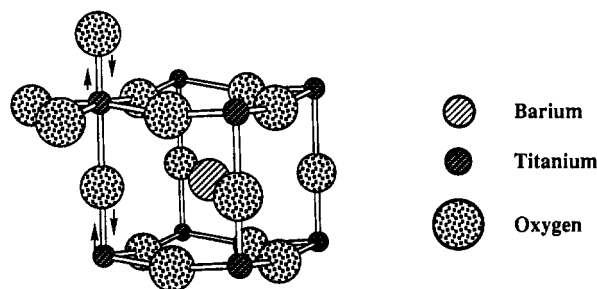| crystallographic system	point group	crystallographic system	point group
triclinic	1	trigonal	3
monoclinic	2		32
	m		$3m$
orthorhombic	222	hexagonal	6
	$mm2$		$\bar{6}$
tetragonal	4		622
	$\bar{4}$		$6mm$
	$4mm$		$\bar{6}m2$
	$\bar{4}2m$	cubic	23
			$\bar{4}3m$

Figure 6. Diagrammatic representation of the distorted Ti environment in tetragonal $BaTiO_3$.

conduction generally cannot provide enough current to compensate for the change in polarization with temperature in a polar crystal. As a result, the crystal develops an electric charge on its surface and therefore polar crystals are pyroelectric. In an alternative view, the pyroelectric coefficient (p_i) relates electric polarization (P_i) with temperature change according to eq 5. Centrosymmetric crystals require that $p_i = 0$ because

$$P_i = p_i \Delta T \qquad (5)$$

the property does not remain unchanged after application of the symmetry operation (i.e. it is inverted) and so violates Neumann's principle. This is the only value of p_i that is consistent with a center of symmetry and as a result, centrosymmetric groups are nonpyroelectric.

Ferroelectric materials are a subgroup of polar materials and therefore they are both pyroelectric and piezoelectric.[33,38] Ferroelectric materials are generating a great deal of current interest because their electric dipole can be reoriented by the application of an electric field. However, all of these materials lose their polar properties above the Curie temperature, T_C, and the nonpolar state above this temperature is called the paraelectric phase. For example, barium titanate changes from the tetragonal ferroelectric phase to the paraelectric cubic phase at 130 °C, the Curie temperature. In $BaTiO_3$, the spontaneous polarization (P_S) is due to the distortion of the perovskite structure (e.g. the tetragonal phase) by the displacement of the titanium ions in one direction and some of the oxygen ions in the opposite direction (Figure 6). The large Ba cation "swells" the unit cell, leaving the smaller Ti cation room to move inside the octahedral hole formed by the oxygen ions. The strong interaction between the Ti and the displaced oxygen ion polarizes these unit cells and builds linear chains of dipoles all aligned in the same direction along the c-polar axis. The material is less
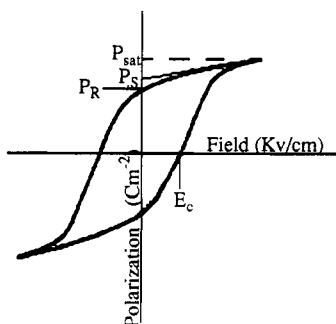
Figure 7. Typical hysteretic behavior of electrical polarization versus applied field for thin-film ferroelectric ceramics.

polarizable along the c-polar axis than in a perpendicular direction such as the a-axis because this distortion in the c-axis limits the mobility of the titanium and oxygen ions in this direction.[39] However, the atoms are free to move in the a- and b-axis directions, which can polarize the cell and hence produce a large dielectric constant. Thus, below the Curie temperature the individual titanium–oxygen octahedra are polarized all the time and this can produce areas where the dipoles are all aligned in the same crystallographic direction. These regions of homogeneous polarization are called domains and the line between two domains is called a domain wall or boundary. The size of these domains is variable and they can be observed by the use of a microscope with a polarized light source in some ferroelectrics. The net polarization of a ferroelectric material is the vector sum of the polarization of each individual domain. The effect of applying an electric field across a ferroelectric is to cause the individual dipoles to align with the field and change the net polarization. There are several mechanisms to explain this effect in polydomain ferroelectrics:[23] (a) Domains which are oriented favorably with the electric field may grow at the expense of less favorably aligned domains, i.e., the domain walls move out. (b) The direction of the domain polarization changes to align with the field. A plot of variation of polarization with applied electric field is shown in Figure 7. As the field is increased the polarization of the sample increases to a maximum called the saturation polarization, P_{Sat}. As the magnitude of the applied field decreases, the polarization decreases until, at zero field, the material retains an amount of polarization called the remanent polarization, P_R. In order to reduce the polarization to zero, another field must be applied in the reverse direction and this is the coercive field, E_C. This characteristic hysteretic behavior is illustrated in Figure 7.

The properties of ferroelectric materials change significantly and show a maximum as the temperature approaches T_c. In the case of BaTiO₃, the dielectric constant increases from 1000 to ~10 000 in the 10 K interval below the T_c while above this temperature there is a gradual decrease in the dielectric constant. The main applications for BaTiO₃ are based around this phase transition, especially applications as a dielectric. The temperatures at which these phase transitions occur can be modified by the partial substitution of other metal oxides into BaTiO₃ to give solid solutions.[40] These substitutions by dopants change the cell dimensions and hence the temperatures at which the phase changes occur. This is shown in Figure 11.

Table II. Perovskite-Phase Metal Oxides: Their Properties and Applications

materials	properties	applications
BaTiO₃	dielectric	capacitors, sensors
(Ba,Sr)TiO₃	pyroelectric	pyrodetector
PbTiO₃	pyroelectric	pyrodetector
	piezoelectric	acoustic transducer
Pb(Zr,Ti)O₃	dielectric	nonvolatile memory
	pyroelectric	pyrodetector
	piezoelectric	surface acoustic wave device substrate
	electro-optic	wave guide device
(Pb,La)(Zr,Ti)O₃	pyroelectric	pyrodetector
	electro-optic	wave guide device optical memory display
LiNbO₃	piezoelectric	pyrodetector surface acoustic wave device
(LiNbO₃/Ti)	electro-optic	wave guide device second harmonic generation optical modulator
K(Ta,Nb)O₃	pyroelectric	pyrodetector
	electro-optic	wave guide device frequency doubler
Pb(Mg₁/₃Nb₂/₃)O₃	dielectric	memory capacitor

Not all perovskite-phase metal oxides of this type exhibit ferroelectric properties. For example, CaTiO₃ and SrTiO₃ exhibit simple linear dielectric behavior; they possess high dielectric strength and have low dielectric loss. In addition, other non-perovskite-phase metal oxides can exhibit these properties; for example, tungsten bronzes exhibit ferroelectric behavior.

Perovskite-type oxides exhibit a number of interesting chemical properties including catalytic activity and oxygen-transport phenomena. Their catalytic activity includes CO oxidation, oxidation of hydrocarbons, NO reduction, hydrogenation and hydrogenolysis of hydrocarbons, CO and CO₂ hydrogenation, SO₂ reduction, and various electro- and photocatalytic reactions.[41] There is a variety of dense perovskite-phase mixed-metal oxides which are capable of high oxygen transport fluxes at elevated temperatures (T > 600 °C).[42,43] In fact, at high temperatures, the oxygen permeability of some of these materials exceeds that of porous membranes. Among the perovskite-type oxides that have been used for oxygen transport are La₁₋ₓSrₓMnO₃₋δ, La₁₋ₓSrₓCo₁₋ᵧFeᵧO₃₋δ, LiNbO₃, SrCeO₃, and SrTiO₃. Membranes made from these materials are dense, and as a result, their separation selectivity for oxygen is perfect. The oxygen-transport mechanism for these materials involves oxidation and reduction of O₂ at the membrane surface, with diffusion of oxide ions and electrons through the dense ceramic matrix, driven by an oxygen potential difference across the membrane. Both electronic and ionic conduction are necessary to allow continuous operation of the membrane without polarization, which will eventually curtail the transport. Their stability and high oxygen flux potential at high temperature provides considerable potential for application in high temperature membrane reactor applications, such as oxidation reactions.

2.4. Applications of Perovskite-Phase Materials

The properties and applications of a number of important perovskite-phase mixed-metal oxides are listed in Table II. The uses for these materials are
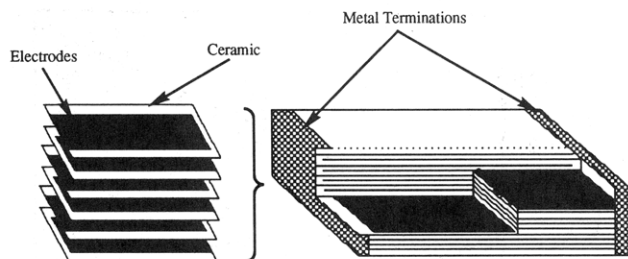
Figure 8. Cross section of a multilayer ceramic capacitor. The electrodes are connected to the metal terminations at the ends in an alternate fashion, so all the layers are in parallel. The capacitor can be mounted as shown and does not require leads. The thickness of the ceramic layers is ~15 μm and the overall dimensions of the capacitor can be as low as 1 mm × 0.5 mm × 0.5 mm.[44]
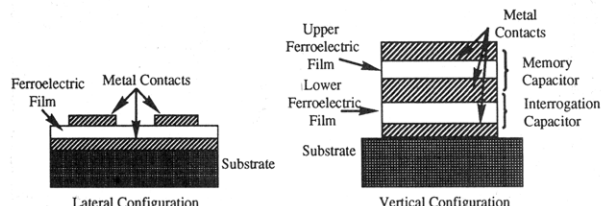
Figure 9. Designs for memory devices which utilize ferroelectric materials.

Figure 10. Schematic representation of an erasable read/write optical storage device based on a ferroelectric material.

based on their dielectric, ferroelectric, piezoelectric, and pyroelectric properties. All ferroelectric materials are both pyroelectric and piezoelectric and they have additional uses based on these properties.

The applications for ferroelectric materials utilize their ability to have their polarization reversed (switched) for memories as well as their nonswitching uses and high dielectric constant at or near T_C.[42] The drive for size reduction in electronic components has lead to the development of ceramic capacitors, especially the multilayer ceramic capacitor (MLCC), using ceramic dielectric materials with the highest permittivity values and multilayer configurations to fulfill the need for increased capacitance and reduced size.[44] A cross section of a MLC capacitor is shown in Figure 8, which illustrates the composite assembly of these structures. If the MLC capacitor has x dielectric layers then its capacity should be equivalent to x disk capacitors linked in parallel comprised of the same dielectric material, with the same thickness (down to 10 μm) and surface area of the electrodes.[32]

Another area which is attracting a good deal of interest is the use of ferroelectric thin films as nonvolatile computer memories.[27] Current static and dynamic memory chips lose the data they contain when the power to the memory is interrupted and the information leaks off. Magnetic storage facilities provide one answer to this problem, but the desire for fast, light-weight memories with low power consumption being integrated into silicon chips remains for some applications. These materials are also unaffected by radiation and magnetic fields which destroy the data stored on a standard memory chip. Two designs for a nonvolatile memory are shown in Figure 9. One of the key features of these designs is the nondestructive readout method, which has been a general problem for these types of memory devices. To read the memory cell, it must be poled, which erases the information the cell contained. This drawback can be overcome by designing a system to
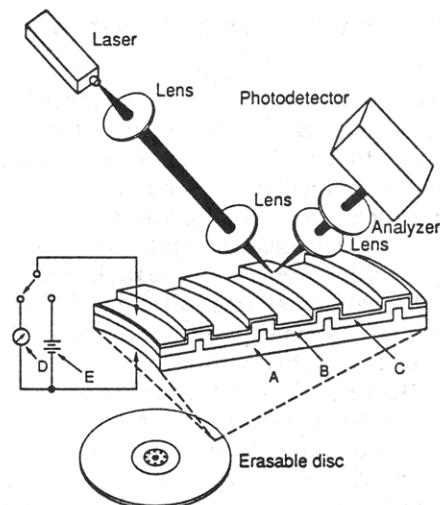
rewrite the information back into the memory once the cell has been read.

Another application which is under investigation is the use of ferroelectric materials as electro-optic switching devices for optical computers.[27,45] This is based on the ability of the ferroelectric to change its refractive index under an applied field. The response of the material for the electro-optic application is influenced by many factors such as film thickness, wavelength of the light, and the properties of the electrodes. Another application for thin films could be as a read/write optical storage device. In this case the material such as lead lanthanum zirconate titanate (PLZT) is switched between the ferroelectric state and the antiferroelectric state by application of a light beam while the film is under an applied field. The signal-to-noise ratio, which is typically poor for thin films, has been significantly improved in thin PZT films (~0.5 μm) under conditions that optimize interference effects. A schematic diagram of a proposed erasable optical read/write disk is shown in Figure 10. This type of optical storage device is unaffected by magnetic fields and would be the optical equivalent of the magnetic hard disks in computers.[46,47] Further applications of "smart" materials, especially electroceramics which have performance abilities other than those described here, such as sensing and actuating, have been reviewed recently.[48]

For the successful integration of these ceramics into silicon-based devices, the problems of high crystallization temperatures (>400 °C) and kinetically slow crystallization must be overcome. Low crystallization temperatures are required to prevent the degradation of the underlying materials (especially aluminum) in the device structure. To achieve this goal a great deal of research has been carried out using the sol–gel process to deposit thin films at low temperatures via metal–organic precursors. (See section 3.) By this route, thin films can be spin-coated onto a silicon wafer and fired to give the crystalline ceramic material. It is worth noting that in conventional ceramic syntheses, temperatures of >900 °C (often >1200 °C) are needed to produce crystalline materials.

2.5. Control of the Physical Properties

The different physical properties related to the phase transitions are sensitive to chemical composition, purity, number of surface and bulk defects, grain size, and sintering conditions.[40] The need to control these parameters is critical for the quality control of the devices produced from these materials. For example, the loss of Pb from lead titanate precursors during thermal processing is common due to the high volatility of PbO. This can be detrimental as any deviation from the correct stoichiometry will introduce TiO_2 as an impurity (or lead to Pb vacancies) and will be detrimental to the ferroelectric properties of the product. Studies have been conducted on the effect of the crystallite size on the crystalline structure adopted by $BaTiO_3$ at the surface and in the bulk.[49] At the surface of the crystallite, $BaTiO_3$ is cubic and is only tetragonal in the bulk with the two phases separated by a transition zone. As the crystallite size decreases below a few micrometers, the proportion of the crystal influenced by the surface effect increases and any undistorted tetragonal phase disappears. Thus, if the crystallite is small enough, then the ferroelectric state fades and is replaced by a pseudocubic, super-paraelectric state.[50]

The physical properties of these materials are often tailored through formation of nonintegral stoichiometry phases or solid solutions. The reasons for producing these materials are to tailor the properties for the particular application. For many applications, $BaTiO_3$ is not useful in its pure form because the high permittivity values are limited to a narrow temperature range near the Curie point at 130 °C, which is outside the temperature range for electronic applications. For capacitor applications, the goal of forming solid solutions with $BaTiO_3$ is to lower the T_C to room temperature and to broaden the temperature range over which the permittivity is high. To achieve this, partial substitution of Ca for Ba and Zr or Sn for Ti is used to give formulations of the type $Ba_{1-x}Ca_xTi_{1-y}Zr_yO_3$. A systematic study of the effect of isovalent substitutions on the transition temperatures of $BaTiO_3$ has been carried out and is shown in Figure 11.[40] By utilizing these substitutions the three phase transitions which exist in pure $BaTiO_3$ can be moved into a narrow band around room temperature to give a high permittivity under these conditions.

2.6. General Routes to Perovskite-Phase Materials

2.6.1. Introduction

The common means of processing ferroelectric materials is by traditional powder processing methods. This is because for capacitor applications the use of powders is desirable since the powder can be cast as a tape or a slurry and processed to the final multilayer or disk capacitor.[39] The methods for producing powders are reviewed in section 3.1. The traditional methods for producing ceramics have been based on powder techniques and it is still the preferred method in industry today. The ease by which powder methods can be used on an industrial scale and primarily the low costs associated with the use of inorganic precursors such as $BaCO_3$ and TiO_2 are two of the main attractions for this route. In some cases the prefiring of the
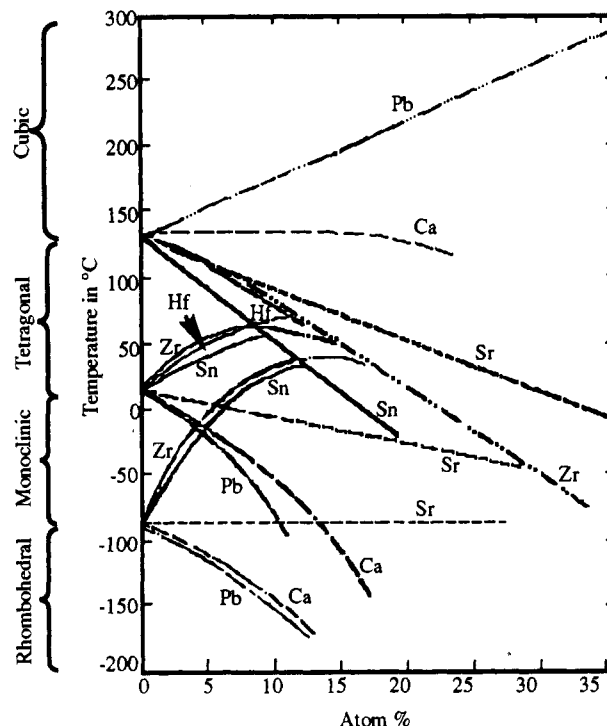
Figure 11. The effect of isovalent substitutions on the phase transitions of $BaTiO_3$.

precursors to form powders is desirable when the properties of the precursors themselves are not useful. For example the particle size distribution or rheological properties may be poor, so firing and grinding the ceramic may be necessary. Powders can be shaped into green bodies which are then sintered to give the final product. The temperature required for sintering the green body depends not only on the material but also on the crystallite and particle size of the powder. The smaller the particle and crystallite size, the lower the temperature required because the increased surface forces cause the particles to flow together at lower temperatures. This has been one of the driving forces behind the formation of nanoscale particles in which the sintering temperatures will be greatly reduced. The formation of the nanoscale particles of the final ceramic powders has the advantage that side reactions can be avoided compared to nanoscale mixing of the reactants. For example, the inorganic precursors, BaO and $Ba(OH)_2$ can react with atmospheric CO_2 to produce the impurity $BaCO_3$, but $BaTiO_3$ is unreactive toward CO_2 under ambient conditions. The amount of water absorbed onto the ceramic powder is also limited, as is the amount of shrinkage the green body undergoes during sintering.

2.6.2. Solution Routes

For some applications, especially the preparation of thin films, liquid-phase processing is one of the most convenient methods of preparation.[51] This method also has the potential advantages of (a) allowing control over the stoichiometry of the metals, (b) producing fully dense materials at temperatures hundreds of degrees lower than those required for powder compaction, (c) producing homogenous materials, (d) allowing formation of complex shapes, and (e) allowing preparation of composite materials. However, there are several disadvantages to this process: (a) the high cost of the

precursors, (b) the large shrinkage during processing, (c) the presence of fine pores, (d) the retention of hydroxyl groups, (e) the presence of carbon as an impurity, and (f) the possibility of long processing times. Thus, it appears that solution routes will only replace conventional techniques if they can produce materials which are superior or are only available through this method.

2.6.3. Vapor-Phase Routes

Due to the high cost of the chemical vapor deposition reactors and the shortage of suitably volatile precursors required to produce perovskite-phase ceramic material, usually thin films, this method appears to be limited to high-value-added products. The advantages of this route include (a) the potential purity of the materials produced, (b) the possibility of selective deposition, and (c) the production of nanophase particles with a narrow size distribution.

2.6.4. Hybrid Methods

A number of methods to prepare metal oxide powders and films exist which are a hybrid of the vapor phase and solution techniques. Spray pyrolysis is a method that can be used to form either powders or films at high rates and it requires only soluble metal–organic precursors. Aerosol-based methods rely on the formation of submicron-sized droplets of soluble metal–organic precursors in solution which can be processed in a number of different ways. The solvent can evaporate from the droplets to form solid particles which thermally decompose and form small metal oxide particles by intraparticle reactions. Alternatively, the solvent and the precursors can evaporate, if the precursors are volatile, and chemical vapor deposition may occur.[52,53]

3. Metal–Organic Routes to Perovskite-Phase Materials

3.1. Traditional Routes

Conventional routes to perovskite-phase ceramics are based on solid-state reactions and often involve the use of readily available starting materials. These reactions generally involve mixing of powders, grinding, milling, or firing and are generally followed by other grinding and calcination steps. Perovskite-phase materials are no exception, and the synthesis of $BaTiO_3$, for example, is achieved from barium carbonate ($BaCO_3$) and titania (TiO_2).[15,54] The synthesis has been studied extensively and requires high-temperature processes (ca. 1050–1150 °C). The first step involves a reaction at the grain interface (eq 6) to form $BaTiO_3$ with the liberation of

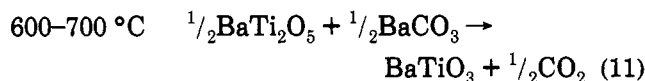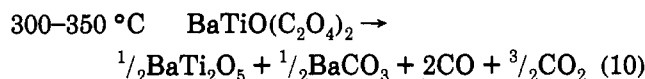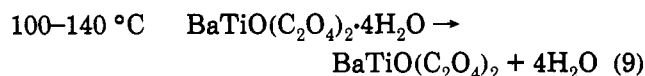$$BaCO_3 + TiO_2 \rightarrow BaTiO_3 + CO_2 \qquad (6)$$
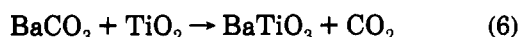
CO_2. In the bulk material, reactions are limited by the diffusion of the barium cations in the titania matrix, and the following reactions (eq 7 and 8) occur:

$$BaCO_3 + BaTiO_3 \rightarrow Ba_2TiO_4 + CO_2 \qquad (7)$$

$$Ba_2TiO_4 + TiO_2 \rightarrow 2BaTiO_3 \qquad (8)$$
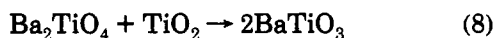
However, this route does not produce pure $BaTiO_3$. Ba_2TiO_4 obtained from the reaction of barium carbonate

and $BaTiO_3$ (eq 7) as well as other oxide phases ($Ba_6Ti_{17}O_{40}$, $Ba_4Ti_{13}O_{30}$) are present in the final material and contribute to deleterious effects on the electrical properties of the material. Moreover, as a result of high-temperature synthesis, the powders obtained are usually coarse and inhomogeneous. The use of readily available materials (of "low purity") and the necessity of grinding or milling also contribute to the introduction of impurities such as sulfur, phosphorus, silica, and alumina that lower the overall performance of the material. An alternative pathway could involve the thermal decomposition of $BaCO_3$ to form BaO and reaction of the latter with TiO_2. Although this intermediate is postulated during the calcination of a barium carbonate–titania mixture under vacuum, no BaO was detected.[54]

An alternative approach is the so-called oxalate process.[55] This process is used industrially to obtain $BaTiO_3$ powders in large quantities with precise stoichiometry. The result of mixing $BaCl_2$, $TiCl_4$, water, and oxalic acid is precipitation of $BaTiO(C_2O_4)_2 \cdot 4H_2O$. Crystalline *pseudocubic* $BaTiO_3$ is formed via thermal decomposition and a number of different pathways have been proposed. In one study the following pathway (eqs 9–11) was proposed:[55]

$$100\text{–}140\ ^\circ\text{C} \quad BaTiO(C_2O_4)_2 \cdot 4H_2O \rightarrow$$
$$BaTiO(C_2O_4)_2 + 4H_2O \qquad (9)$$

$$300\text{–}350\ ^\circ\text{C} \quad BaTiO(C_2O_4)_2 \rightarrow$$
$${}^1\!/_2BaTi_2O_5 + {}^1\!/_2BaCO_3 + 2CO + {}^3\!/_2CO_2 \qquad (10)$$

$$600\text{–}700\ ^\circ\text{C} \quad {}^1\!/_2BaTi_2O_5 + {}^1\!/_2BaCO_3 \rightarrow$$
$$BaTiO_3 + {}^1\!/_2CO_2 \qquad (11)$$

It should be noted that in this reaction scheme, the bis(oxalate) species does not convert directly to $BaTiO_3$ according to this study. In fact, the mechanism is similar to the conventional process described earlier where a mixed metal oxide of the wrong stoichiometry is formed as an intermediate. As a result, doubts can be raised about the "molecular mixing" using this technique, but the size of the $BaCO_3$ and $BaTi_2O_5$ particles is small due to the low reaction temperature and result in lowering the sintering temperatures for $BaTiO_3$. The resulting *pseudocubic* barium titanate phase is converted to the *tetragonal* phase on additional heat treatment.

In other studies, the thermal decomposition of barium titanyl oxalate was proposed to proceed via different intermediates according to the reactions of eqs 12–15.[57–59] It has been proposed that the broad peaks observed by X-ray powder diffraction after heating to 500 °C,[60] which some workers have been interpreted as the formation of weakly crystalline intermediates such as $BaCO_3$, $BaTi_2O_5$, or TiO_2, is not conclusive evidence for their formation.[59]

This reaction has been the subject of a large number of studies in the literature, and the phase purity and crystallinity of the $BaTiO_3$ product has been shown to depend subtly on the reaction conditions.[61–65] The controversy concerning the exact nature of the barium titanyl oxalate intermediate[60,64–66] was recently put to
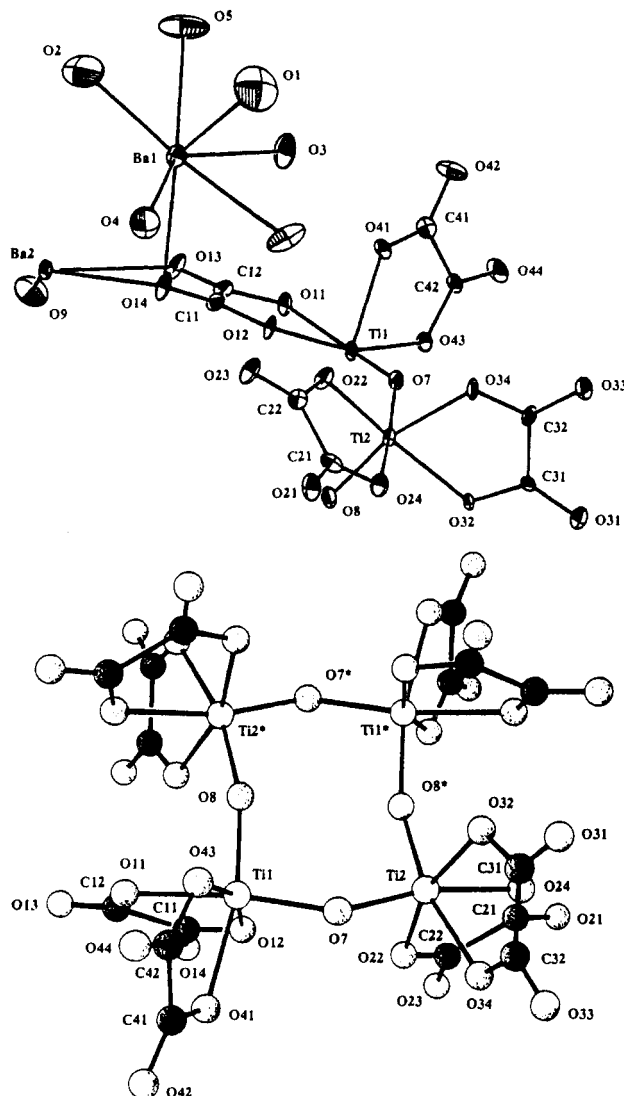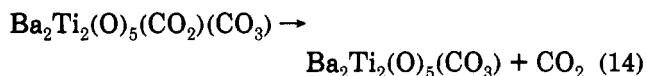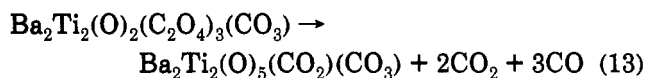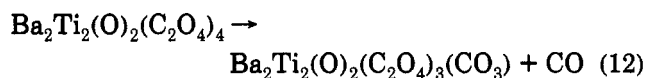
Figure 12. Solid state structure of $BaTi(O)(C_2O_4)_2 \cdot 5H_2O$ as determined by single-crystal X-ray diffraction.

$$Ba_2Ti_2(O)_2(C_2O_4)_4 \rightarrow$$
$$Ba_2Ti_2(O)_2(C_2O_4)_3(CO_3) + CO \quad (12)$$

$$Ba_2Ti_2(O)_2(C_2O_4)_3(CO_3) \rightarrow$$
$$Ba_2Ti_2(O)_5(CO_2)(CO_3) + 2CO_2 + 3CO \quad (13)$$

$$Ba_2Ti_2(O)_5(CO_2)(CO_3) \rightarrow$$
$$Ba_2Ti_2(O)_5(CO_3) + CO_2 \quad (14)$$

$$Ba_2Ti_2(O)_5(CO_3) \rightarrow 2BaTiO_3 + CO_2 \quad (15)$$

rest as the result of a single crystal X-ray diffraction study of $BaTi(O)(C_2O_4)_2 \cdot 5H_2O$ formed by the reaction between barium nitrate and ammonium titanyl oxalate, $(NH_4)_2Ti(O)(C_2O_4)_2 \cdot CH_2O$.[59] The solid-state structure is best described by the formula $Ba_2Ti_2(O)_2(C_2O_4)_4 \cdot 10 H_2O$ and is polymeric. A portion of the structure is shown in Figure 12 and consists of 6-coordinate Ti centers where $[Ti(O)(C_2O_4)_2]_4{}^{8-}$ form 8-membered rings while the Ba atom is 10-coordinate, including seven of the 10 water molecules. The remaining three water-molecules were found in interstitial sites in the structure and are not closely associated with either the Ba or Ti

centers. This probably results in a difference in strength of coordination of the water molecules, which has led to ambiguity in the interpretation of the TGA data of this material in the past.

A similar approach, the Pechini or citrate process,[67] patented in 1967, involves the thermal decomposition of a 1:1 mixed crystalline Ba·Ti tris(citrate)·water adduct $(BaTi(C_6H_6O_7)_3 \cdot xH_2O)$[68,69] to give tetragonal $BaTiO_3$ at 800 °C. The barium titanium citrate is obtained by mixing titanium and barium citrate solutions and adjusting the pH to <2.6 to precipitate the 1:1 Ba:Ti adduct. At higher pH, ≥3.6, a 2:1 Ba:Ti salt $(Ba_2Ti(C_6H_5O_7)_2(C_6H_6O_7) \cdot 7H_2O)$ was obtained.[70] It should be noted that these results were independent of the initial barium to titanium ratio (1:1 to 3:2). Thermal decomposition of $BaTi(C_6H_6O_7)_3 \cdot xH_2O$ has been studied[70] (eqs 16–22), and above 360 °C (eq 20), the presence

20–200 °C
$$BaTi(C_6H_6O_7)_3 \cdot 6H_2O \rightarrow$$
$$BaTi(C_6H_6O_7)_3 + 6H_2O \quad (16)$$

200–210 °C
$$BaTi(C_6H_6O_7)_3 \rightarrow$$
$$BaTi(C_6H_4O_6)_3 + 3H_2O \quad (17)$$

210–250 °C
$$BaTi(C_6H_4O_6)_3 \rightarrow$$
$$BaTi(C_5H_4O_4)_3 + 3CO_2 \quad (18)$$

250–360 °C
$$BaTi(C_5H_4O_4)_3 \rightarrow$$
$$TiO_2 \cdot Ba(C_5H_4O_4) + 2C_5H_4O_3 \quad (19)$$

360 °C
$$C_5H_4O_3 + O_2 \rightarrow 5CO_2 + 2H_2O \quad (20)$$

360–600 °C
$$BaTi(C_5H_4O_4)_3 \rightarrow$$
$$BaCO_3 + CO_2 + H_2O + TiO_2 \quad (21)$$

>500 °C
$$(BaCO_3)_x \cdot (TiO_2)_y \rightarrow$$
$$BaTiO_3 + CO_2 \quad (22)$$
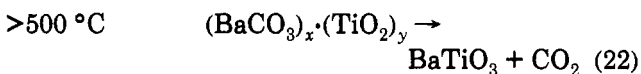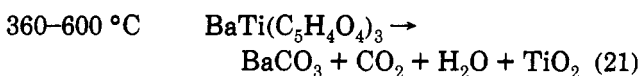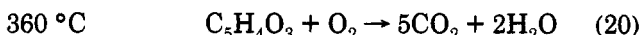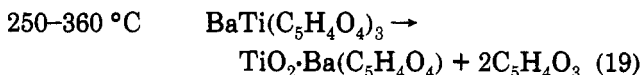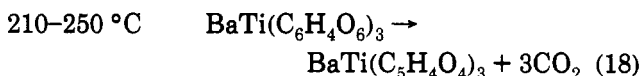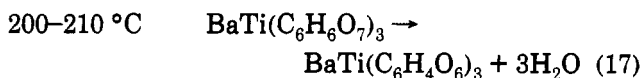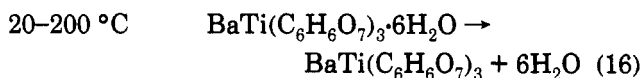
of small $BaCO_3$ crystallites (150 Å) was observed by X-ray powder diffraction. The small size of barium carbonate and titanium dioxide particles resulted in a sintering temperature lower than that of traditional routes (typically <800 °C), but the process does not offer perfect homogeneity until completion of the reaction. This process has been applied to a variety of mixed metal oxides (Mg, Ca, Sr, Ba, Pb, Zn, Cd, La, rare earths, Ga, Ti, Zr, Sn, Nb, Ta, Mo, W, Bi, Sb) and gives good control over the stoichiometry of the final materials.[68] However, disadvantages of this method include its high weight loss (low ceramic yield) and agglomeration during calcination. A variety of other organic reagents have been used in similar processes including tartaric acid and catechol, often to form analogous intermediates such as $Ba(Ti(catecholate)_3) \cdot 3H_2O$.[71-73]

Similar reactions for the preparation of lead-containing mixed-metal oxides are more difficult to achieve due to the volatility of PbO. Very often Pb is introduced in excess or the reaction is carried out under an atmosphere of lead oxide.[29]

3.2. Metal Alkoxide Based Routes

The synthetic approach to perovskite-phase metal oxides using metal alkoxide compounds generally involves the hydrolysis of solutions containing mixtures of metal alkoxide compounds to form sols or gels or to coprecipitate the metal oxides or hydrous metal oxides. Hydrolysis is then followed by a thermal treatment to remove the remaining hydroxyl groups and crystallize the final material.

Reaction of $Ba(OCH_2CH_2OCH_3)_2$ and $Ti(O-CH_2CH_2OCH_3)_4$ in the parent alcohol, 2-methoxyethanol, led to a white powder of the general formula $BaTi(OCH_2CH_2OCH_3)_6$[74] after removal of the solvent, as confirmed by elemental analysis and NMR spectroscopy. Hydrolysis of this material with 1 equiv of water per alkoxide ligand gave the oxo species $Ba_4Ti_{13}O_{18}(OCH_2CH_2OCH_3)_{24}$ (see Figure 37). This change in stoichiometry is believed to occur in the early stage of the sol–gel process. However, addition of an *excess* of water to a solution of $BaTi(OCH_2CH_2OCH_3)_6$ afforded *perovskite*-phase powders of $BaTiO_3$ at a temperature as low as 400 °C. So, although the stoichiometry may not be retained during the hydrolysis of the 1:1 mixed barium titanium alkoxide complex, the desired material was obtained at low temperature. The same precursors led to the formation of thin films at 600–700 °C.[75] Crystalline barium carbonate could be detected at 550 °C but was absent above 650 °C. The hydrolysis of barium and titanium isopropoxides in a CO_2-free atmosphere was proposed to result in formation of a water adduct of $BaTiO_3$ which on dehydration at 50 °C for 12 h resulted in formation of crystalline material.[76-78] This material has also been crystallized on thermal treatment at 100 °C.[79]

Lithium niobate has been prepared from the reaction of lithium and niobium ethoxide compounds in ethanol via formation of $LiNb(OEt)_6$, followed by hydrolysis and thermal treatment.[80,81] $LiNbO_3$ doped with Ti and $K(Ta_{0.65}Nb_{0.35})O_3$ thin films were also obtained at low temperatures (550 and 675 °C, respectively) starting from individual metal ethoxide complexes.[82] The species $Ta(OEt)_5$ and $Nb(OEt)_5$ were mixed in ethanol in the appropriate ratio. Then a stoichiometric amount of KOEt was then added and the solution was refluxed for 24 h. After partial hydrolysis, $^{13}C\{^1H\}$ NMR spectroscopy revealed the disappearance of the peaks corresponding to alkoxide ligands which indicated a condensation–polymerization process. These observations were confirmed by FT-IR spectroscopy.

The reaction of $Pb(OR^1)_2$, $Mg(OR^2)_2$, and $Nb(OR^3)_5$ ($R^1, R^3 = C_3H_7$ or C_4H_9, $R^2 = C_2H_4OCH_3$ or $C_2H_4OC_2H_5$) in a 3:1:2 ratio in a mixture of the parent alcohols afforded clear sols that could be coated on different substrates and dried at 150 °C.[83,84] Firing in air at 600–800 °C gave perovskite-phase $Pb(Mg_{1/3}Nb_{2/3})O_3$ (PMN) thin films (pyrochlore free). The kinetically favored pyrochlore phase formed at 200–300 °C was slowly converted to the perovskite-phase PMN at higher temperature. No attempt was made to characterize the intermediate species. Under these conditions a number of different reactions can occur. It is likely that alkoxide ligand redistribution, which is known to be rapid at room temperature, occurs in the first step (see section 4.6). Furthermore, it has been demonstrated that, unless special precautions are taken,
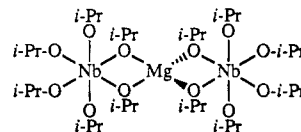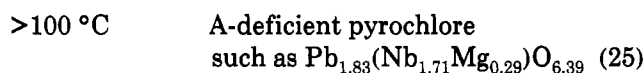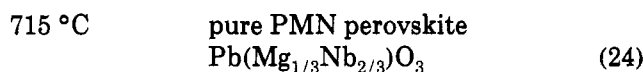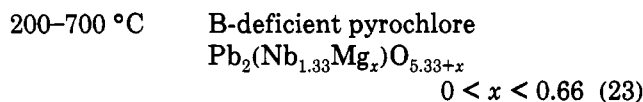

Figure 13. Schematic representation of the structure proposed for $Mg[Nb(O-i-Pr)_6]_2$.

lead(II) alkoxide compounds react to form oxo–alkoxide species.[85,86] In related chemistry, Hubert-Pfalzgraf et al.[87] have demonstrated the formation of Pb_6O_4-$(OEt)_4[Nb(OEt)_5]_4$ from the reaction of $Pb_6O_4(OEt)_4$ and $[Nb(OEt)_5]_2$. Furthermore, the reaction of $Mg(O-i-Pr)_2$ and $[Nb(O-i-Pr)_5]_2$ led to a mixed metal alkoxide $Mg[Nb(O-i-Pr)_6]_2$ as determined by elemental analysis. The structure shown in Figure 13 was proposed for this species on the basis of the analogy with Ca and Sr niobium isopropoxide complexes for which molecular weights were determined in solution and the reasonable assumption that magnesium(II) prefers a coordination number of four.[88] It is noteworthy that the similar species $MgNb_2(OAc)_2(O-i-Pr)_{10}$ was found to exhibit a different structure in solution as shown in Figure 60 with a six-coordinate magnesium(II) center.[89] Translucent gels were obtained from further reaction of $Mg[Nb(OEt)_6]_2$ with the appropriate amount of lead alkoxide in ethanol and hydrolysis with a 5-fold excess of water.[90] After removal of the solvent, the solid-state reaction is believed to proceed according to equations 23–25, as determined by X-ray diffraction data. The

200–700 °C	B-deficient pyrochlore
	$Pb_2(Nb_{1.33}Mg_x)O_{5.33+x}$

$$0 < x < 0.66 \quad (23)$$

715 °C	pure PMN perovskite
	$Pb(Mg_{1/3}Nb_{2/3})O_3$ $\quad$ (24)

>100 °C	A-deficient pyrochlore
	such as $Pb_{1.83}(Nb_{1.71}Mg_{0.29})O_{6.39}$ $\quad$ (25)

B-deficient pyrochlore phase (deficient in B cation) proposed in eq 23 was inconsistent with the $Pb_{1.83}$-$(Nb_{1.71}Mg_{0.29})O_{6.39}$ phase proposed previously.[91] The lead-deficient pyrochlore phase (equation 25) is thought to be derived from the loss of PbO.

The superconducting mixed-metal oxide $YBa_2Cu_3O_{7-\delta}$ can also be obtained at relatively low temperatures from metal alkoxide complexes.[92-98] Most reactions of this type led to the formation of $BaCO_3$, Y_2O_3, and CuO as intermediates, and have few advantages over conventional solid-state syntheses. However, the smaller particle size and better mixing of the different components results in a lowering of the firing temperature to 800 °C.[99] The thermal stability of $BaCO_3$ precludes any further reduction in crystallization temperature.[100] Calcination of thin films under argon atmosphere[100] shows the presence of traces of $BaCO_3$ at 550 °C by X-ray diffraction. At temperatures higher than 600 °C, crystallization of the superconducting phase occurs and no other crystalline phases were detected. These observations led the authors to postulate that the carbonate must be introduced into the film after calcination.
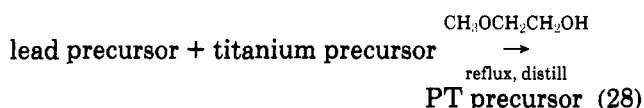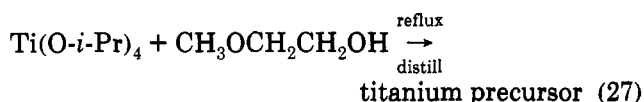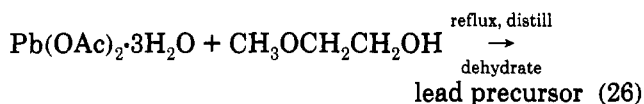
3.3. Metal Carboxylate and Metal Alkoxide Based Routes

Substitution of one or more of the alkoxide ligands on one or more of the metals by a carboxylate functionality has also been widely used as a method of formation of perovskite-phase materials. For example, the synthesis of $PbTiO_3$ (PT) or $Pb(Zr_{0.53}Ti_{0.47})O_3$ (PZT) can be achieved via the reaction of lead acetate with titanium and zirconium alkoxides. In a typical experiment, lead acetate trihydrate is dissolved in acetic acid and Ti(O-i-Pr)$_4$, Zr(OR)$_4$ (R = i-Pr, n-Bu), or a mixture of titanium and zirconium precursors is added. The solution is stirred before adding at least a stoichiometric amount of water. The resulting sols or gels can then be cast into films, or powders can be obtained by removal of the volatile components. Thermal treatment to remove the residual organic ligands (300–500 °C) and a calcination step (600 °C for 6 h) is necessary to condense the remaining hydroxyl groups and crystallize the material. Many variations of the theme have been reported.[101,102] However, in this section, we shall not try to make an exhaustive list of these different variations but shall focus on those where intermediates have been identified or at least postulated.

Schwartz and co-workers have recently reported that the electrical properties of PZT thin films are very dependent upon the synthetic scheme and reagents.[103,104] Unfortunately, as with many studies, a number of variables were changed between experiments, so the origin of different effects is not clear. The two synthetic approaches employed were "sequential precursor addition" (SPA) and "inverted mixing order" (IMO). The SPA method involved the dissolution of lead(II) acetate in acetic acid followed by dehydration, addition of Ti and Zr alkoxides, and addition of water and methanol. The IMO method involved mixing Ti and Zr alkoxide precursors, reaction with acetic acid, addition of methanol, and addition of $Pb^{(IV)}(OAc)_4$ in acetic acid followed by addition of water and methanol. Evidence for the formation of esters in the final solution was obtained by ^1H and $^{13}C\{^1H\}$ NMR spectroscopy. Solid-state CP/MAS ^{13}C NMR of the dried SPA product under vacuum indicated that acetate ligands were the major species present, consistent with formation of oxo–acetate rather than alkoxide containing species such as oxo–alkoxide or oxo–acetato alkoxide polymers. It was also proposed that, on the basis of the amount of ester formed, more water was liberated in the SPA method compared to the IMO method. However, ester may also be formed without liberation of water via the reaction between metal alkoxide and metal acetate species (see eq 44). For both methods, removal of the acetate ligands was achieved on heating to 300 °C, and crystallization of the perovskite-phase occurred after heating to 650 °C for 30 min (although the onset of crystallization was observed at 400 °C). The thin films were characterized by a remanant polarization of 18.7 and 26.2 μC cm^{-2} and a coercive field of 55.2 and 43.3 kV cm^{-2}, for SPA and IMO methods, respectively.

The evolution of structure has been studied in the barium/titanium system by FT-IR.[105] Two different methods were used to prepare the sol. In one method, Ba metal, polished by emery paper in kerosene, was reacted with anhydrous ethanol at room temperature to form Ba(OEt)$_2$. To this solution was added Ti(O-

i-Pr)$_4$, followed by a sufficient amount of acetic acid to form a yellow transparent solution. In the other method, Ba was reacted with an excess of glacial acetic acid at room temperature and then reacted with Ti(O-i-Pr)$_4$ to form a yellow transparent solution. Both solutions were then treated with water to a sol from which fibers were drawn and fired. IR spectra of the gel fibers were recorded at various temperatures after the hydrolysis and a drying step. Unfortunately, it is not clear which method was used to prepare these gels. On heating to 100 °C both acetate and alkoxide groups were present, but it appears that crystalline Ba(OAc)$_2$ was not present by comparison with the data for authentic Ba(OAc)$_2$. At 400 °C, the vibrational modes of CO_3^- (produced by decomposition of acetate groups) were detected at 1370 cm^{-1}. However, this is apparently not due to *crystalline* BaCO$_3$ since these gels are still amorphous according to X-ray diffraction experiments at this temperature. At 600 °C, a broad band at 600 cm^{-1} was consistent with the presence of TiO$_6$ octahedra. Above this temperature, no peak other than that of the TiO$_6$ entity (560 cm^{-1}) was observed. However, thermal treatment to 1000 °C was required to produce crystalline, perovskite-phase BaTiO$_3$.

Payne and co-workers have been investigating the chemistry behind these types of reactions. Using NMR (^1H, $^{13}C\{^1H\}$, and ^{207}Pb) and mass spectroscopies, they studied the formation of lead titanate (PbTiO$_3$) from dehydrated lead acetate trihydrate and Ti(O-i-Pr)$_4$ in 2-methoxyethanol (eqs 26–29; see also eq 53).[106,107]

$$Pb(OAc)_2 \cdot 3H_2O + CH_3OCH_2CH_2OH \xrightarrow[\text{dehydrate}]{\text{reflux, distill}}$$
$$\text{lead precursor} \quad (26)$$

$$Ti(O\text{-}i\text{-}Pr)_4 + CH_3OCH_2CH_2OH \xrightarrow[\text{distill}]{\text{reflux}}$$
$$\text{titanium precursor} \quad (27)$$

$$\text{lead precursor} + \text{titanium precursor} \xrightarrow[\text{reflux, distill}]{CH_3OCH_2CH_2OH}$$
$$\text{PT precursor} \quad (28)$$

The lead precursor was prepared by refluxing Pb(OAc)$_2 \cdot 3H_2O$ in 2-methoxyethanol (eq 26), and the volatile components were then removed in vacuo. Chemical ionization mass spectroscopy analysis showed a molecular ion peak at 343 amu corresponding to the molecular formula Pb(OAc)(OCH$_2$CH$_2$OCH$_3$) plus a proton. ^{207}Pb NMR spectroscopy of this species in 2-methoxyethanol solution revealed an up-field shift, the value of which was not reported, compared to lead acetate trihydrate, but interpretation of this change is difficult to assess (see section 5). $^{13}C\{^1H\}$ and ^1H NMR spectra confirmed the ratio of acetate:2-methoxyethoxy ligands but ^1H NMR also shows the presence of a peak ascribed to <0.5H$_2$O. On the basis of these analyses the following structure was proposed: Pb(OAc)(OCH$_2$CH$_2$OCH$_3$)·xH$_2$O (x < 0.5) (although the connectivity of the ligands to the lead center was not unambiguously established). A similar reaction between Ti(O-i-Pr)$_4$ and 2-methoxyethanol (eq 27) resulted in the formation of a complex of molecular formula Ti$_2$(OCH$_2$CH$_2$OCH$_3$)$_8$ as determined by mass spectrometry. Low-temperature ^{13}C NMR spectro-

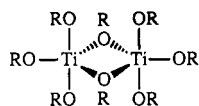**Figure 14.** Proposed structure for $Ti_2(OCH_2CH_2OCH_3)_8$.

scopy showed two different chemical shifts for the α-carbon, leading the authors to propose the structure shown in Figure 14, where the two bridging alkoxide ligands are chemically inequivalent to the terminal groups and, as a result, possess different chemical shifts.

Chemical inequivalence between the two different types of terminal alkoxide ligands might have been expected,[108] but was not observed. A single type of alkoxide ligand was observed at room temperature, probably due to fast alkoxide ligand exchange. No experiments were performed to investigate the degree of aggregation of this species. The modified lead and titanium precursors were then mixed in refluxing 2-methoxyethanol (eq 28) followed by removal of the volatile components in vacuo. Three possible compositions for these solutions were proposed: (i) a simple mixture of molecules, (ii) formation of a double alkoxide compound, and (iii) a mixture of Ti and Pb polymers analogous to the possibilities presented in Figure 1. The mass spectral data did not show the ions observed for the individual precursors, which disfavors i, although $[Ti_2(OR)_7]^+$ was observed. The mass spectral data were used to support the second possibility, where formation of the fragment $[Pb_2Ti_2(OR)_{12}]^+$ could account for m/e = 790. The isotope distribution pattern which might have confirmed this assignment was not discussed. ^1H and $^{13}C\{^1H\}$ NMR spectroscopies revealed the presence of only a small amount of acetate ligand. The loss of acetate ligands was not interpreted, but one could imagine that esterification reactions take place with formation of Pb-O-Ti or hydroxyl groups.

In other work, similar solutions have been hydrolyzed with water and nitric acid. Spin coating of films from this solution followed by annealing (400 °C) and calcination (700-800 °C) in an oxygen atmosphere affords perovskite-phase $PbTiO_3$.[109] Synthesis of $Pb(Ti_{0.47}Zr_{0.53})O_3$ (PZT) from $Pb(OAc)_2$, $Ti(O\text{-}i\text{-}Pr)_4$, $Zr(O\text{-}n\text{-}Pr)_4$, and 2-methoxyethanol has also been investigated using FT-IR and NMR spectroscopies.[110] The titanium and zirconium species were refluxed in 2-methoxyethanol at 120 °C and the excess solvent removed by distillation prior to reaction with the lead complex at 120 °C. The volatile components were then removed by distillation. Mass spectroscopic investigations of the Zr/Ti solution are consistent with formation of a mixed metal alkoxide compound although the isotope distribution data that could confirm this assignment were not discussed. Upon addition of anhydrous lead acetate to 2-methoxyethanol, a significant change in the IR spectra was observed. The bonds associated with $\nu_{as}(CO_2)$ and $\nu_{sym}(CO_2)$, 1572 and 1409 cm^{-1}, respectively, were shifted compared with those of crystalline lead(II) acetate in the solid state, 1428 and 1419 cm^{-1}, respectively. These observations were interpreted as providing evidence for monodentate carboxylate ligands based on the difference Δ, defined as the difference $\nu_{as}(CO_2) - \nu_{sym}(CO_2)$, compared to the value for the free acetate ion. However, the values of Δ available for the free acetate ion are in conflict with other literature data,[111] which makes interpretation ambiguous.

The IR spectrum of this solution also gave rise to a band at ~ 1740 cm^{-1}, which is consistent with the presence of either a free carboxylic acid or an ester. $^{13}C\{^1H\}$ NMR data were found to be consistent with the presence of an ester. NMR spectroscopies show the formation of the ester 2-methoxyethyl acetate and liberation of an equivalent amount of water that had to be removed by distillation to avoid adventitious hydrolysis and condensation. The formation of an ester was also consistent with IR data. Upon hydrolysis, alkoxide ligands were progressively removed, but acetate ligands and some remaining alkoxy groups could be identified by IR spectroscopy. Thermal treatment (400 °C) resulted in the removal of most of these organic fragments (~ 10 weight %) although a weak band at ~ 1000 cm^{-1} was still observed, even at 500 °C. Firing at 700 °C crystallized perovskite-phase PZT. It is noteworthy that the perovskite phase appeared as a weak peak in the X-ray powder pattern in the major pyrochlore phase at a temperature as low as 400 °C. On heating to 650 °C, virtually all the pyrochlore phase disappeared. The influence of water content on the crystallization behavior of the films was also studied on gels fired at 650 °C for 30 min. Gels formed with low water content tended to have little or no pyrochlore phase, whereas higher water contents tended to result in more extensive pyrochlore-phase formation. To examine these aspects further, two precursor solutions were prepared. In the first, all the volatile components were removed by vacuum distillation whereas, in the second, the volatile components were not removed. All films formed from these solutions were fired at 700 °C for 30 min on platinized silicon substrates. Films derived from the first solution hydrolyzed under basic conditions gave a mixture of pyrochlore and perovskite phases while those hydrolyzed under acidic conditions appeared to be mainly perovskite, predominantly oriented in the [111] direction. Consistent with the presence of perovskite phase, these films exhibited better ferroelectric parameters than those derived from the second procedure. The second solution gave poorly defined hysteresis loops which could be improved by a pretreatment at 450 °C for 30 min and resulted in more extensive perovskite-phase development.

Synthesis of $PbZrO_3$ (PZ) from addition of zirconium propoxide to a 2-methoxyethanol solution of lead acetate has also been studied by FT-IR and Raman spectroscopies.[112] In the first stage of the reaction, in which lead acetate was refluxed in 2-methoxyethanol, it was proposed that ester formation occurs (growth of a band at ~ 1740 cm^{-1}) and the $\nu(CO_2)$ stretching mode shifts to higher wavenumbers (~ 1558 cm^{-1}) compared to lead acetate, which was probably due to the formation of a bidentate acetate binding mode, unlike that of the crystalline solid. Addition of $Zr(O\text{-}n\text{-}Pr)_4$ to this solution resulted in growth of a band at 1740 cm^{-1} and a shift in $\nu_{asym}(CO_2)$ to 1576 cm^{-1}. These data were interpreted in terms of formation of a bimetallic species rather than a trimetallic species, in which case the acetate ligand would have been completely removed by esterification. Bands attributed to $\nu(Zr\text{-}O)$ in ZrO_2 were also observed. In contrast to the $PbTiO_3$ (PT) system,[113] the bands at ~ 1740 and ~ 1576 cm^{-1} did not change dramatically in intensity upon aging, indicating a faster

reaction in the case of Zr. Upon hydrolysis and aging, the band corresponding to the alcohol and ester slowly decreased due to the evaporation of these molecules. Bands associated with acetate ligands, attributed to lead acetate, remain even upon solidification of the gel and no new Pb–O bonds seem to be formed. Acetate species disappeared upon heat treatment (300–400 °C) and Zr–O modes characteristic of PZ appeared after heating to 500 °C. X-ray diffraction data revealed the formation of metallic lead when the PZ precursor was heated at 400 °C. Formation of metallic lead was not observed in the PT system. Mixed phases were observed on heating to 700 °C, including monoclinic ZrO_2 as determined by Raman spectroscopy and orthorhombic PbO on heating to 500 °C for 6 h. Perovskite-phase PZ was obtained at or above 800 °C. In contrast to the PT system, no PbO band was observed in the PZ system after treatment to 450–750 °C.[114]

Chandler et al. have synthesized lead titanate from the reaction of $Ti(O\text{-}i\text{-}Pr)_4$[114,115] or $Ti(O\text{-}i\text{-}Pr)_2(acac)_2$[116] with either lead glycolate or lead dimethyl glycolate, which has some analogy with the citrate or Pechini processes (chelation of two metals by a common polydentate ligand). $Pb(OOCCH_2OH)_2$, characterized in the solid state by single crystal X-ray diffraction, reacts in pyridine with $Ti(O\text{-}i\text{-}Pr)_2(acac)_2$ to liberate 2 equiv of 2-propanol as determined by gas chromatography. A species believed to be $[Pb(OOC\text{-}CH_2O)_2Ti(acac)_2]$ was precipitated, although no satisfactory elemental analysis (probably due to a slight excess of lead glycolate) nor NMR data (due to insolubility problems) was obtained. Thermogravimetric analysis (TGA) showed a complete weight loss (observed, 40%; calculated, 39%) corresponding to $PbTiO_3$ at 400 °C. After a bulk sample of this white precipitate was heated to 400 °C for 1 h, perovskite-phase PT contaminated with PbO (probably from coprecipitation of $Pb(OOCCH_2OH)_2$) was formed. Studies of the crystallization behavior as a function of temperature by X-ray powder diffraction and transmission electron microscopy techniques were consistent with the formation of the pyrochlore phase, initially at low temperatures. Further heat treatment resulted in development of the perovskite phase with no significant pyrochlore crystallite growth. This is illustrated in the X-ray diffraction data shown in Figure 15 as a function of temperature and in the TEM data shown in Figure 16. The both techniques show that the perovskite crystallite size is on the order of 30 nm while the pyrochlore crystallites are on the order of 2 nm.[117] Substitution of the methylene protons of the glycolate ligand by methyl groups circumvents the insolubility encountered in the case of the glycolate complexes and further characterization of intermediate species was possible.[114] Reactions of $A[OOCC(CH_3)_2OH]_2$ (A = Pb, Ca, Sr, and Ba) and $B(OR)_4$ (B = Ti, R = i-Pr; Zr, i-Pr; B = Sn, R = t-Bu) in pyridine (C_5H_5N) afforded clear solutions. ^1H and $^{13}C\{^1H\}$ NMR data were consistent with complexes of the general formula $A[OOCC\text{-}(CH_3)_2O]_2B(OR)_2\cdot2ROH\cdot xC_5H_5N$ (Figure 17). However, TGA and elemental analysis (C, H, and N) are consistent with an entity without the alcohol molecules: $A[OOCC(CH_3)_2O]_2B(OR)_2\cdot xC_5H_5N$. Hydrolysis of the pyridine solutions results in formation of clear sols.
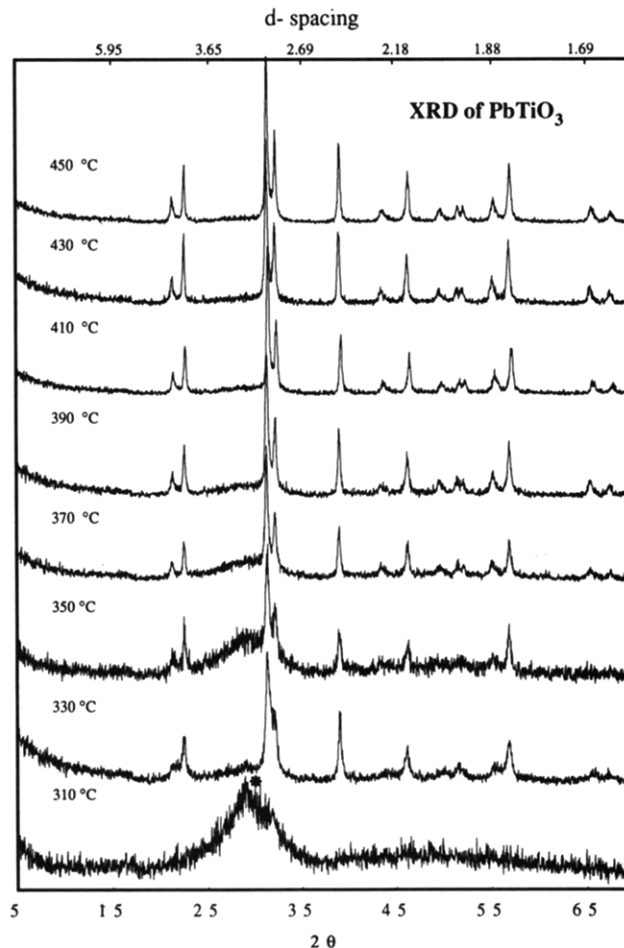

Figure 15. X-ray powder diffraction data recorded as a function of temperature for $PbTiO_3$ formed via thermal decomposition of $[Pb(OOCCH_2O)_2Ti(acac)_2]$. The broad peak labeled with an asterisk shows the presence of the pyrochlore phase. The other (sharper) peaks are due to the perovskite phase.
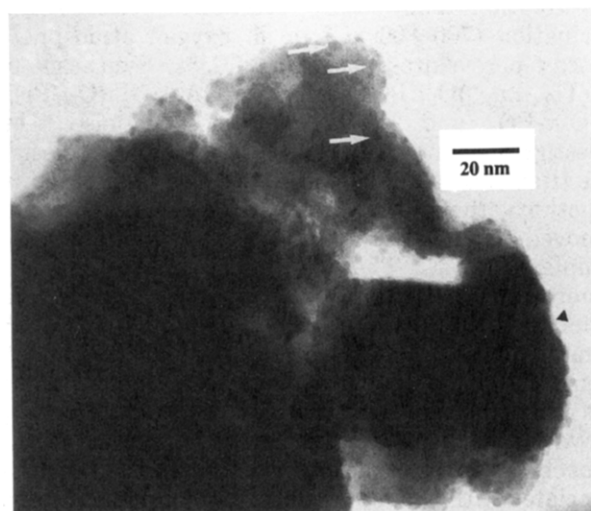

Figure 16. TEM data showing the morphology of the $PbTiO_3$ obtained via thermal decomposition of $[Pb(OOC\text{-}CH_2O)_2Ti(acac)_2]$. White arrows show some of the 2-nm pyrochlore crystallites and the triangle shows a larger (30 nm) perovskite-phase crystallite, revealing the lattice fringes on close inspection.

Removal of the volatile species affords white or pale-yellow powders consistent with the empirical formula $A[OOCC(CH_3)_2O]_2B(OH)_2\cdot xH_2O\cdot yC_5H_5N$. ^1H and
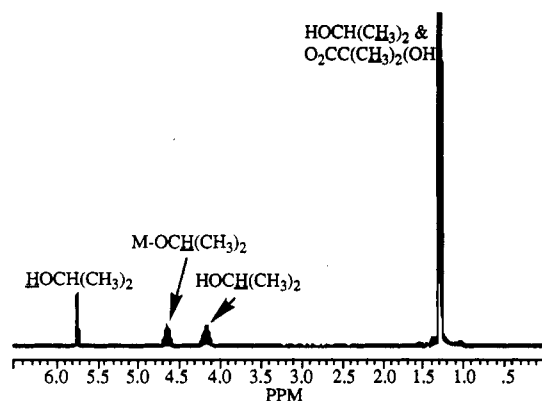
Figure 17. ^{1}H NMR spectrum of Ba[OOCC(CH$_3$)$_2$O]$_2$Ti(O-i-Pr)$_2$·2HO-i-Pr in C$_5$D$_5$N.
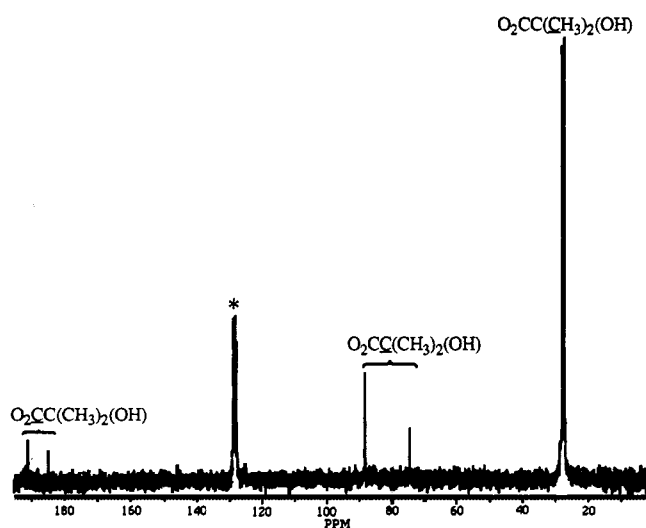
Figure 18. ^{13}C NMR spectrum of Ba[OOC-C(CH$_3$)$_2$O]$_2$Ti(OH)$_2$ in D$_2$O referenced to internal C$_6$D$_6$ (*).
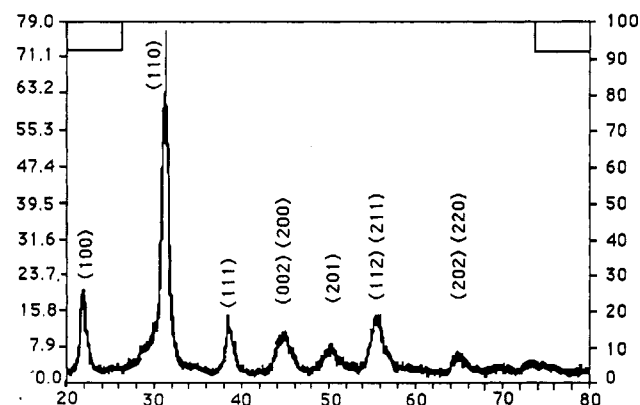
Figure 19. X-ray powder diffraction data for PbZr$_{0.52}$Ti$_{0.48}$O$_3$ as prepared by the method described above.[114]

^{13}C{^{1}H} NMR spectroscopies confirmed the removal of the alkoxides and the presence of the glycolate ligand (Figure 18). Thermolysis of the hydrolyzed products at 350 °C under an oxygen atmosphere gave perovskite-phase crystalline materials. Large crystallites (ca. >1000 Å) were formed in all cases except PZ (300 Å), as determined by X-ray diffraction. Synthesis of PZT 52:48 (PbZr$_{0.52}$Ti$_{0.48}$O$_3$) was also probed using this method. Mixing of PT and PZ precursors (A[O$_2$CC-(CH$_3$)$_2$O]$_2$B(OR)$_2$) followed by hydrolysis or mixing the hydrolyzed species (A[O$_2$CC(CH$_3$)$_2$O]$_2$B(OH)$_2$) in a 0.48 (A = Pb, B = Ti) to 0.52 (A = Pb, B = Zr) ratio afforded

clear solutions from which solvents could be removed in vacuo and perovskite-phase PZT could be obtained by thermal treatment at low temperature (350 °C under O$_2$ atm, 30 min) as shown in Figure 19. It was proposed that homogeneity at the molecular level may be responsible for the low crystallization temperature of PZT rather than formation of individual phases PZ and PT. These reactions are summarized in eqs 29–32, below.

$$A(CO_3) + 2HO_2CCR_2OH \xrightarrow{H_2O}$$
$$A(O_2CCR_2OH)_2 + H_2O + CO_2 \quad (29)$$

$$A(O_2CCR_2OH)_2 + B(OR')_4 \rightarrow$$
$$A(O_2CCR_2O)_2B(OR')_2 + 2HOR' \quad (30)$$

$$A(O_2CCR_2O)_2B(OR')_2 \rightarrow ABO_3 \quad (31)$$

$$xA(O_2CCR_2O)_2B(OR')_2 +$$
$$(1-x)A(O_2CCR_2O)_2B'(OR')_2 \rightarrow AB_xB'_{(1-x)}O_3 \quad (32)$$

A = Ca, Sr, Ba, Pb; B = Ti, Zr, Sn;
$$R = H, Me; R' = i\text{-}Pr$$
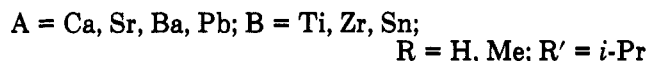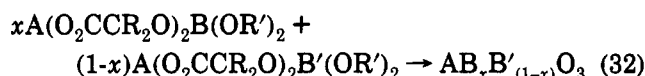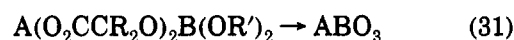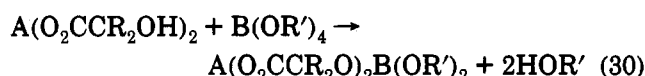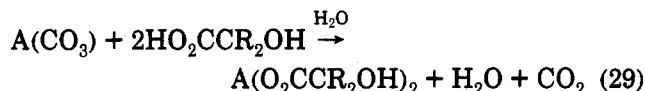
3.4. Other Routes

Other solution routes to mixed metal oxides include hydrothermal synthesis. This aqueous process is generally effected above room temperature and at high pressures. Typically, the temperature varies from the boiling point to the critical point of water, 100–374 °C, and the pressure can be as high as 15 MPa.[14] Generally, but not always, a subsequent thermal treatment is required to crystallize the final material. Readily available starting materials are used (metal oxide or metal hydroxide) which allow a low-cost processing of mixed metal oxide. By avoiding the use of organic ligands, no calcination step is necessary.

Hydrothermal synthesis of BaTiO$_3$ powder has been achieved between 150 and 200 °C by reaction between barium and titanium hydroxides[118] in strongly alkaline (pH >12) solutions in an autoclave at >5 MPa or from barium titanium acetate gels.[119] However, the materials produced by this method exhibit some anomalous behavior thought to be derived from the incorporation of water and the presence of hydroxyl groups in the crystal lattice.[120]

More recently, hydrothermal–electrochemical methods have been investigated.[119] At temperatures as low as 55 °C, crystalline BaTiO$_3$ thin films were electrochemically deposited on Ti metal as the anode using barium acetate–sodium hydroxide solutions under an oxygen atmosphere.[121] The films were contaminated with a small amount of BaCO$_3$ which was derived from reaction of the electrolyte with atmospheric CO$_2$ (probed by AES depth-profile analysis).

Other synthetic methods using metal salts (i.e. M(NO$_3$)$_x$, MCl$_x$) have been studied. For example, PZT 52:48 was obtained from Pb, Ti, and ZrNO$_3$ salts in the presence of ethylenediaminetetraacetic acid (EDTA) at a constant pH of 5.[122] After removal of the solvents and drying at 80 °C, crystallization of perovskite-phase PZT is observed at temperatures as low as 250 °C during
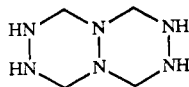
Figure 20. Structure of TFTA as reported by Mashina.[124]

the firing step. However, pure crystalline PZT is only obtained above 600 °C. The role of EDTA in this solution is unknown and was not discussed. Unfortunately control experiments in the absence of EDTA were not performed.

Using metal nitrates $MTiO_3$ and $MZrO_3$ (M = Ca, Sr, Ba, and Pb), PZT 53:47 and $Pb_{0.92}La_{0.08}(Zr_{0.65}Ti_{0.35})_{0.98}O_3$ were synthesized upon heating to 350 °C. Perovskite phases of these materials were obtained contaminated with approximately 5-20% of pyrochlore phases.[123] These materials were also prepared by combustion (hypergolic reaction) of tetraformal triazine (TFTA, Figure 20) in the presence of metal nitrates mixed in the proper stoichiometry. Thermal decomposition of TFTA occurs at 350 °C (in air), producing HNCO and NH_3 and the mixed TFTA-metal nitrates ignite and burn with a flame of ca. 1000 °C. Reaction of the metal nitrates and the decomposition products of TFTA is highly exothermic and formation of mostly perovskite-phase materials occurs instantaneously.

Schwartz and Payne carried out an interesting comparative study of the crystallization behavior of $PbTiO_3$ by three different methods.[32] These methods involved a sol-gel route (lead acetate and titanium isopropoxide), coprecipitation (lead nitrate and titanium tetrachloride), and splat cooling where $PbTiO_3$ was prepared from a molten lead titanate bar. Coprecipitated $PbTiO_3$ crystallized at the lowest temperature of 375 °C (>600 min) followed by sol-gel derived $PbTiO_3$ at 425 °C (>600 min) and rapidly solidified materials at 425 °C (>600 min), but with the presence of multiple phases in the latter case.

4. The Chemistry of Metal–Organic Precursors

4.1. Introduction

The goal of this section is to review the fundamental aspects of the chemistry of metal–organic compounds that are relevant to the reactions discussed in the previous section. As a result, it may be possible to draw some useful conclusions and provide insight into sol-gel metal–organic routes to perovskite-phase materials. Therefore, this discussion is not necessarily limited to the metal–organic complexes of the elements found in perovskite-phase materials but is focused on the relevant metal–organic precursor reaction chemistry in general. Emphasis has been placed on structural and mechanistic aspects of metal–organic precursor chemistry where known. To date, most structural data is derived from solid-state single-crystal X-ray diffraction data. In many cases, these structures are unlikely to be retained in solution, especially where polar and/or coordinating solvents are used. However, discussion of the structural data is useful in providing a data base for the variety of ligand binding modes that can be encountered and for confirmation of empirical and molecular formulae.

The hydrolysis and condensation of metal alkoxide compounds have been extensively reviewed in recent years, and the reader is referred to these articles for a discussion of the details of this topic.[11-25] The hydrolysis

of metal alkoxide compounds is only one aspect of the reaction chemistry that occurs during the formation of mixed metal oxides from liquid-phase routes. The metal–organic precursors used for the preparation of perovskite-phase materials often contain other ligands in place of, or in addition to, alkoxides. For example, metal carboxylates are commonly used as precursors in these systems and are likely to react with other metal alkoxide precursors prior to, during, or subsequent to hydrolysis. Furthermore, in the formation of multicomponent metal oxides, the different metal–organic reagents are often mixed in a solvent (generally an alcohol) prior to hydrolysis. In this section, various aspects of the chemistry relevant to that which occurs in these solutions are discussed in detail.

4.2. Hydrolysis of Metal Alkoxide Compounds

Numerous examples of metal alkoxide compounds exist, and the principles that determine the structures adopted by these species have been addressed.[11,22] In contrast to silicon alkoxide compounds, non-silicate metal alkoxide compounds can exhibit a variety of coordination numbers (2–8) and geometries and readily oligomerize in the absence of other donor molecules to satisfy their coordination number. As a result, the factors which control the evolution of structure and the connections between polymer structure and microstructure in non-silicate metal oxide systems are significantly more complex and poorly understood compared to the silicate system. It is expected that the greater condensation rates of non-silicates establish diffusion-limited conditions, but this has not been well-documented to date, suggesting perhaps that restructuring (to form compact structures) occurs with kinetics commensurate to condensation.

In order to exhibit greater control over the evolution of microstructure, it is desirable to separate the steps of hydrolysis and condensation. In particular, Livage and co-workers have attempted to control the relative rates of hydrolysis and condensation by various synthetic approaches.[125] They emphasize that oligomerization, alcohol interchange, acid/base catalysis, or complexation may be used to slow down hydrolysis and separate nucleation and growth steps in order to achieve monosized powders. For example, titanium alkoxide compounds with primary alkoxide groups are thought to form trimers in alcohol solution with 5-coordinate titanium centers, while those with secondary or tertiary alkoxide ligands remain monomeric due to the greater steric demands of the ligands.[126] Calculations based on the partial charge model[21,127] and electronegativity data indicate that for $[Ti(OR)_4]_n$, where R = Et (n = 4), $\Delta G° = 110$ kJ mol^{-1}, and for R = i-Pr (n = 1) and t-Bu (n = 1), $\Delta G° = 90$ kJ mol^{-1}. This was rationalized by assuming that primary alkoxides are hydrolyzed more easily than secondary or tertiary alkoxide ligands; this difference in energy was attributed to the energy required to break the $[Ti(OR)_4]_3$ trimer. It has been observed that monomeric titanium alkoxide compounds such as $Ti(O-i-Pr)_4$ undergo hydrolysis and condensation simultaneously, leading to polydispersed powders while under similar conditions oligomeric alkoxide compounds such as $[Ti(OEt)_4]_4$ form monosized spherical particles.[128,129] Other authors report that the rate of hydrolysis of metal alkoxide compounds increase in the order primary < secondary < tertiary.[21] This is in

contrast to the assumption made above. However, no definitive study has addressed the kinetic distinction between the rate of hydrolysis of either primary, secondary, and tertiary alkoxide ligands, unambiguously, or alkoxide ligands of different coordination modes namely terminal, doubly bridging, and triply bridging, in non-silicate systems.

Acid or base catalysis can also be used to enable separation of the hydrolysis and condensation steps. It has been demonstrated that acid catalysis increases hydrolysis rates and ultimately crystalline powders are formed from fully hydrolyzed precursors. Base catalysis is thought to promote condensation with the result that amorphous powders are obtained, containing unhydrolyzed alkoxide ligands. For example, monosized particles of pure or doped SnO_2, TiO_2, ZrO_2, Ta_2O_5, and $ZrO_2Al_2O_3$ have been prepared by the hydrolysis of homoleptic metal ethoxide precursors.[130-139] These particles are composed of small crystallites which apparently have undergone an ordered aggregation process. This hierarchical structure is apparent in many non-silicate metal oxide particles. However, the principles described above may not be generally applicable since crystalline metal oxides have been obtained upon basic hydrolysis of metal alkoxides at room temperature.[137]

The paucity of structural data on metal polyoxo–alkoxide species, the likely intermediates in the formation of metal oxides derived from the hydrolysis of unmodified metal alkoxide compounds, reflects the difficulty in characterizing complex mixtures that are likely to be formed in these solutions and in limiting the rates of these reactions. However, a number of species have been isolated and structurally characterized in the solid state. While this information is useful, it is clearly more important to develop methods to characterize such species in solution because the solution structures might be substantially different from those observed in the solid state. An ingenious method was recently reported for the solution structural characterization of $Ti^{(IV)}$ polyoxo–alkoxides derived from the partial hydrolysis of alcohol/toluene solutions of $[Ti(OEt)_4]_4$.[140,141] This technique involves hydrolysis with 40 atom % ^{17}O-enriched H_2O, which results in selective enrichment at the oxide relative to the alkoxide ligands. The denticity of the ^{17}O-enriched oxo ligands was then established through their ^{17}O NMR chemical shift, and the variation in intensity of certain ^{17}O NMR resonances enabled assignment of their connectivity. The mixture of species formed was identified by independent high-yield synthesis and characterization of specific Ti(IV) oxo–alkoxide clusters which included $[Ti_7O_4](OEt)_{20}$, $[Ti_8O_6](OBz)_{20}$ (where Bz = benzyl), and $[Ti_{10}O_8](OEt)_{24}$ (Figures 21–23). The correlation between the solid-state and solution structures of the isolated metal oxo–alkoxides is particularly satisfying. This system also demonstrates the complexity of these reactions wherein it was demonstrated that both $[Ti_7O_4](OEt)_{20}$ and $[Ti_8O_6](OEt)_{20}$ were formed as hydrolysis products of $[Ti(OEt)_4]_4$ and that $[Ti_{10}O_8](OEt)_{24}$ was prepared independently from the reaction between $[Ti_7O_4](OEt)_{20}$ and $[Ti_8O_6](OEt)_{20}$. However, $[Ti_{10}O_8](OEt)_{24}$ was not observed as a product of the hydrolysis of $[Ti(OEt)_4]_4$! Extension of this methodology of solution structure determination in
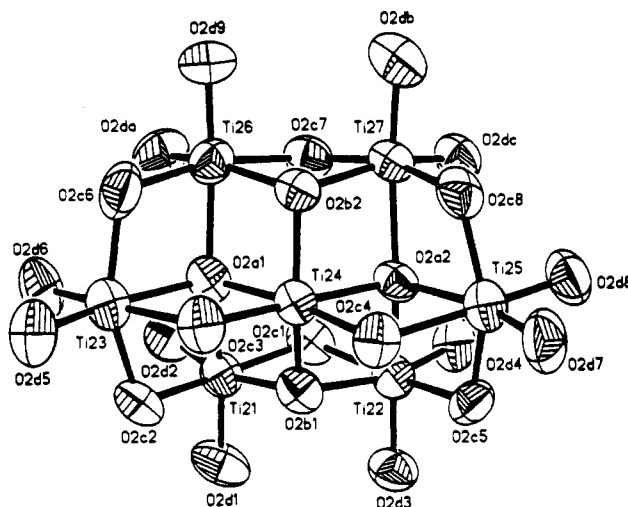
Figure 21. Solid-state structure of $[Ti_7O_4](OEt)_{20}$.
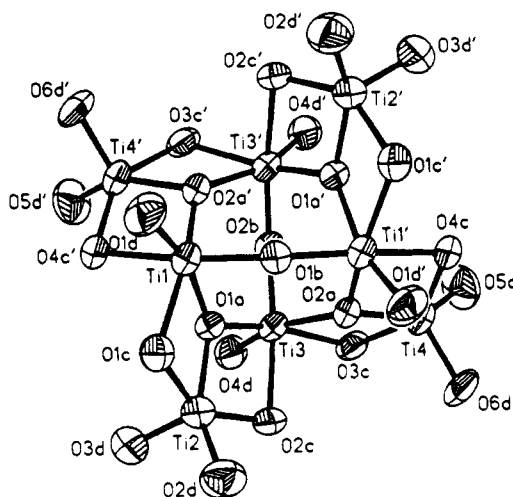
Figure 22. Solid-state structure of $[Ti_8O_6](OBz)_{20}$.
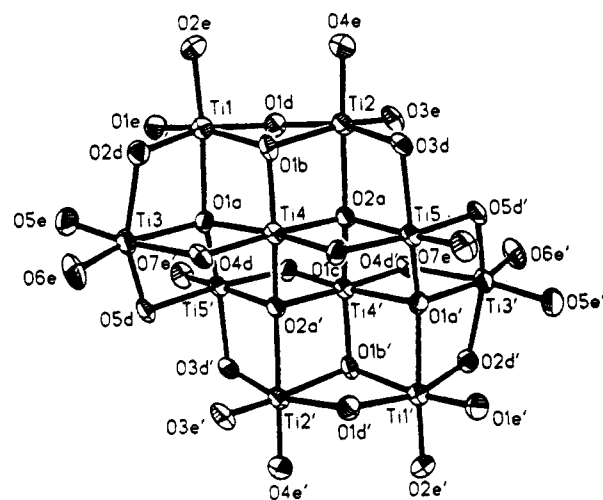
Figure 23. Solid-state structure of $[Ti_{10}O_8](OEt)_{24}$.

perovskite-phase metal titanates would clearly be very interesting.

The only reported oxo–alkoxides of aluminum were formed by the hydrolysis of aluminum alkoxide precursors. The species $Al_4O(O\text{-}i\text{-}Bu)_{11}H$ was isolated from the reaction of aluminum tri-sec-butoxide with isobutyl alcohol containing 150 ppm of water.[142] This species is structurally related to the other aluminum oxo–

◯ = Oxygen, R group omitted

⊘ = μ_4-Oxygen

⬤ = μ_3-Oxygen

◉ = Aluminum

Figure 24. Solid-state structure of $Al_4O(O\text{-}i\text{-}Bu)_{11}H$.

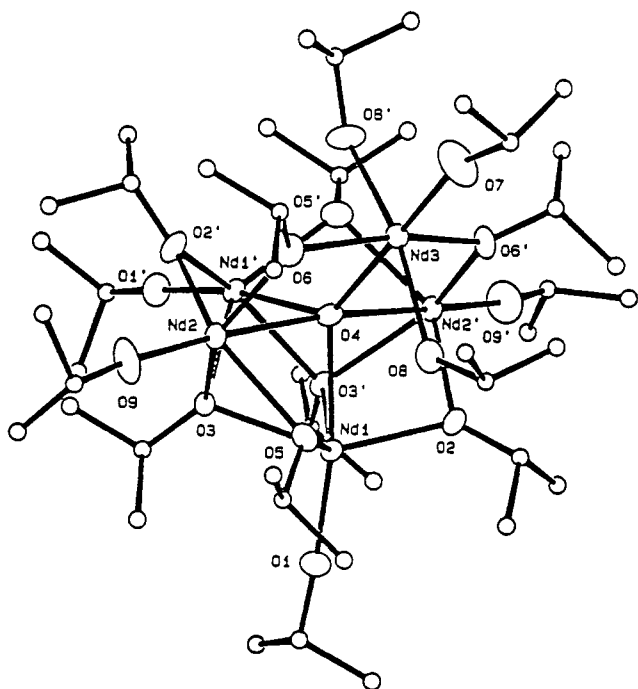**Figure 25.** Solid-state structure of $Al_{10}O_4(OEt)_{22}$.

alkoxide $Al_{10}O_4(OEt)_{22}$ as shown schematically in Figures 24 and 25.[143]

A number of lead oxo–alkoxide compounds have been prepared by a variety of reaction methods. The reaction of alcohols with $Pb[NSi(Me_3)_2]_2$ resulted in isolation of a number of homoleptic lead(II) alkoxide compounds, two of which, $Pb(O\text{-}t\text{-}Bu)_2$ and $Pb(OCH_2CH_2OMe)_2$, were structurally characterized in the solid state by single-crystal X-ray diffraction.[85] However, these species appear to be quite sensitive to the reaction conditions under which they are formed. Their thermal stability appears to be purity-dependent and their decomposition in reaction mixtures is promoted by the presence of water, other impurities, high temperatures, and concentration effects.[85,144,145] In addition, the use of a lead(II) carboxylate as starting material often results in the formation of an oxo–alkoxide product which might arise as a result of ester elimination (see section 4.7). Papiernik et al.[86] report that lead(II) alkoxide compounds decompose on alcoholysis to form the species $Pb_4O(OR)_6$ and $Pb_6O_4(OR)_4$ (Figures 26 and 27). The structure of $Pb_4(\mu^4\text{-}O)(OSiPh_3)_6$ has previously been determined[146] and is analogous to a number of basic metal acetates such as $Be_4(\mu^4\text{-}O)(OAc)_6$[147] and $Zn_4(\mu^4\text{-}O)(OAc)_6$.[148] The compound $Pb_6O_4(O\text{-}i\text{-}Pr)_4$ was structurally characterized in the solid state[149] and is analogous to the structures observed for $Sn_6O_4(OR)_4$, $R = H$, Me.[150,151]

Figure 26. Solid-state structure of $Pb_4O(OR)_6$.

Figure 27. Solid-state structure of $Pb_6O_4(OR)_4$.

Figure 28. Solid-state structure of $Y_5(\mu^5\text{-}O)(\mu^3\text{-}OR)_4(\mu^2\text{-}OR)_4(OR)_5$.

It is also noteworthy that a number of other metal oxo–alkoxide compounds have been isolated and structurally characterized, some of which were originally formulated as homoleptic metal alkoxide compounds. For example the compound formulated as $[Y(O\text{-}i\text{-}Pr)_3]$ appears to be more accurately formulated as $Y_5(\mu^5\text{-}O)(\mu^3\text{-}OR)_4(\mu^2\text{-}OR)_4(OR)_5$ (Figure 28).[152] The reaction of neodymium chips with 2-propanol in the presence of a catalyst resulted in formation the oxo–alkoxide compound $Nd_5(\mu^5\text{-}O)(\mu^3\text{-}OR)_2(\mu^2\text{-}OR)_6(OR)_5(ROH)_2$

Figure 29. Solid-state structure of $Nd_5(\mu^5\text{-}O)(\mu^3\text{-}OR)_2(\mu^2\text{-}OR)_6(OR)_5(ROH)_2$.

(Figure 29).[153] In the absence of a catalyst, no reaction between neodymium and 2-propanol was observed. The use of mercuric chloride as a catalyst can result in a halide transfer reaction, and it has been proposed that mercuric acetate is a better choice. However, the acetate ligand could be responsible for the formation of an oxo-alkoxide species via an ester elimination reaction (see section 4.7). A number of other derivatives display the $M_5O(O\text{-}i\text{-}Pr)_{13}$ structure, M = In, Sc, Yb, even under conditions where exceptional precautions against adventitious hydrolysis were taken.[154]

4.3. Hydrolysis and Condensation of Modified Metal Alkoxide Compounds

Complexation is a method of controlling *condensation* of metal alkoxide compounds through coordination of additional "modifying" ligands, such as carboxylates or β-diketonates, that hydrolyze more slowly than alkoxide ligands.[12,21,155] The choice of the "modifying" ligand is generally determined by the fact that the pK_a of the free modifying acid must be lower than that of the free alcohols corresponding to the alkoxide ligand. This enables thermodynamic distinction between the hydrolysis of the alkoxide ligands and the other type of ligand coordinated to the metal center. The choice of β-diketonate or carboxylate ligands is particularly judicious because of the strength of basicity of the ligand, or the pK_a of the conjugate acid, can be manipulated through substitution to control the conditions under which it is removed. The other feature of the modifying ligands which can be exploited to control the evolution of structure is the preferred coordination mode. In general, β-diketonate ligands predominantly form metal *chelates*,[156] whereas carboxylate ligands have a strong propensity to *bridge* metal centers.[112,157] As a result, it might be anticipated that, in metal alkoxide complexes modified with these ligands, when all the alkoxide (and hydroxide) ligands
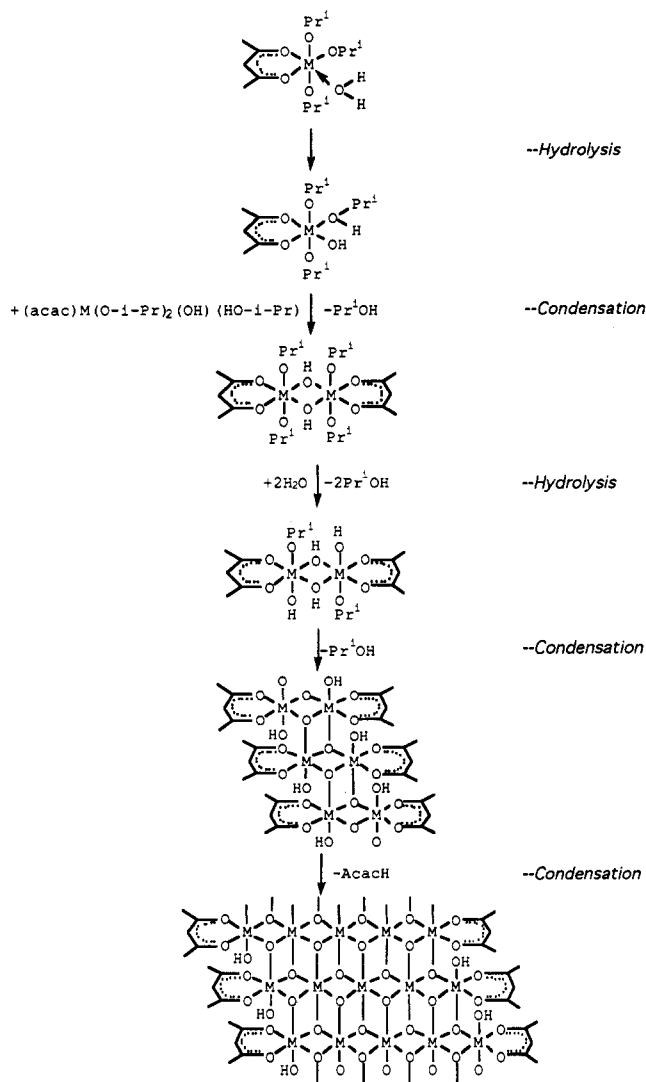

Figure 30. Proposed mechanism for the hydrolysis and condensation of $[Ti(O\text{-}i\text{-}Pr)_3(acac)]$.

have been consumed by hydrolysis and condensation, the β-diketonate ligands can "cap" the surface of the structure[125] (see Figure 30) whereas carboxylate ligands are likely to become "trapped" in the bulk of the material in addition to the surface of the particle. Furthermore, the β-diketonate ligands are likely to be more labile compared to carboxylate ligands and, through reversible dissociation, may be preferential recoordinated at the surface of a growing cluster. This would also account for the loss of β-diketonate ligands observed during some reactions.

It has been observed that, whereas hydrolysis of $Ti(O\text{-}i\text{-}Pr)_4$ is very rapid and leads to formation of polydisperse 10–20-nm particles, hydrolysis of $[Ti(O\text{-}i\text{-}Pr)_3(acac)]$[158,159] results in formation of a three-dimensional colloidal sol consisting of $\sim$5 nm particles, and hydrolysis of $(acac)_2Ti(O\text{-}i\text{-}Pr)_2$ results in formation of weakly branched polymers which may be useful precursors for formation of fibers. Hydrolysis and condensation of $[Ti(O\text{-}i\text{-}Pr)_3(acac)]$ was studied by a variety of spectroscopic techniques including NMR, IR, Xanes, and EXAFS.[158,159] The results showed that hydrolysis was essentially complete for a H_2O:Ti ratio of 3 and some acac ligands were present even when a large excess of water was used. The proposed mech-
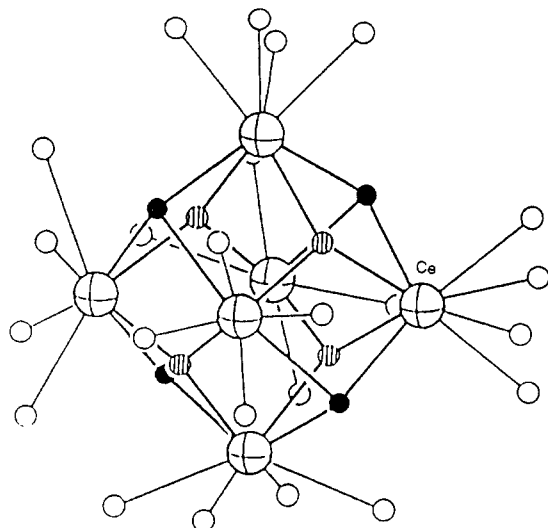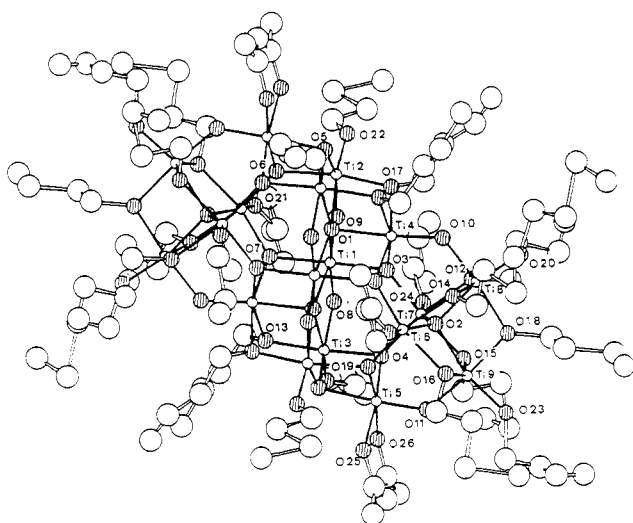
Figure 31. Solid-state structure of $Ce_6O_4(OH)_4(acac)_{12}$.

Figure 32. Solid-state structure of $[Ti_{18}O_{22}(O\text{-}n\text{-}Bu)_{26}(acac)_2]$.

anism for the nucleation and growth of this material is shown in Figure 30.

Gradually, quantitative data are emerging concerning the progressive structural evolution in these modified metal alkoxide systems. The hydrolysis of $Ce_2(O\text{-}i\text{-}Pr)_4(acac)_4$ resulted in isolation of the species Ce_6O_4-$(OH)_4(acac)_{12}$, which was structurally characterized by single crystal X-ray diffraction.[160–162] The structure is shown in Figure 31. Hydrolysis of $Ti(O\text{-}n\text{-}Bu)_{4-x}(acac)_x$ resulted in the isolation of the species $[Ti_{18}O_{22}(O\text{-}n\text{-}Bu)_{26}(acac)_2]$. This species was also structurally characterized in the solid state (Figure 32).[163] The acetate-modified metal alkoxide compound $Ti_2(OR)_6(OAc)_2$ has been prepared and, via ester elimination reactions (see section 4.7), the oxo–acetate compound $Ti_6O_4(OAc)_4$ was isolated (Figure 33). A variety of species were proposed as intermediates in the formation of this material.[162,164]

4.4. Mixed-Metal Species as Precursors

4.4.1. Homoleptic Mixed-Metal Alkoxide Species

The synthesis, structural principles, and reactivity of heterometallic alkoxide compounds were recently extensively reviewed.[25] The species that are noteworthy
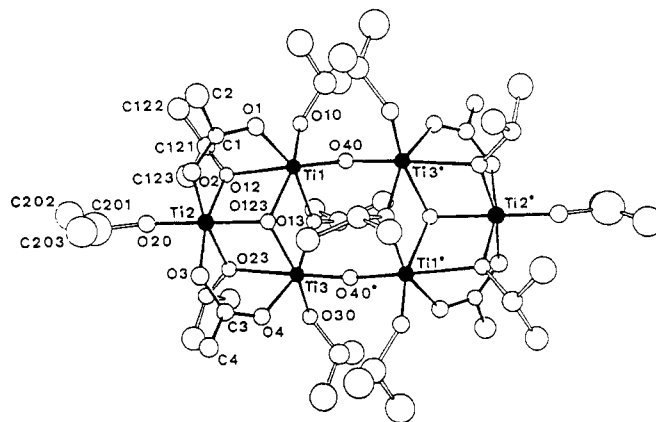

Figure 33. Solid-state structure of $Ti_6O_4(OAc)_4$.

in this context are those that have the correct stoichiometry for the formation of a perovskite-phase material (or a component of one), and those that provide insight into the rational design of such precursors. Mixed-metal alkoxide complexes of a large number of elements have been prepared, notably by Mehrotra et al.[165]

A number of strategies have been explored for the formation of mixed-metal alkoxide compounds with a particular, desired stoichiometry. The most common strategy is to simply mix the parent metal alkoxide compounds and rely on their acid–base behavior (eq 33). While this strategy has resulted in formation of

$$xM(OR)_m + M'(OR')_n \rightarrow M_xM'(OR)_m(OR')_n \quad (33)$$
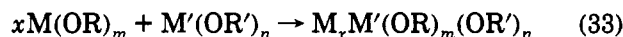
a number of valuable species, there is little control over these reactions. A classic example of a useful "single-component" precursor to a perovskite-phase ceramic material is $LiNb(OEt)_6$. This species is prepared by simply refluxing an ethanol solution of lithium ethoxide and niobium ethoxide in the correct ratio.[166] Spectroscopic evidence has been presented that a single species is formed in these solutions,[167] and recently the solid-state structure of this material was obtained (Figure 34).[168] The structure consists of 1-dimensional infinite helical polymers of niobium octahedra linked via one edge through tetrahedral lithium. In numerous studies, solutions of this compound have been hydrolyzed to form high-quality $LiNbO_3$ films and powders.[80–82]

Two barium zirconium alkoxide compounds have been prepared via the reaction of either Ba metal or $Ba[N(SiMe_3)_2]_2(THF)_2$ with $Zr_2(O\text{-}i\text{-}Pr)_8(HO\text{-}i\text{-}Pr)_2$.[167] The compound $[BaZr_2(O\text{-}i\text{-}Pr)_{10}]_2$ was characterized in the solid-state by single-crystal X-ray diffraction (Figure 35), where the two Zr_2 cores characteristic of $Zr_2(O$-$i\text{-}Pr)_8(HO\text{-}i\text{-}Pr)_2$ remain intact and are bridged by two barium atoms. The barium centers are then bridged by isopropoxide ligands. The species $Ba[Zr_2(O\text{-}i\text{-}Pr)_9]_2$ is believed to have a similar structure, in which two $[Zr_2(O\text{-}i\text{-}Pr)_9]^-$ groups surround one 8-coordinate Ba ion, although the X-ray data could not be satisfactorily refined. The preparation of various other relevant mixed-metal alkoxides have been claimed including $KNb(OR)_5$, R = Et and n-Pr,[170] $BaTi(OR)_6$,[171] Mg-$[Al(OR)_4]_2$,[172] $Mg[Nb(OEt)_6]_2$,[89] $ZnSn(OEt)_6$,[137] $PbZr$-$(OEt)_6$,[173] $BaTi(OCH_2CH_2OMe)_6$,[74] and $Zn[Nb(OEt)_6]_2$,[89] but their structures either in solution or in the solid state have not been unambiguously established.

One flaw associated with this strategy is that the formation of mixed-metal alkoxides is at the mercy of
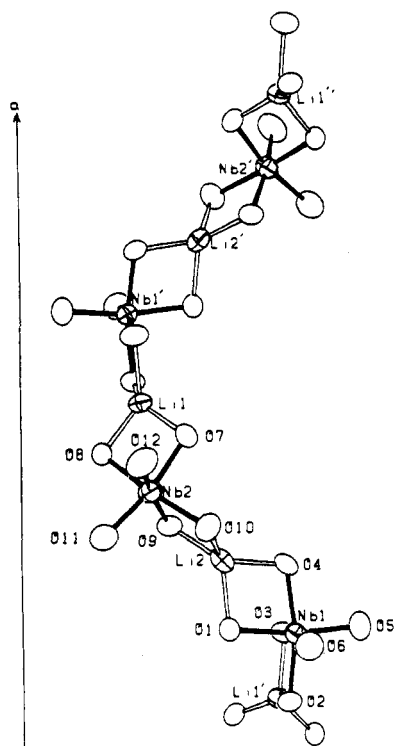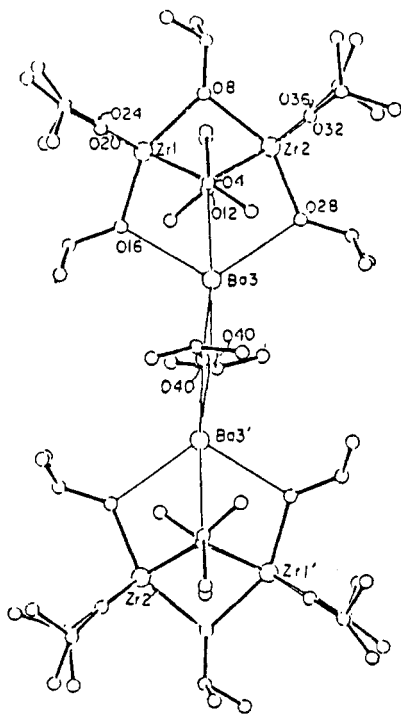
Figure 34. Solid-state structure of $LiNb(OEt)_6$.

Figure 35. Solid-state structure of $[BaZr_2(O\text{-}i\text{-}Pr)_{10}]_2$.

thermodynamic control and the factors which influence the product distribution are not well-understood. This limitation is illustrated by the reaction of a 1:1 ratio of $Sr(O\text{-}i\text{-}Pr)_2$ with $Ti(O\text{-}i\text{-}Pr)_4$ in $HO\text{-}i\text{-}Pr$/toluene, which yields $Sr_2Ti(O\text{-}i\text{-}Pr)_8(HO\text{-}i\text{-}Pr)_5$ as the only mixed metal alkoxide product.[174] This species was characterized in the solid state and the structure is shown in Figure 36.

Another strategy that has been explored for the preparation of homoleptic mixed-metal alkoxide compounds is the salt-elimination reaction in which a mixed-metal alkoxide compound, where one of the metal ions is exchangeable, is reacted with another metal halide
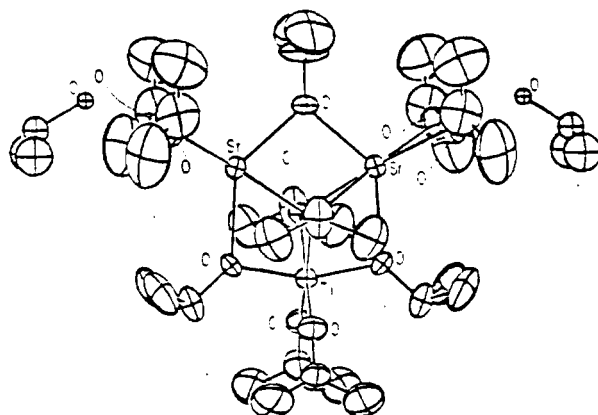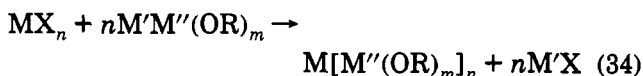

Figure 36. Solid-state structure of $Sr_2Ti(O\text{-}i\text{-}Pr)_8(HO\text{-}i\text{-}Pr)_5$.

to eliminate a metal halide (salt) according to the stoichiometry of eq 34. Although this reaction method

$$MX_n + nM'M''(OR)_m \rightarrow$$
$$M[M''(OR)_m]_n + nM'X \quad (34)$$

has been used to form a large variety of mixed-metal alkoxide compounds, it is a rather poor strategy for the synthesis of specific stoichiometry products. This method relies on (i) the formation of a species, $M'M''(OR)_m$, of appropriate stoichiometry and (ii) control over stoichiometry of the "ion exchange" reaction. In many cases metal halide containing products have been isolated from incomplete reactions,[25] although it may be possible to replace the halide with an alkoxide in a subsequent metathesis step. In a number of cases, and probably in many more than have been reported in the literature, no reaction occurs when a mixed alkali metal alkoxide compound (i.e. M' = Li, Na, K) is reacted with a metal halide. This is probably the result of the covalent nature of metal alkoxide compounds and the strong desire for ions that are typically considered as exchangeable, such as Li, Na, K, for hard donors such as the oxygen atoms of alkoxide ligands. A number of mixed-metal homoleptic alkoxide compounds containing alkali metals have been structurally characterized in the solid state.[167,108,175,176] They typically show that the alkali metal is coordinated to alkoxide oxygen atoms sometimes even in the presence of a donor solvent.
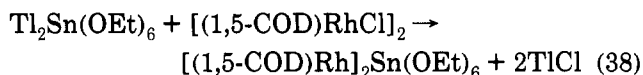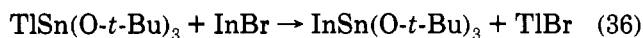
There are a number of obvious methods for circumventing this problem. One is to use a stronger donor to sequester the alkali metal center and attempt to generate a more ionic reagent. When recrystallized from polydentate oxygen donor solvents, the solvent often sequesters the alkali metal as in the case of $K(\eta^2\text{-}DME)_3(\eta^1\text{-}DME)][Y(OSiPh_3)_4(\eta^2\text{-}DME)]$, where the potassium ion exists in a 7-coordinate environment of oxygen ions of 1,2-dimethoxyethane (DME).[177] Another example is shown in eq 35.[25] However, it is quite likely

$$LiV(OR)_4 \cdot THF + 12\text{-crown-4} \rightarrow$$
$$[Li(12\text{-crown-4})]^+[V(OR)_4]^- \quad (35)$$
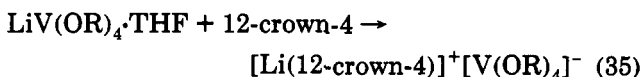
that the alkoxide oxygen atoms are at least as efficient as classical reagents such as crown ethers at sequestering alkali metal cations.

Another method of inducing a salt elimination reaction is to use a large, soft, polarizable cation[178] that

has a lower affinity for oxygen donors or which forms particularly insoluble salts. Thallium is a good choice for such reactions and has been shown to result successfully in ion-exchange reactions particularly for tin(II)[179] and tin(IV) alkoxide[137,176] compounds according to the examples shown in eqs 36–38.

$$TlSn(O\text{-}t\text{-}Bu)_3 + InBr \rightarrow InSn(O\text{-}t\text{-}Bu)_3 + TlBr \quad (36)$$

$$Tl_2Sn(OEt)_6 + ZnCl_2 \rightarrow ZnSn(OEt)_6 + 2TlCl \quad (37)$$

$$Tl_2Sn(OEt)_6 + [(1,5\text{-}COD)RhCl]_2 \rightarrow$$
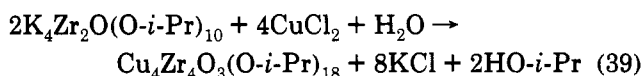$$[(1,5\text{-}COD)Rh]_2Sn(OEt)_6 + 2TlCl \quad (38)$$

4.4.2. Mixed-Metal Oxo–Alkoxide Compounds

A number of methods for the preparation of mixed metal oxo–alkoxide compounds have been reported. Some methods are designed to form these species intentionally and some are accidental. One reaction that leads to formation of these species in particular is the reaction between a metal alkoxide and a metal carboxylate compound with the elimination of an ester. A separate section is devoted to the discussion of this reaction (section 4.7). Where metal oxo–alkoxide species are formed unintentionally, the origin of the oxo group is not necessarily known. This will be pointed out where possible.

Controlled hydrolysis of homoleptic mixed metal alkoxide compounds is an obvious method for the formation of mixed metal oxo–alkoxide compounds. However, there are very few examples of these reactions. A notable recent example is the partial hydrolysis of a 2-methoxyethanol solution of $BaTi(OCH_2CH_2OMe)_6$ which after 2 months produced colorless, transparent crystals in 30% yield.[74] Analytical, spectroscopic, and X-ray diffraction data showed this species to be $Ba_4Ti_{13}O_{18}(OCH_2CH_2OMe)_{24}$ in which the Ba:Ti stoichiometry was different than the overall solution stoichiometry. The solid-state structure of this rather complicated molecule is shown in Figure 37.

Reaction of 2 equiv of KH or $KN(SiMe_3)_2$ with $Zr_2(O\text{-}i\text{-}Pr)_8(HO\text{-}i\text{-}Pr)_2$ resulted in formation of $K_4Zr_2O(O\text{-}i\text{-}Pr)_{10}$ in which the oxygen atom occurs at the center of an octahedron of metal atoms.[180] This product appears not to be derived from the double protonation of the coordinated alcohol ligand, and extensive precautions were taken against impurity contamination (i.e. KOH in the KH or surface adsorbed water on the glassware). Significantly, no propene or diisopropyl ether were observed on reaction of KH with $Zr_2(O\text{-}i\text{-}Pr)_8(HO\text{-}i\text{-}Pr)_2$, but propane, isopropyl alcohol, and a trace of acetone were observed. As a result of these observations and a labeling study using KD, it was proposed that oxygen abstraction occurred at the $(\mu^3\text{-}O\text{-}i\text{-}Pr)$ ligand.

The oxo–alkoxide species $K_4Zr_2O(O\text{-}i\text{-}Pr)$ (Figure 38) undergoes a salt elimination reaction with copper(II) chloride in the presence of water according to eq 39 to give the species $Cu_4Zr_4O_3(O\text{-}i\text{-}Pr)_{18}$.[181]

$$2K_4Zr_2O(O\text{-}i\text{-}Pr)_{10} + 4CuCl_2 + H_2O \rightarrow$$
$$Cu_4Zr_4O_3(O\text{-}i\text{-}Pr)_{18} + 8KCl + 2HO\text{-}i\text{-}Pr \quad (39)$$

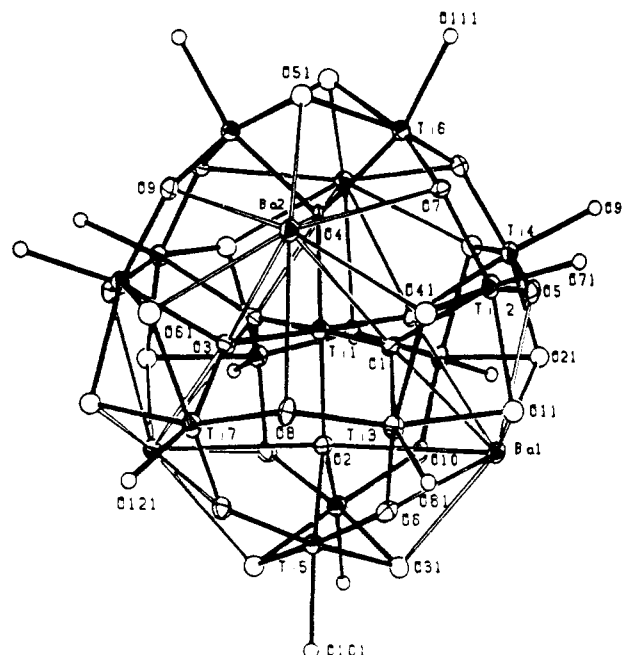A number of bismuth oxo–alkoxide compounds have been prepared by the reaction of alkali-metal alkoxides

Figure 37. Solid-state structure of $Ba_4Ti_{13}O_{18}(OCH_2CH_2OMe)_{24}$.

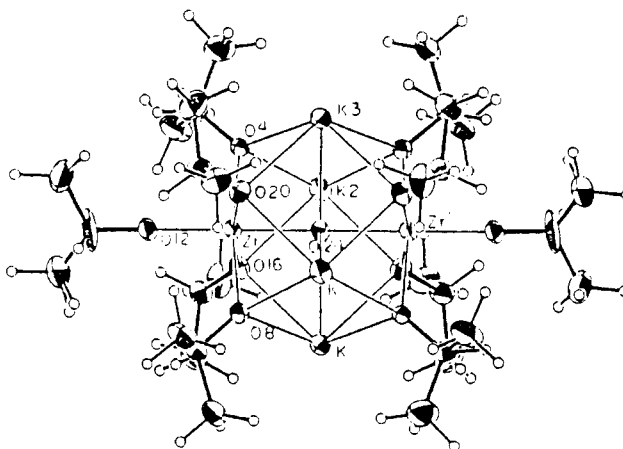**Figure 38.** Solid-state structure of $K_4Zr_2O(O\text{-}i\text{-}Pr)_{10}$.

with bismuth halides.[182] For example, whereas $BiCl_3$ reacts with 3 equiv of $Na(O\text{-}CH(CF_3)_2)$ in THF results in formation of $[Bi(OCH(CF_3)_2(THF)]_2$, the reaction of $BiCl_3$ with $NaOC_6F_5$ results in formation of a variety of different species, depending upon the origin of alcohol from which the salt was made. From this reaction, the species, $NaBi_3(\mu^4\text{-}O)(OR)_8(THF)$, $Bi_6(\mu^3\text{-}O)_4(\mu^3\text{-}OR)\{(\mu^3\text{-}O)Bi(OR)_4\}_3$, $NaBi_4(\mu^3\text{-}O)_2(OR)_9$, and $Na_2Bi_4(\mu^3\text{-}O)_2(OR)_{10}$ have been isolated and structurally characterized. Two examples are given in Figures 39 and 40.

A number of mixed-metal oxo–alkoxide compounds have been prepared by the reaction of metal alkoxide compounds with metal oxo–alkoxide compounds. For example, $Pb_6Nb_4(\mu^4\text{-}O)_4(\mu^3\text{-}OEt)_4(\mu^2\text{-}OEt)_{12}(OEt)_8$ (Figure 41) was prepared in 46% yield from the reaction between $Pb_4O(OEt)_6$ and $Nb_2(OEt)_{10}$ in ethanol at room temperature.[183] This complex can be viewed as a Lewis acid/base adduct of the lead(II) oxo–alkoxide with $Nb(OEt)_5$ monomers coordinated to four faces of the octahedron. However, in solution, [207]Pb NMR and IR spectroscopy reveal that, even in nonpolar solvents such as toluene, a variety of species are formed, and it is
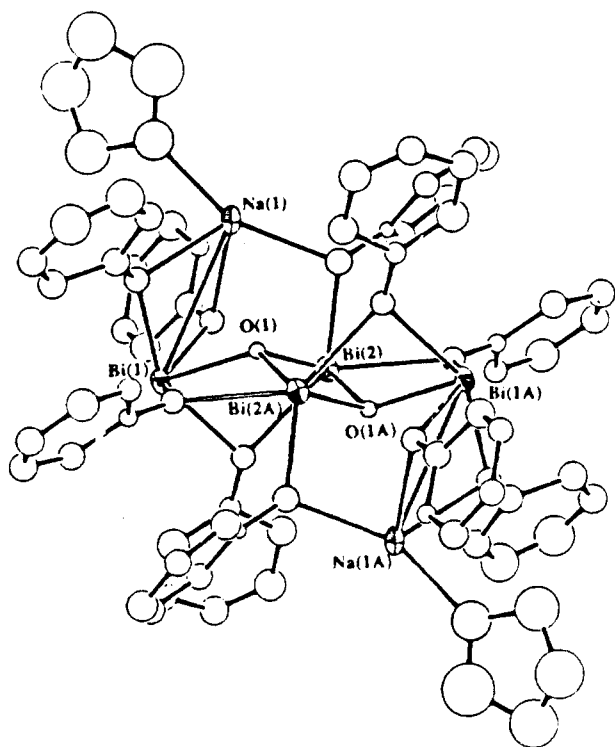
Figure 39. Solid-state structure of $Na_2Bi_4(\mu^3\text{-}O)_2(OR)_{10}$, R $= C_6F_5$.
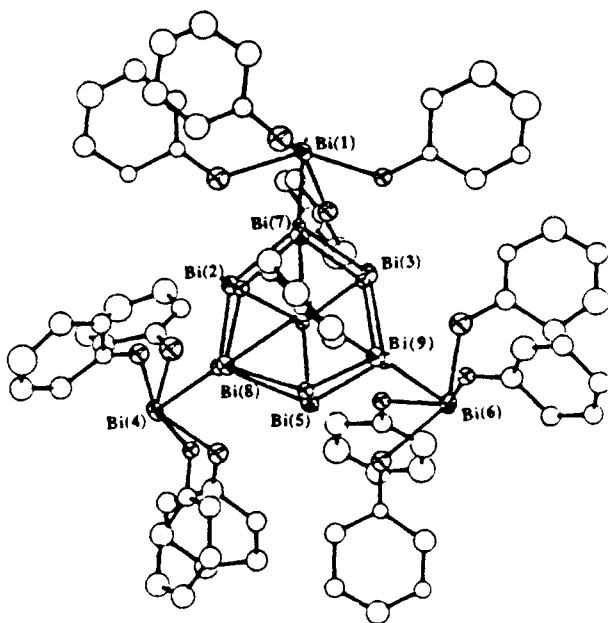
Figure 40. Solid-state structure of $Bi_6(\mu^3\text{-}O)_4(\mu^3\text{-}OR)\{\mu^3\text{-}O\text{-}Bi(OR)_4\}_2(THF)_2$, R $= C_6F_5$.

believed that this heterometallic species dissociates in solution.

4.4.3. Mixed-Metal Alkoxide–Carboxylate Compounds

The reaction of lead(II) and zinc(II) acetates in a 3:1 molar ratio in 2-methoxyethanol at 124 °C resulted in formation of the mixed-metal compound Pb_2Zn_2-$(OAc)_4(OCH_2CH_2OMe)_4$ in which the solvent had reacted and been incorporated in the coordination sphere of the metals.[185,186] A single-crystal X-ray diffraction study revealed that the zinc ions were 4-coordinate and the lead(II) ions were 6-coordinate with a stereochemically active lone pair as shown in
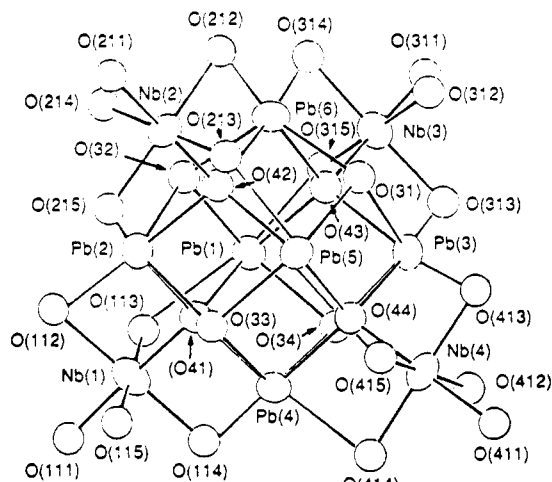

Figure 41. Solid-state structure of $Pb_6Nb_4(\mu^4\text{-}O)_4(\mu^3\text{-}OEt)_4(\mu^2\text{-}OEt)_{12}(OEt)_8$.
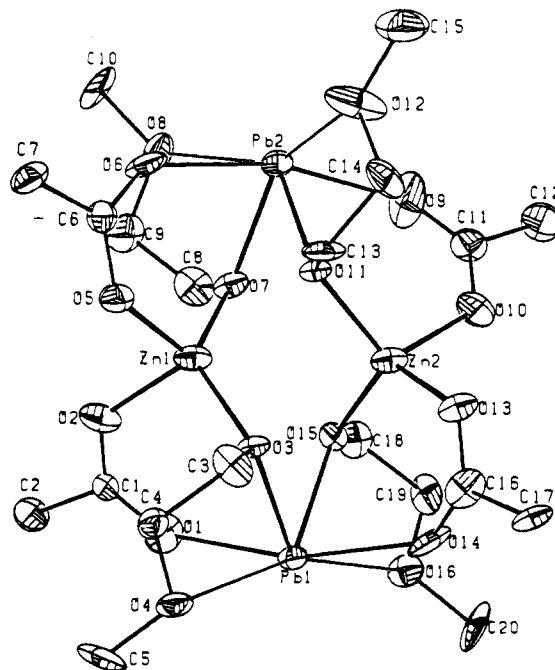

Figure 42. Solid-state structure of $Pb_2Zn_2(OAc)_4$-$(OCH_2CH_2OMe)_4$.

Figure 42. Further reaction with niobium alkoxide compounds resulted in formation of $Pb(Zn_{0.33}Nb_{0.66})O_3$, PZN.[127] The reaction of $Pb_4O(OAc)_6\cdot H_2O$ with $Ti(O\text{-}i\text{-}Pr)_4$ in a 1:1 Pb:Ti ratio in refluxing ethanol resulted in formation of a mixed-metal complex with a Pb to Ti ratio of 2:1 with empirical formula $Pb_2Ti_4(\mu^4\text{-}O)_2(\mu\text{-}OEt)_8(OEt)_6(OAc)_2$.[184] The compound was structurally characterized in the solid state (Figure 43).

4.5. Metal Alkoxide Compounds with Multidentate Ligands

There has been growing interest in the use of multidentate solvents and/or metal–organic precursors which contain multidentate ligands. In particular the use of polyether alcohols as solvents and polyether alkoxides as ligands has seen rapid growth in recent years. The rationale behind the use of such solvents or ligands is that, through chelate effects, it is thought likely that these ligands are removed less easily by hydrolysis and may impart solubility to a growing metal
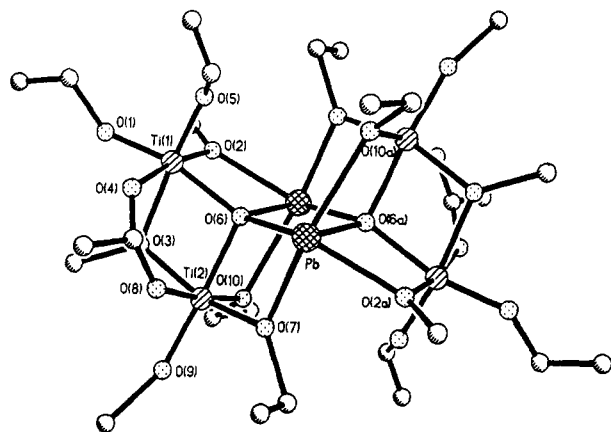
Figure 43. Solid-state structure of $Pb_2Ti_4(\mu^4\text{-}O)_2(\mu\text{-}OEt)_8\text{-}(OEt)_6(OAc)_2$.

oxide cluster extending the time to the gel point. It is likely that, when many metal alkoxide compounds are dissolved in such multifunctional alcohol solvents, alcoholysis reactions occur, leading to the formation of new species perhaps prior to hydrolysis and condensation reactions. Here we review the structural and solution chemistry of metal alkoxide compounds in which the alkoxide ligand contains additional functional groups to investigate the molecular basis for this hypothesis. Specific attention is given to ether and amine functionalities because they have been used in the preparation of mixed-metal oxides.

Buhro and co-workers have been most prolific in the preparation and characterization of metal polyether alkoxide species. Their rationale for the synthesis of these complexes has been to investigate whether the ether oxygens can coordinate and reduce the tendency for oligomerization and as a result improve solubility. An additional bonus of this strategy is that, if successful, a low degree of oligomerization will also improve vapor pressure and the same species might also be useful as precursors for vapor-phase synthetic routes to metal or metal oxide films. The compounds $Cu(OR)_2$, where R = CH_2CH_2OMe or $CH_2CH_2OCH_2CH_2OMe$ and for comparison $(CH_2)_6Me$, were prepared by the alcoholysis of copper(II) methoxide shown in eq 40.[187] The

$$Cu(OMe)_2 + 2HOR \rightarrow Cu(OR)_2 + 2HOMe \qquad (40)$$
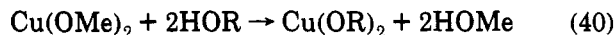
compounds $Cu(OCH_2CH_2OMe)_2$ and $Cu(O(CH_2)_6Me)_2$ were found to be insoluble in a range of organic solvents including benzene, toluene, THF, hexane and 2-methoxymethanol. However, $Cu(OCH_2CH_2OCH_2CH_2OMe)_2$ was soluble in benzene, but cryoscopic molecular weight determination conformed to a degree of aggregation greater than 5. The ^1H NMR spectrum provided insight into the solution structure of this compound where only one ^1H resonance ascribed to a methylene group was highly shifted and broadened, consistent with close proximity to a paramagnetic center. The remaining ^1H resonances were progressively less paramagnetically shifted from their expected isotropic, diamagnetic chemical shifts. In considering the two limiting structures for this molecule, in which the polyether oxygen atoms are either coordinated or not coordinated to the copper(II) center, the structure in which none of the ether oxygens are coordinated (on the NMR time scale) seems most appropriate (Figure 44). Replacement of
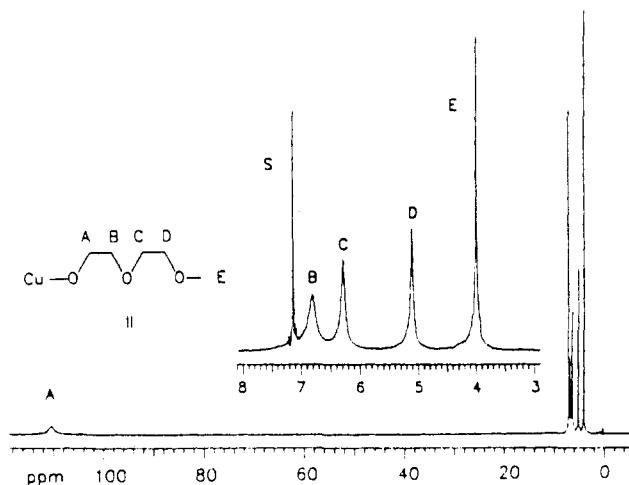

Figure 44. Proposed solution structure for $Cu(OCH_2\text{-}CH_2OCH_2CH_2OMe)_2$ based on ^1H NMR data.
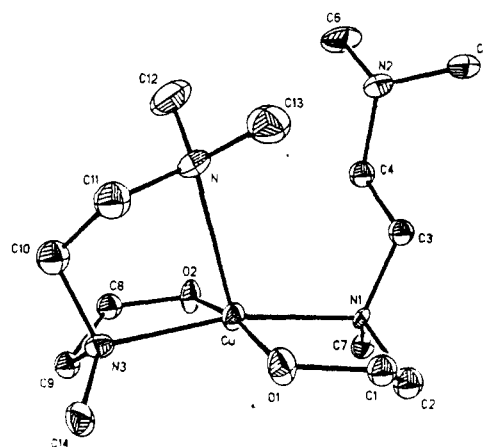
Figure 45. Solid-state structure of $Cu(OCH_2CH_2\text{-}N(Me)CH_2CH_2NMe_2)_2$.
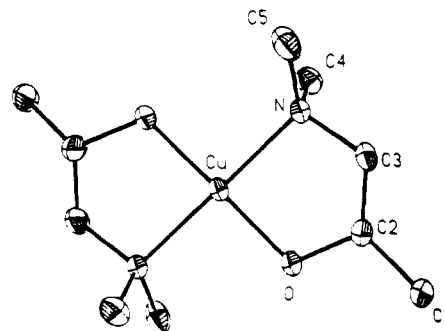
Figure 46. Solid-state structure of $Cu(OCH(Me)CH_2NMe_2)_2$.

the oxygen donors in the polyether ligands with more basic amino groups resulted in the isolation of a number of monomeric, volatile metal alkoxide compounds, $Cu(OR)_2$, where R = $CH_2CH_2NMe_2$, $CH(Me)CH_2NMe_2$, and $CH_2CH_2N(Me)CH_2CH_2NMe_2$.[188] The solid-state structure of two of these species confirmed the notion that the amino group is coordinated to the metal center and results in the observed decrease in oligomerization compared to the ether analogues (Figures 45 and 46).

A number of other metal 2-methoxyethoxide complexes have been isolated and structurally characterized. Lead(II) bis(2-methoxyethoxide) crystallizes as a 1-dimensional infinite polymer with 4-coordinate lead centers where the potentially chelating ligands do not coordinate but adopt dangling conformations.[85] The

Figure 47. Solid-state structure of $Pb(OCH_2CH_2OMe)_2$.

Figure 48. Solid-state structure of $Bi(OCH_2CH_2OMe)_3$.

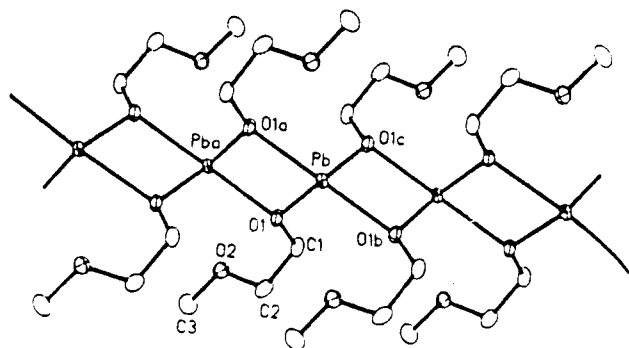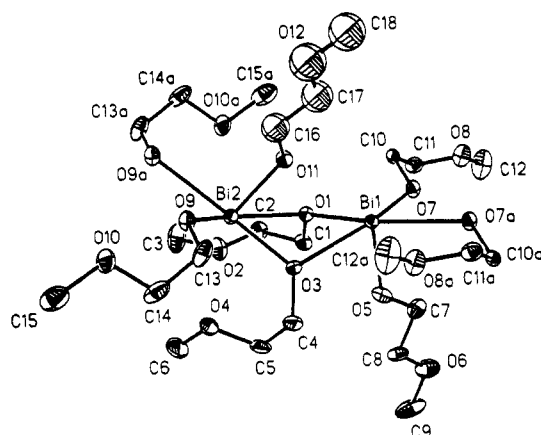**Figure 49.** Solid-state structure of $Ca_9(OCH_2CH_2-OMe)_{18}(HOCH_2CH_2OMe)_2$.

Figure 50. Solid-state structure of $[Y(OCH_2CH_2OMe)_3]_{10}$.

geometry about lead(II) is approximately trigonal bipyramidal, assuming one of the coordination sites is occupied by a stereochemically active lone pair, as shown in Figure 47. The compound $Pb(OCH(Me)CH_2NMe_2)_2$ was also prepared in this study and found to exhibit a molecularity of 1.3 in benzene solution.

The compounds $Bi(OR)_3$, R = i-Pr, CH_2CH_2OMe, $CH_2CH_2NMe_2$, $CH(Me)CH_2NMe_2$, and CMe_2Et, were prepared by alcoholysis of $Bi(NMe_2)_3$.[189] While the low solubility of $Bi(O-i-Pr)_3$ precluded a cryoscopic molecular weight determination in benzene and is likely to be consistent with the presence of an oligomer, the remaining compounds were found to be dimeric (R = CH_2CH_2OMe), or approximately monomeric, in benzene solution. However, a solid-state structural study of $Bi(OCH_2CH_2OMe)_3$ revealed the presence of a 1-dimensional infinite polymer in which the Bi center is approximately octahedral, assuming the presence of a stereochemically active lone pair in the vacant coordination site, and none of the ether oxygen atoms are coordinated to the metal center (Figure 48). A different structure must be adopted in solution since a molecular complexity of 2.1 was measured and this species was readily soluble in a variety of common organic solvents. In solution, the change in degree of aggregation could be derived from the coordination of the ether oxygen atoms to the metal center.

Interestingly the polyether alkoxides $Ba(OR)_2$, where R = $CH_2CH_2OCH_2CH_2OMe$ and $CH_2CH_2OCH_2CH_2-OCH_2CH_2OMe$, were proposed to adopt a structure in which the ether oxygen atoms are chelated to the metal center, as determined by their monomeric nature, their NMR and mass spectra, and their high solubility in common organic solvents.[190] These species were prepared from the reaction of barium metal with the
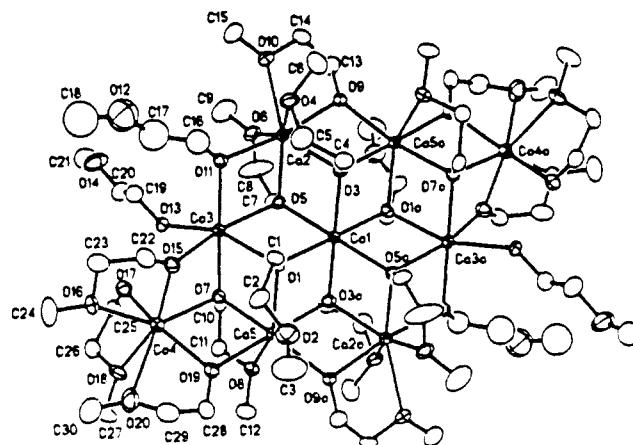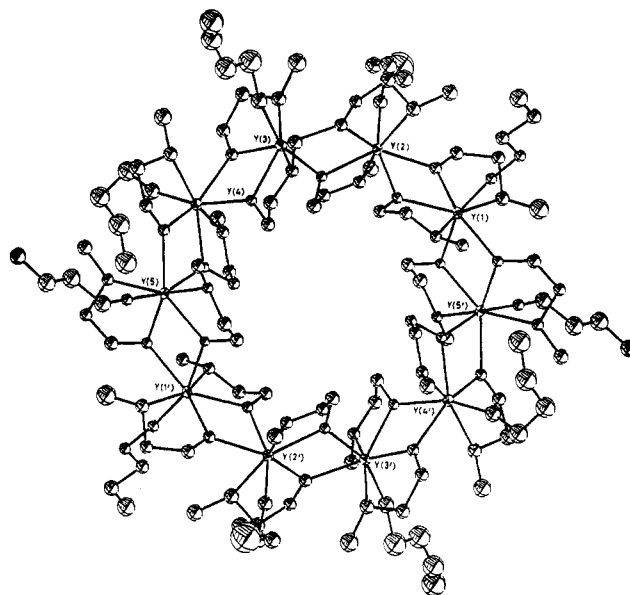
corresponding alcohol according to eq 41 and exist as liquids at room temperature.

$$Ba + 2HOR \rightarrow Ba(OR)_2 + H_2 \qquad (41)$$

The calcium and yttrium derivatives of 2-methoxyethanol were both prepared by the reaction of the metal with an excess of the alcohol and formed high nuclearity species, $Ca_9(OCH_2CH_2OMe)_{18}(HOCH_2CH_2OMe)_2$[191] and $[Y(OCH_2CH_2OMe)_3]_{10}$.[192] These structures are shown in Figures 49 and 50. In contrast to the other structures described above, $Ca_9(OCH_2CH_2OMe)_{18}(HOCH_2CH_2-OMe)_2$ exhibits a structure in which all but two of the ether oxygens are chelated to the Ca centers. In addition there are two coordinated, but nonchelated, alcohols. A similar phenomenon was observed for the yttrium derivative where only one of the three alkoxide ligands for each yttrium atom is *not* chelated. The structure of $[Y(OCH_2CH_2OMe)_3]_{10}$ is quite unusual in that (i) the yttrium coordination number is 7, which is higher than that observed in some phases of Y_2O_3,[31] and (ii) the structure adopted bears no relation to a close-packed structure which is likely to maximize enthalpy while minimizing entropic considerations. On the other hand, the structure of $Ca_9(OCH_2-$
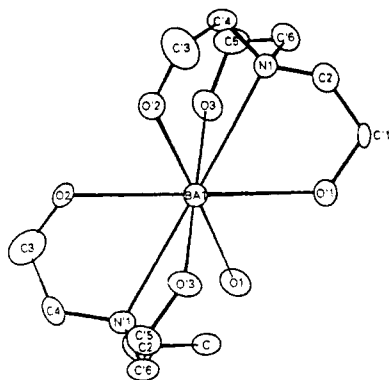
Figure 51. Solid-state structure ofBa[(OCH₂CH₂)N(CH₂-CH₂OH)₂]₂·2EtOH.

CH₂OMe)₁₈(HOCH₂CH₂OMe)₂ was likened to that of CdI₂. It was proposed that the structures adopted by metal alkoxide aggregates are likely to be a subtle trade off between the enthalpic driving force to attain coordinative saturation and the loss in translational entropy. These ideas corroborate Bradley's structural theory, which was based on empirical arguments. Oligomerization should proceed to the point at which coordinative saturation of the metal is satisfied in the absence of other complications. However, the conditions under which 2-methoxyethoxide ligands chelate rather than dangle and other donor ligands such as the free alcohol are used to satisfy the metal coordination environment are not clear at this stage. Furthermore, the reason why enthalpic considerations dominate entropic considerations in the case of the yttrium derivative and represent an exception to the structure theory are not clear.

A number of alcohol amine complexes of metals relevant to this review have been isolated and characterized. Ethanolamine ligands typically chelate and this is demonstrated by the complex [Cu(OCH₂-CH₂NH₂)(SCN)], which exists as a polymer in the solid state through bridging thiocyanate ligands.¹⁹³ Triethanolamine has been used extensively as a solvent in sol–gel processing, but few discrete complexes have been isolated and characterized unambiguously. The tin(IV) compound Sn[(OCH₂CH₂)₂N(CH₂CH₂OH)]₂ has been structurally characterized in two different crystalline modifications, both of which exhibit 6-coordinate, octahedral tin(IV) environments with four alkoxide and two nitrogen donor ligands.¹⁹⁴,¹⁹⁵ The compound Ba[(OCH₂CH₂)N(CH₂CH₂OH)₂]₂·2EtOH was recently prepared¹⁹⁶ from the reaction of Ba and triethanolamine and structurally characterized in the solid state (Figure 51). In this case, with the larger Ba(II) ion compared to Sn(IV), the triethanolamine ligands are each tetradentate resulting in a coordination number of 8. However, the 8-coordinate Ba units are associated through intermolecular hydrogen bonding arising from the ethanol lattice molecules resulting in formation of a two dimensional network.

In an analogous reaction, Ba granules were mixed with 2,6-di-*tert*-butylphenol using gaseous ammonia as a catalyst to form the unexpected product Ba(2,6-(*tert*-Bu)₂C₆H₃O)₂(HOCH₂CH₂NMe₂)₄.¹⁹⁷ It was proposed that the 2-(dimethylamino)ethanol ligand was generated in situ on the basis of the Ba-induced cleavage of THF that had previously been observed to produce
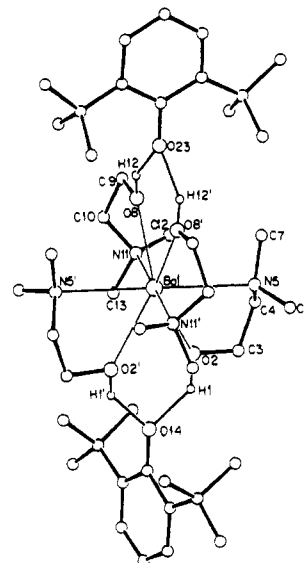
Figure 52. Solid-state structure of Ba(2,6-(*t*-Bu)₂C₆-H₃O)₂(HOCH₂CH₂NMe₂)₄.
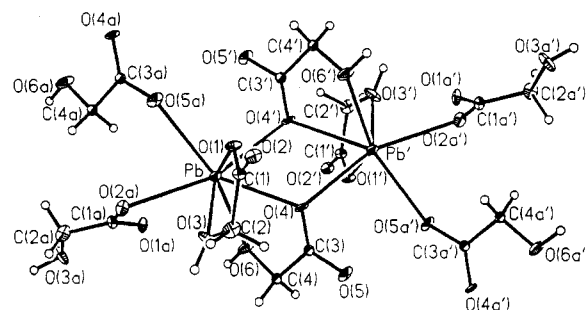
Figure 53. Solid-state structure of Pbᴵᴵ(O₂CCH₂OH)₂.

diols.¹⁹⁸ The product was structurally characterized in the solid state by single-crystal X-ray diffraction to reveal an unusual feature that the ethanolamine ligands had displaced the alkoxide ligands from the coordination sphere of the Ba ion. The alkoxide ligands are hydrogen bonded to the 2-(dimethylamino)ethanol alcoholic protons as shown in Figure 52.

A number of α-hydroxy carboxylate complexes of lead(II) have been prepared and structurally characterized. While it is most likely that the carboxylic rather than the alcoholic group has been deprotonated, these species are relevant to the discussion here because they have been used as precursors to perovskite-phase materials. The reaction of lead(II) carbonate with glycolic acid (HO₂CCH₂OH)¹¹⁶ and dimethylglycolic acid (HO₂CC(Me)₂OH),¹¹⁴,¹¹⁵ according to eq 29, resulted in the formation of the corresponding Pbᴵᴵ⁾-(O₂CCR₂OH)₂ complexes. These species were structurally characterized in the solid state and their structure are shown in Figures 53–55. Both species exhibit extensive hydrogen bonding, a variety of carboxylate coordination modes, and a number of different lead(II) coordination geometries. In this context it is noteworthy that the α-hydroxy carboxylate ligands chelate through the carboxylate and alcohol ligands in every case. These compounds, together with a number of related metal–organic complexes, have also been characterized by both solution and solid-state ²⁰⁷Pb NMR spectroscopy.¹⁹⁹ Crystalline Pb(OAc)₂·3H₂O exhibited a single resonance at −1897 ppm relative to PbMe₄, and Pb(O₂CCH₂OH)₂ exhibited a single reso-
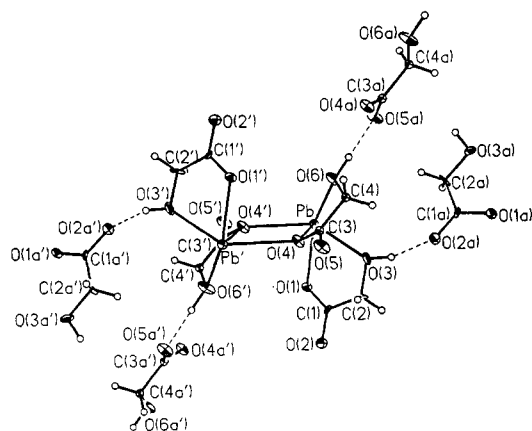
Figure 54. Molecular structure of $Pb^{II}(O_2CCH_2OH)_2$ emphasizing hydrogen bonding.
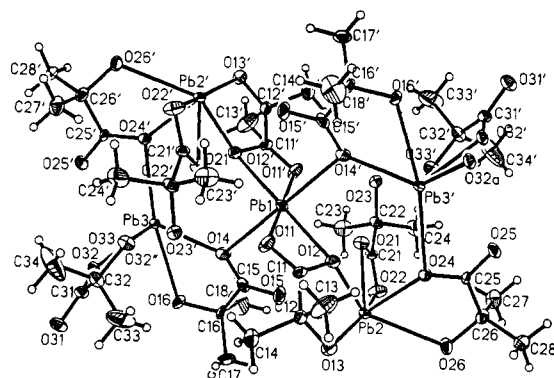
Figure 55. Solid-state structure of $Pb^{II}(O_2CCMe_2OH)_2$.
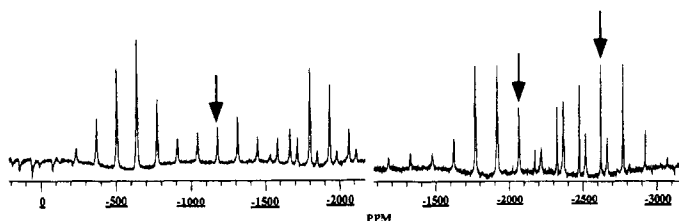
Figure 56. Solid-State CP/MAS ^{207}Pb NMR spectrum of $Pb(O_2CC(Me)_2OH)_2$. The arrows indicate the position of the isotropic chemical shifts.

nance at −2031 ppm, both consistent with the single type of lead atom observed by single-crystal X-ray diffraction data. The compound $Pb(O_2CC(Me)_2OH)_2$ exhibited three crystallographically different lead environments in a 2:2:1 ratio according to single-crystal X-ray diffraction data. Solid-state CP/MAS ^{207}Pb NMR spectroscopy of the same sample of crystals used for X-ray diffraction studies also revealed three ^{207}Pb chemical environments at −1177, −2077, and −2623 ppm in the ratio 2:2:1, consistent with the structural data as shown in Figure 56. Clearly, many more experiments are required to create a data base from which useful predictions of coordination environment can be made, but at least these results demonstrate the potential utility of this technique. Extending these principles to solution ^{207}Pb NMR spectroscopy should also be possible provided caution is exercised in interpretation of the data where coordinating solvents are employed.

Finally, it is worth noting in this section that a number of groups have investigated the use of neutral cyclic and acyclic polyether ligands including crown ethers to control metal ion coordination environments in metal–

organic precursors. These studies have resulted in formation of soluble and sometimes volatile complexes including Ba(2,5,8,11,14-pentaoxapentadecane)(hfac)$_2$,[200] Ba(hfac)(18-crown-6),[201] and Pb(OAc)$_2$(18-crown-6).[202] In some cases, such ether complexes react with the metal center to form olefin complexes, or with cleavage of a C–O bond resulting in formation of an alkoxide species.[203]

A large number of crown ether and polyethylene glycol complexes of the main group and transition metals have also been prepared and characterized, many of which are beyond the scope of this text.[204,205] However, some of these reactions have resulted in the deprotonation of the glycols, resulting in formation of metal polyether alkoxides. A notable recent example was that of the reactions between Bi(NO$_3$)$_3$ and a number of polyethylene glycols which resulted in formation of soluble Bi(III) alkoxides. A number of dimeric species were formed as shown in Figure 57. In each case the ether oxygens of the ethylene glycol ligands are all coordinated to the metal center, and it was noted that pentaethylene glycol (EO5) has sufficient chain length for all six oxygen atoms to bind to one Bi atom, and in addition, the two alcohol oxygens bridge to an adjacent Bi atom. It is also noteworthy that extensive ligand redistribution can occur during these reactions as evidenced for example by the isolation of the salt [Bi(NO$_3$)$_2$(EO5)]-[Bi(NO$_3$)$_2$(EO5^{2-})Bi(NO$_3$)$_3$]$_2$·H$_2$O. This topic is the subject of the next section.

4.6. Ligand-Exchange Reactions

In this section the reactions between two different reagents which result in transfer or exchange of ligands will be discussed. This is relevant to the chemistry that occurs en route to mixed metal oxides because the transfer of a ligand can lead to a change in stoichiometry and structural control in these systems. The most relevant aspect of these reactions is the transfer of ligands between a metal alkoxide compound and a metal carboxylate compound. Often these reactions have been investigated as an approach to form mixed metal intermediates or to induce ester elimination.

The 1:1 reaction of Bi(O-t-Bu)$_3$ with copper(II) acetate is represented by eq 42, in which a mixed metal

$$6Bi(O\text{-}t\text{-}Bu)_3 + 6[Cu(OAc)_2]_2 \rightarrow$$
$$[Cu(O\text{-}t\text{-}Bu)(OAc)]_6 + 3[Cu(OAc)_2]_2$$
$$[Bi(O\text{-}t\text{-}Bu)_2(OAc)]_2 \quad (42)$$
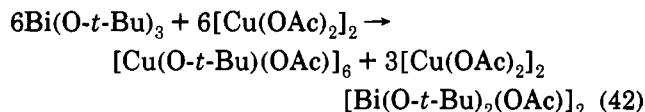
species is formed and in addition acetate for alkoxide exchange occurs at copper to form a copper(II) hexameric species, [Cu(O-t-Bu)(OAc)]$_6$.[206] The reaction between [Y(OCH$_2$CH$_2$OMe)$_3$]$_{10}$ and Cu(acac)$_2$ results in ligand exchange to form a variety of species from which a mixed alkoxide, β-diketonate of yttrium was isolated (eq 43).[207] The yttrium product,

$$[Y(OCH_2CH_2OMe)_3]_{10} + 30Cu(acac)_2 \rightarrow$$
$$3Y_3(OCH_2CH_2OMe)_5(acac)_4 + [Cu(OCH_2CH_2OMe)$$
$$(acac)]_n + \text{others} \quad (43)$$
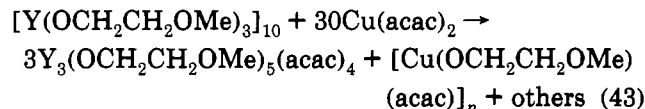
$Y_3(OCH_2CH_2OMe)_5(acac)_4$, was isolated as white crystals and the structure was solved by single-crystal X-ray diffraction. The yttrium atoms form a triangle capped

[Bi(NO₃)₂(EO4⁻)]₂·2MeOH.

[Bi(NO₃)₂(EO6⁻)]₂.

A portion of the polymeric anion in [Bi(NO₃)₂(EO5)][Bi-
(NO₃)₂(EO5²⁻)Bi(NO₃)₃]·2H₂O. O(4)ᵃ and O(6)ᵃ coordinated to Bi(2)
are related to O(4) and O(6) by x, ¹/₂ – y, z – ¹/₂.

Figure 57. Solid-state structure of Bi polyethylene glycol complexes.

above and below with triply bridging alkoxide oxygens
of chelating 2-methoxyethoxide groups. The metals
are also linked by two doubly bridging alkoxide ligands
of a chelating methoxymethoxide and a doubly bridging
alkoxide oxygen of a dangling 2-methoxyethoxide. The
coordination sphere is completed by the β-diketonate
ligands which chelate to the metals and result in
8-coordination at yttrium.

The first example of a molecular barium–copper
cluster, Ba₂Cu₂(acac)₄(OCH₂CH₂OMe)₄·2(HOCH₂CH₂-
OMe), was isolated from the reaction of [(acac)Cu-
(OCH₂CH₂OMe)] withBa(OCH₂CH₂OMe)₂].²⁰⁸ The
structure is shown in Figure 58 and indicates that a
β-diketonate ligand has been transferred from the
copper center to Ba. It is interesting to note that, in
this case, the 2-methoxyethoxide ligands all chelate
while the 2-methoxyethanol ligands dangle.

4.7. Ester-Elimination Reactions

Mixed-metal oxide species have been prepared ex-
tensively by reactions between metal alkoxide com-
pounds and metal carboxylates. Solutions of these
species are generally prepared in alcohols or carboxylic
acids as solvents and subsequently hydrolyzed and

○ Carbon

⊗ Oxygen

⊕ Cu, Ba

Figure 58. Solid-state structure of Ba₂Cu₂(acac)₄-
(OCH₂CH₂OMe)₄·2(HOCH₂CH₂OMe).

pyrolyzed, as discussed in section 3. However, on
mixing, solutions containing metal alkoxide and metal

carboxylate compounds can undergo a number of reactions which might dictate the evolution of structure on formation of the final mixed-metal oxide. The possibility of ligand exchange has been discussed above. Another possibility is a reaction in which an alkoxide and a carboxylate ligand react to form an oxo ligand and an ester, the so-called ester-elimination reaction. This reaction stoichiometry is presented for a general case in eq 44. Free alcohol and/or carboxylic acid can

$$M(OR)_n + M'(O_2CR')_m \rightarrow$$
$$(RO)_{n-1}MOM'(O_2CR')_{m-1} + RO_2CR' \quad (44)$$
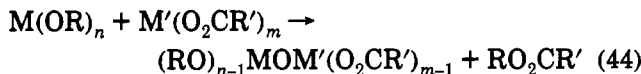
also react with metal–organic precursors to form hydroxide species which may be capable of further condensation to liberate 0.5 equivalent of water for each ester formed (eqs 45–47). However, the reaction of eq 46 is unlikely due to the higher pK_a of alcohols compared to carboxylic acids.

$$M(OR)_n + HO_2CR' \rightarrow (RO)_{n-1}MOH + RO_2CR' \quad (45)$$

$$M(O_2CR')_n + HOR \rightarrow$$
$$(R'CO_2)_{n-1}MOH + RO_2CR' \quad (46)$$

$$2(X)_{n-1}MOH \rightarrow$$
$$(X)_{n-1}MOM(X)_{n-1} + H_2O \quad (X = OR \text{ or } O_2CR) \quad (47)$$
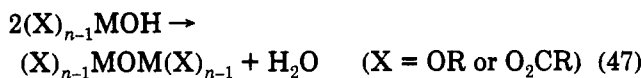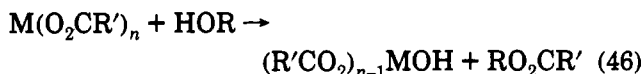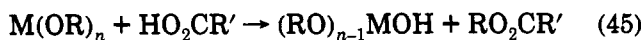
The elimination of esters has also been used extensively in the formation of metal siloxide compounds where an acyloxysilane is reacted with a metal alkoxide to eliminate the corresponding ester according to eq 48.[209-211] In this case ester elimination does not lead to

$$Ti(OR)_4 + 4R'_3SiOCOR'' \rightarrow$$
$$Ti(OSiR'_3) + 4ROCOR'' \quad (48)$$

formation of an oxo species, but rather a new homoleptic metal alkoxide compound. This reaction is successful for the formation of Ti, Zr, V, and Nb siloxide complexes. While this reaction is not "useful" in this context because it leads to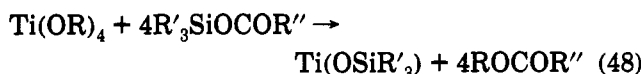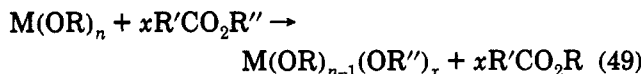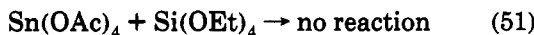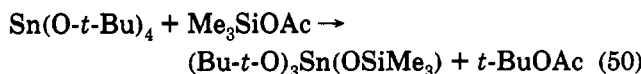 neither hydrolysis nor condensation of the starting materials, it demonstrates that if an ester is present in such a reaction mixture, it could be responsible for alcoholysis or transesterification reactions as illustrated in eq 49.[22]

$$M(OR)_n + xR'CO_2R'' \rightarrow$$
$$M(OR)_{n-1}(OR'')_x + xR'CO_2R \quad (49)$$

The importance of controlling the functionality at the metal center has been demonstrated in the reactions described in eqs 50 and 51. The reaction of eq 50

$$Sn(O\text{-}t\text{-}Bu)_4 + Me_3SiOAc \rightarrow$$
$$(Bu\text{-}t\text{-}O)_3Sn(OSiMe_3) + t\text{-}BuOAc \quad (50)$$

$$Sn(OAc)_4 + Si(OEt)_4 \rightarrow \text{no reaction} \quad (51)$$

successfully gave ester elimination (as determined by NMR and GC–MS), but the reaction of eq 51 did not result in any new products (as determined by NMR spectroscopy), even on heating to 80 °C.[212] The ester elimination reaction to prepare metal oxo–alkoxide
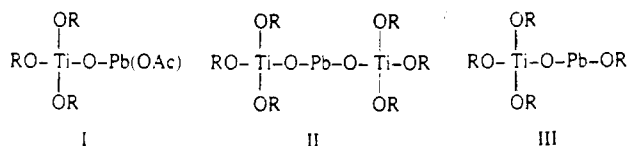

Figure 59. Proposed structures formed on ester elimination between $Pb(OAc)_2$ and $Ti(O\text{-}i\text{-}Pr)_4$.

compounds has been used extensively by Teyssie et al.,[213-215] where, in an early example, the reaction of an aluminum alkoxide with iron(II) acetate resulted in formation of the corresponding iron aluminum oxo–alkoxide according to eq 52. These species were

$$2Al(OR)_3 + Fe(OAc)_2 \rightarrow$$
$$Fe[OAl(OR)_2]_2 + 2ROAc \quad (52)$$
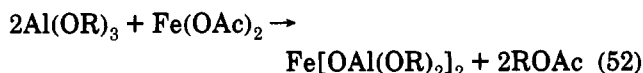
prepared to investigate their catalytic activity. Unfortunately, the details of these synthesis have not been published in the open literature. These species are thought to be oligomeric in solution as a result of the formation of bridging oxide and alkoxide ligands in an analogous fashion to metal alkoxide compounds. The degree of association was calculated from cryoscopic measurements and examples include $M[OAl(OR)_2]_n$, where M = Zn, R = n-Bu, n = 6; M = Co, R = n-Bu, n = 4.1; and M = Co, R = i-Pr, n = 2. It is interesting to note that for $Zn[OAl(O\text{-}n\text{-}Bu)_2]_n$, n = 8 for a fresh solution, but on standing for 2 days a value of n = 6 was observed, indicating the presence of time-dependent phenomena in these solutions. Teyssie et al. have proposed that the size and shape of oxo–alkoxide aggregates can be controlled by modification of three parameters: the nature of the alkoxide groups, the nature of the central metal, and the nature of the solvent.[213]

The use of ester eliminations reactions was identified in the reaction between lead(II) acetate and $Ti(O\text{-}i\text{-}Pr)_4$ in the work of Gukovich and Blum.[216,217] They dehydrated lead(II) acetate by refluxing the hydrated salt in 2-methoxyethanol and then reacted it with $Ti(O\text{-}i\text{-}Pr)_4$ in refluxing 2-methoxyethanol to liberate an undetermined amount of isopropyl acetate. They also proposed that a number of bi- or trimetallic mixed-metal oxo–alkoxide species were formed and speculated on their structures, which are shown in Figure 59. This system was also investigated by Dekleva et al.[218] These workers found that refluxing lead(II) acetate trihydrate in 2-methoxyethanol results in formation of basic lead acetate, $Pb_4O(OAc)_6 \cdot H_2O$, with liberation of 0.5 equiv of ester (eqs 53 and 54) in contrast to the results of Payne et al.,[106] where the lead acetate trihydrate was first dehydrated. The reaction of the basic lead acetate

$$4Pb(OAc)_2 + H_2O \rightarrow Pb_4O(OAc)_6 + 2HOAc \quad (53)$$

$$HOAc + ROH \rightarrow ROAc + H_2O \quad (54)$$
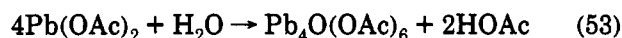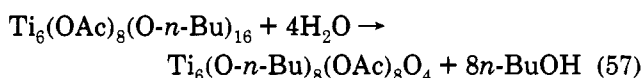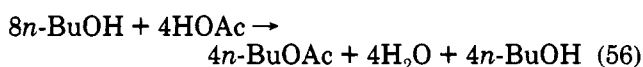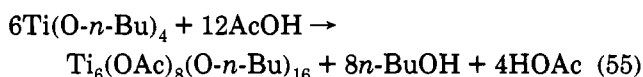
with titanium isopropoxide was then thought to be responsible for the formation of the mixed-metal oxo species, but they proposed that extended polymers were unlikely to be formed on the basis of the reaction stoichiometry. It was also shown that more ester was eliminated on reaction with $Ti(O\text{-}i\text{-}Pr)_4$. In the same paper, these authors also addressed the observations
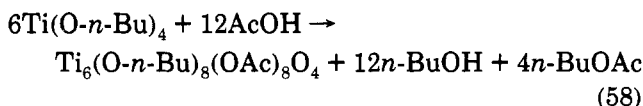
of Payne et al.[106] that, in this system, the lead titanate precursor powders derived from Ti(O-i-Pr)$_4$ differed from those derived from Ti(O-n-Pr)$_4$ according to DTA data. At first glance this seems strange, as Dekleva et al. point out, because it might be expected that trans alcoholysis reactions would result in virtually complete replacement of the titanium alkoxide ligands when 2-methoxyethanol is used as a solvent. However, these reactions will depend markedly on the reaction conditions. The replacement of the primary alkoxide O-n-Pr ligand by another primary alkoxide ligand, 2-methoxyethoxide, is likely to be slow unless forcing conditions are used, and the hydrolysis of primary alkoxides is known to be fast.

According to a later paper of Hayashi and Blum,[219] the reaction between Ti(O-i-Pr)$_4$ and Pb(OAc)$_2$ resulted in a distillation product which was thought to be composed of isopropyl acetate together with a small amount of 2-propanol as determined by Raman spectroscopy.
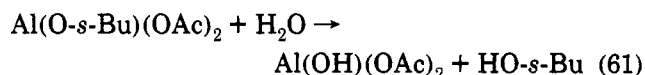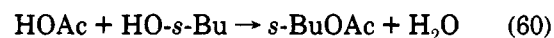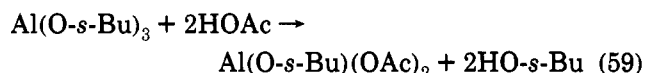
The addition of acetic acid in the sol–gel processing of metal alkoxide compounds has been used to prevent precipitation. For example, when acetic acid is added to solutions of titanium(IV) alkoxide compounds, stable transparent sols and gels can be reproducibly obtained. These colloidal materials can be used to deposit electrochromic TiO$_2$ coatings. The role of acetic acid in these systems has recently been investigated. The crystalline compound Ti$_6$(O-n-Bu)$_8$(OAc)$_8$O$_4$ was obtained from the reaction of 2 equiv of acetic acid with 1 equiv of Ti(O-n-Bu)$_4$.[144] It is believed that the acetic acid promotes an esterification reaction and the presence of butyl acetate was identified by infrared spectroscopy. This leads to generation of water, in situ, which promotes hydrolysis and condensation reactions. The following reactions have been proposed to account for these observations:
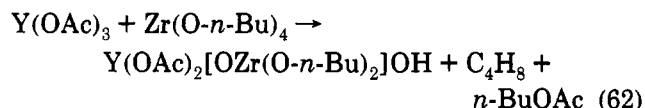
$$6Ti(O\text{-}n\text{-}Bu)_4 + 12AcOH \rightarrow$$
$$Ti_6(OAc)_8(O\text{-}n\text{-}Bu)_{16} + 8n\text{-}BuOH + 4HOAc \quad (55)$$

$$8n\text{-}BuOH + 4HOAc \rightarrow$$
$$4n\text{-}BuOAc + 4H_2O + 4n\text{-}BuOH \quad (56)$$

$$Ti_6(OAc)_8(O\text{-}n\text{-}Bu)_{16} + 4H_2O \rightarrow$$
$$Ti_6(O\text{-}n\text{-}Bu)_8(OAc)_8O_4 + 8n\text{-}BuOH \quad (57)$$

The overall reaction can be written as:

$$6Ti(O\text{-}n\text{-}Bu)_4 + 12AcOH \rightarrow$$
$$Ti_6(O\text{-}n\text{-}Bu)_8(OAc)_8O_4 + 12n\text{-}BuOH + 4n\text{-}BuOAc \quad (58)$$

In another example, Al(O-s-Bu)$_3$ was reacted with acetic acid to liberate s-BuOH.[220] It was proposed that the alcohol in turn reacted with the acetic acid present to form the corresponding ester and liberate water. The water reacted with the remaining alkoxide ligands to produce aluminum basic acetate, Al(OH)(OAc)$_2$, which was insoluble in the reaction solvent (diethyl ether) and precipitated (eqs 59–61). The formation of the ester was supported by a comparison of the IR spectra of the starting materials and products. In the presence of an excess of acetic acid, a new ν(C=O) band was observed that was attributed to s-BuOAc.
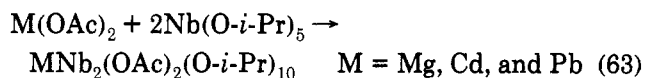
$$Al(O\text{-}s\text{-}Bu)_3 + 2HOAc \rightarrow$$
$$Al(O\text{-}s\text{-}Bu)(OAc)_2 + 2HO\text{-}s\text{-}Bu \quad (59)$$

$$HOAc + HO\text{-}s\text{-}Bu \rightarrow s\text{-}BuOAc + H_2O \quad (60)$$

$$Al(O\text{-}s\text{-}Bu)(OAc)_2 + H_2O \rightarrow$$
$$Al(OH)(OAc)_2 + HO\text{-}s\text{-}Bu \quad (61)$$

Yttria-stabilized zirconia was prepared by the elimination of butyl acetate from the reaction between Y(OAc)$_3$ and Zr(O-n-Bu)$_4$ according to eq 62.[221] The

$$Y(OAc)_3 + Zr(O\text{-}n\text{-}Bu)_4 \rightarrow$$
$$Y(OAc)_2[OZr(O\text{-}n\text{-}Bu)_2]OH + C_4H_8 +$$
$$n\text{-}BuOAc \quad (62)$$

evidence and origin for the formation of butene was not discussed. The ester and some additional n-BuOH were identified by gas chromatography. The structural integrity of this product was not confirmed by spectroscopic techniques.

In some cases, metal acetates react with metal alkoxides to form mixed-metal species which do not undergo ester elimination. A recent example is shown in eq 63, where divalent metal acetates were reacted

$$M(OAc)_2 + 2Nb(O\text{-}i\text{-}Pr)_5 \rightarrow$$
$$MNb_2(OAc)_2(O\text{-}i\text{-}Pr)_{10} \quad M = Mg, Cd, \text{ and } Pb \quad (63)$$

with Nb(O-i-Pr)$_5$.[89] The Mg derivative was structurally characterized in the solid state and found to contain bridging acetate ligands as expected. The solid-state structure is shown in Figure 60. The Cd and Pb analogs exhibited a single resonance in the solution ^{113}Cd and ^{207}Pb NMR spectra consistent with the presence of a single species in solution. In contrast, Ba(OAc)$_2$ does not react with Nb(O-i-Pr)$_5$ at room temperature, but its reactivity was overcome by adding acetic acid to the reaction mixture, which led to formation of a gel. Anhydrous, basic zinc acetate, Zn$_4$O(OAc)$_6$, also reacted with Nb(O-i-Pr)$_5$, but the products were not identified.[89]

Hydrolysis of MgNb$_2$(OAc)$_2$(O-i-Pr)$_{10}$ resulted in formation of a reactive powder which still contained acetate ligands and evidence for the elimination of isopropyl acetate was proposed from ν_{as}(C–O), as determined by FTIR. The reaction of lead(II) acetate with Ti(OEt)$_4$ resulted in formation of a hexane-soluble oxo species formulated as PbTi$_2$O(OAc)$_2$(OEt)$_6$, which was proposed to exhibit a triangular framework based on NMR data.[89] The formation of an oxo cluster was confirmed by a single-crystal X-ray diffraction analysis for the reaction of Zr(O-i-Pr)$_4$ with lead(II) acetate (Figure 61). The species PbZr$_3$(μ^4-O)(μ-OAc)$_2$(μ-O-i-Pr)$_5$(O-i-Pr)$_5$ was isolated from this reaction when [Zr(O-i-Pr)$_4$(HO-i-Pr)]$_2$ was added to Pb(OAc)$_2$ in toluene. Each Zr is 6-coordinate and the lead atom is 6-coordinate, assuming the presence of a stereochemically active lone pair in the vacant coordination site. This species is structurally analogous to Ce$_4$O(O-i-Pr)$_{14}$(HO-i-Pr).[160-162] No mention of the origin of the oxide ligand was made. Hubert-Pfaltzgraf et al. have commented on the order of addition of reagents in these systems.[89] They have observed that, in the lead/zirconium system described above, the same
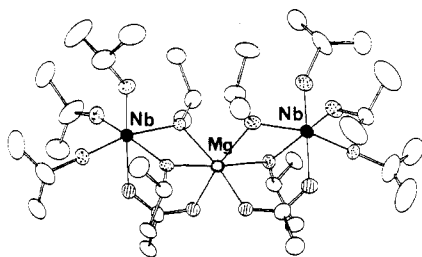
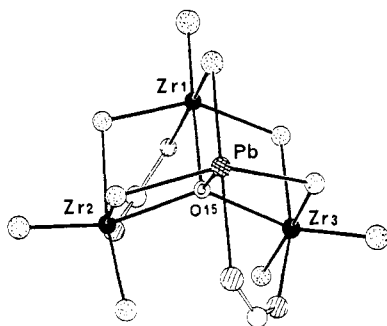**Figure 60.** Solid-state structure of $MgNb_2(OAc)_2(O\text{-}i\text{-}Pr)_{10}$.

Figure 61. Solid-state structure of $PbZr_3(\mu_4\text{-}O)(\mu\text{-}OAc)_2(\mu\text{-}O\text{-}i\text{-}Pr)_5(O\text{-}i\text{-}Pr)_5$.
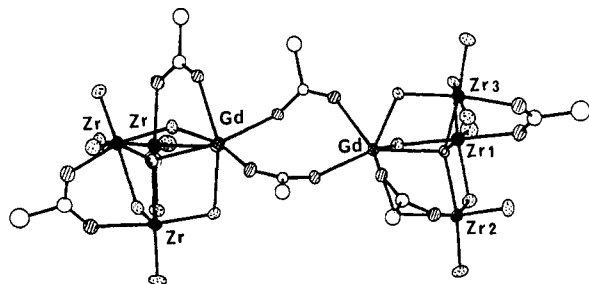

Figure 62. Solid-state structure of $[Gd(OAc)_3Zr_3O(O\text{-}i\text{-}Pr)_{10}]_2$.

solution ^{207}Pb NMR spectrum was observed regardless of the order of addition of the reagents. However, they note that a Zr-rich species, analyzing as $PbZr_4O\text{-}(OAc)_2(O\text{-}i\text{-}Pr)_{14}$, was isolated when $Pb(OAc)_2$ was added to $[Zr(O\text{-}i\text{-}Pr)_4(HO\text{-}i\text{-}Pr)]_2$.

In contrast to these observations, $Gd(OAc)_3$ does not react with $Zr(O\text{-}i\text{-}Pr)_4$ at room temperature, but the metal acetate was observed to dissolve on heating.[89] The species $[Gd(OAc)_3Zr_3O(O\text{-}i\text{-}Pr)_{10}]_2$ was formed in high yield (85%). A solid-state structural study revealed a structure analogous to that of $PbZr_3(\mu^4\text{-}O)(\mu\text{-}OAc)_2(\mu\text{-}O\text{-}i\text{-}Pr)_5(O\text{-}i\text{-}Pr)_5$. Gd is 7-coordinate while all the Zr atoms are 6-coordinate (Figure 62). In this case, ester formation was not observed and the oxo ligand was thought to be derived from the thermal decomposition of an alkoxide ligand. However, when the $O\text{-}i\text{-}Pr$ ligand is replaced by the more reactive $OCH_2\text{-}CH_2OMe$ ligand, reaction between $Ln(OAc)_3$, $Ln = a$ lanthanide, and $Zr(OR)_4$ occurs at room temperature to form an adduct, in the case of yttrium, $YZr\text{-}(OAc)_3(OCH_2CH_2OMe)_4$.[89] On heating, this species reacts to form an insoluble product which has a $\nu_{as}(C\text{-}O)$ stretch analogous to that of (2-methoxyethoxy)-acetate, signifying the elimination of an ester group.

5. Conclusions and Future Directions

It is clear from the discussion above that even the simplest multicomponent metal–organic precursor sys-

tem exhibits extremely complicated reaction chemistry. Unfortunately, few systems have been studied where the reaction intermediates have been, or very often, can be, unambiguously characterized. It is also difficult to draw definite conclusions from comparisons between systems because generally more than one variable is changed. We feel that the perovskite-phase system reviewed here is representative of other (non-silicate) metal oxide systems both in terms of complexity and the level of understanding of fundamental chemical transformations at the molecular level. From the comparison of the information available from spectroscopic studies of systems reviewed in section 3, which lead to formation of perovskite-phase metal oxides, and studies of molecular systems, where very often interesting species have been isolated that are not necessarily en route to interesting materials, a number of common phenomena are apparent.

Alcoholysis reactions are clearly important in systems where a metal alkoxide is dissolved in a different alcohol as a solvent. This is especially pertinent to the cases where (i) the pK_a of the alcohol solvent is lower than the alcohol derived from the alkoxide ligands of the metal–organic complex and (ii) where the steric demands of the alcohol solvent are less than those of the alcohol derived from the alkoxide ligand. Furthermore, it might be expected that if the alkoxide ligand has other functional substituents, such as is the case of 2-methoxyethanol, the chelate effect might play a crucial role in controlling the reaction rates and coordination environment of the metal center during subsequent reactions. However, in the majority of complexes containing 2-methoxyethanol or 2-methoxyethoxide ligands that have been characterized in the solid state and in solution, it appears that the ether oxygen often prefers to dangle rather than chelate. This effect, no doubt, enhances solubility in polar solvents, but may not play as marked a role in controlling aggregation phenomena as might be anticipated if the ether oxygen was coordinated to the metal center, as in the case of β-diketonate ligands (see Figure 30). Polyether alkoxide ligands or polyether alcohols seem to be more effective in binding to the metal center, as demonstrated by a number of studies of the molecular chemistry of these complexes and processing studies (see section 4). In the few amino alkoxide compounds that have been structurally characterized, it appears they exhibit stronger propensity for coordination of the amine lone pair to the metal center compared to analogous ether oxygen lone pair coordination. We therefore conclude that amino alcohol solvents are likely to be more effective in reducing the rates of hydrolysis of metal alkoxide compounds compared to ether alcohol solvents. Interestingly, it has been observed that alcohol amine solutions (such as triethanolamine) of titanium(IV) and tin(IV) alkoxide compounds are indefinitely stable with respect to precipitation on addition of a large excess of water in air.[222-225] However, it should be noted that the preference of the donor atom for the metal depends on the nature of both the donor atom and the metal center. Some predictions may be possible through hard/soft, acid/base concepts.[178]

Ligand exchange reactions between metal–organic complexes which contain different ligands are also

prevalent in these systems. This is likely to be important where one type of ligand is used to control some aspect of the reaction chemistry as in the case of modified metal alkoxide compounds (Figure 30). Where the dimensionality of hydrolysis is expected to be controlled by preferential reaction of one ligand in the presence of another, ligand transfer reactions are likely to alter this reaction pathway and lead to a loss of regiochemistry. However, this may be advantageous where two different homoleptic metal–organic precursors are mixed in solution. These species are likely to have markedly different hydrolysis rates, especially where one is an alkoxide compound, and ligand exchange processes may result in more comparable rates of hydrolysis. Such reactions have been observed in molecular systems.

Reactions between different metal–organic precursors can lead not only to ligand exchange but also the formation of mixed metal species. In many cases, few precautions are taken to control the stoichiometry of the possible intermediates formed, via ligand-controlled reactions for example, and it is possible that the intermediates do not have the appropriate stoichiometry desired for the final metal oxide material. This has been demonstrated in a number of cases on simply mixing metal–organic precursors (e.g. $Sr_2Ti(O\text{-}i\text{-}Pr)_8$-$(HO\text{-}i\text{-}Pr)_5$,[174] $PbZr_3(O)(O\text{-}i\text{-}Pr)_{12}$[89]) and on partial hydrolysis in these systems (e.g. $Ba_4Ti_{13}O_{18}(OCH_2CH_2$-$OMe)_{24}$[74]). The effects of formation of these species as reaction intermediates on the formation of the final ceramic materials is not clear at this stage. In a number of cases, mixing metal organic precursors has resulted in formation of "single-component" precursors, i.e. molecular species with the same stoichiometry as that desired for the final metal oxide material ($LiNb$-$(OEt)_6$,[168] $ZnSn(OEt)_6$,[137] $BaTi(OCH_2CH_2OMe)_6$[74]). The control over stoichiometry in such systems has yet to be demonstrated unambiguously. We speculate that the lack of control over these reactions and possibly that a variety of species with different metal atom ratios may be formed might be responsible for the high crystallization temperatures or long thermal treatments necessary to convert many of these intermediates to metal oxide materials, (see Figure 1, part iii). To elucidate this point, a series of carefully designed and executed experiments are required with the appropriate controls.

Reactions between the ligands in these systems resulting in elimination of organic fragments is also an important aspect, especially the possibility that metal carboxylates can react with metal alkoxide compounds to generate metal oxo species and organic esters. There is the possibility of ambiguity in these systems, however, where hydrolysis (either accidental or intentional) can lead to formation of oxo groups and the FTIR bands attributed to formation of an ester may be derived from the presence of a free carboxylic acid. However, a large number of reactions have been carried out in which data that is consistent with ester elimination have been obtained and lend credence to this pathway. In a number of cases the ester has been identified, unambiguously, by spectroscopic methods.

We had hoped to draw more precise conclusions from a comparison of the studies of model systems and systems that lead to perovskite-phase materials. How-

ever, due to the complexity of these systems and the large number of reaction variables, only broad conclusions concerning the likelihood for common reaction phenomena are possible at this stage. To make significant advances it seems reasonable to pursue studies of model systems and if possible make them more accurately model routes to specific ceramic materials. Model studies are useful to determine the variety of coordination modes possible for ligands that are typically used in real systems. A similar situation has been encountered in the evolution of organometallic chemistry where molecular models for likely catalytic intermediates were sought. In a number of cases, particular binding modes of unsaturated organic ligands to metal atoms were well-characterized in the molecular chemistry literature before they were observed to be formed in reactions of organic molecules with metal surfaces.[226,227]

One of the problems associated with deriving molecular information in systems that ultimately yield useful ceramic materials is the difficulty in characterization of the amorphous phase. In this sense, metal–organic species in solution can be considered "amorphous" since they lack long range 3-dimensional structure. Development of new and existing techniques will probably be crucial to deriving an understanding of fundamental aspects of the reaction chemistry in these systems. In this context, while single-crystal X-ray diffraction data reveal interesting and valuable structural information, it is generally not possible to make a connection between the solid-state and solution structures of metal–organic species in these systems.

Infrared and Raman spectroscopies have been used for the characterization of metal oxide materials and their precursors. Unfortunately, many of the assignments are only tentative. For example, the difference between symmetric and asymmetric $\nu(C\text{-}O)$ stretching frequency in metal carboxylate compounds has been used extensively as a method for determining the coordination mode of the carboxylate ligand in these complexes. However, as Deacon et al.[111] have pointed out, these assignments are only tentative, even in cases where a sound body of model compounds has been prepared and characterized as a data base. Synthetic chemists could make a significant contribution to this aspect by more carefully characterizing molecular species where the structure of these species has been determined unambiguously by other methods (such as single-crystal X-ray diffraction). Raman spectroscopy is a useful tool in probing the local coordination environment of intermediates formed from the reactions of metal–organic compounds. Several papers have appeared concerning the determination of bond length–bond order relationships derived from a series of model metal oxide compounds, and in favorable cases, coordination environment can also be determined.[228]

EXAFS is an alternative method that shows great potential for the structural characterization of amorphous materials.[229] It has been used extensively in studies of extended amorphous materials, such as zeolites, and in molecular chemistry. However, it is again necessary to provide an accurate data base of information of structurally characterized comparative species on which to base the interpretation of these data.

Solid-state NMR spectroscopy is a technique that has been used extensively in the silicate system and is now being extended to the characterization of other materials using less common nuclei. In a number of systems valuable information concerning coordination number and geometry can be discerned.[230] Solid-state ^{27}Al NMR spectroscopy can be used to distinguish octahedral and tetrahedral Al coordination environments in the solid state. This method is also convenient to follow the course of a thermal treatment in situ. The extension of solid-state NMR spectroscopy to perovskite-phase materials is somewhat limited by the suitability of the NMR-active isotopes of the elements involved. While the group 4 (^{49}Ti, ^{47}Ti, and ^{91}Zr) and group 2 (^{43}Ca, ^{87}Sr, ^{137}Ba) elements have NMR-active isotopes, they do not possess high receptivity and in some cases have not been studied in great detail.[231-233] However, the situation is different for ^{207}Pb NMR spectroscopy, where the relative receptivity is high and the nucleus is dipolar ($I = \frac{1}{2}$).[234] There are limited ^{207}Pb chemical shift data available in solution for metal-organic lead compounds[235-237] and most data are available for organo lead(IV) compounds.[238] A number of ^{207}Pb NMR chemical shifts have been reported for lead(II) alkoxide compounds, but these data have yet to be interpreted as a function of a property of the lead coordination environment.[87] This is in contrast to ^{119}Sn NMR spectroscopy of tin(IV) alkoxide compounds, where for a given ligand environment a unit change in coordination number gives rise to a chemical shift change of approximately 150 ppm.[239,240] As a result, it is possible to use ^{119}Sn NMR chemical shifts to derive information concerning coordination number of reaction intermediates in reactions to form stannates.[241,242] An analogous data base of information has not yet been established for ^{207}Pb NMR spectroscopy although similar correlations should be possible. In fact due to the larger chemical shift range of ^{207}Pb NMR compared to ^{119}Sn, more subtle information, such as changes in coordination geometry within a given coordination number, may be discernible. However, it has been demonstrated that ^{207}Pb chemical shifts are very sensitive to solvent and concentration effects and care will be needed to avoid ambiguous results.[199] There are a number of reports of ^{207}Pb NMR chemical shifts in model systems and those that lead to perovskite-phase materials, but in the absence of a data base, the chemical shift information is rarely useful. Solid-state ^{207}Pb NMR spectroscopy has not been investigated extensively, and few chemical shifts of metal-organic lead complexes have been reported. The paucity of data is probably the result of the large chemical shift anisotropy, the lack of information concerning ^{207}Pb and ^{1}H (for cross polarization (CP) experiments) relaxation times and the frequent absence of protons from which to cross polarize. However, an example of the potential utility of solid-state CP/MAS ^{207}Pb NMR spectroscopy was recently demonstrated in the characterization of a number of model lead carboxylate systems (see section 4.5).[199]

Studies based on these techniques in both model systems and those that lead to perovskite-phase materials are likely to yield valuable information concerning reaction pathways and mechanisms. Further studies directed at controlling the evolution of structure

by devising new methods to control the rates of hydrolysis and condensation would also be valuable. Use of modified metal alkoxide compounds has been discussed in section 3 as one method to achieve these goals and some preliminary aspects have been demonstrated in monometallic systems. A number of other methods have been described recently. Buhro et al.[243] have proposed a number of nonhydrolytic processes for converting metal alkoxide compounds and related precursors to intermediate gels and then to metal oxides. These processes use reagents other than water to cause hydrolysis with the possibility of different kinetics with the result that gels with different structures may be formed which would expand the capabilities of sol-gel processing. In one form this process involves the reaction of metal alkoxide compounds, especially zinc(II) alkoxide compounds with acetone according to eqs 64 and 65, which results in formation of a gel
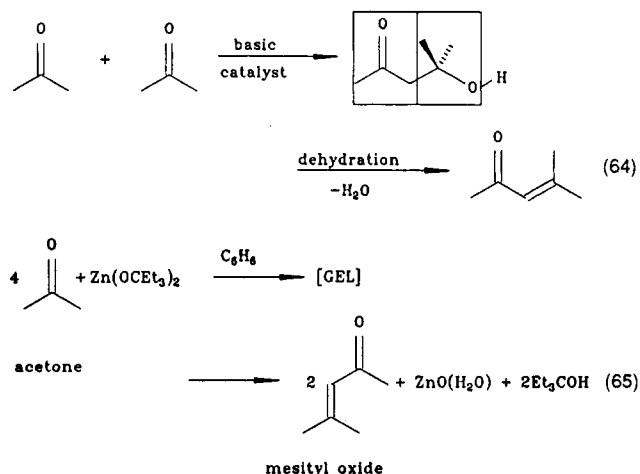
mesityl oxide

ultimately liberating zinc oxide, the alcohol, and mesityl oxide via dehydration of the aldol condensation product. An aldolate complex of zinc(II) was isolated as an intermediate in these reactions, and the overall reaction mechanism was proposed to contain the steps identified in Figure 63. Where the metal alkoxide is nonbasic, such as in the case of Ti(O-i-Pr)$_4$, no reaction was observed with acetone. However, a number of steps can be taken to overcome this problem. The alkoxide ligands can be substituted for more basic ligands such as amido groups, in which case reaction with acetone was observed. Alternatively, the metal alkoxide compound can be reacted with diacetone alcohol directly, which in the case of Ti(O-i-Pr)$_4$ resulted in a gel forming reaction.

Significant advances have yet to be made in the design of ligands for the thermally or photochemically induced decomposition of metal-organic compounds to form metal oxides. The thermal reactivity of metal alkoxide compounds has been investigated for Ti(OR)$_4$ systems and provides useful insight into reaction mechanisms.[244] The reaction of Y$_5$(O)(O-i-Pr)$_{13}$ with acetylacetone resulted in the unexpected formation of Y$_2$(μ-OAc)$_2$(acac)$_4$(H$_2$O)$_2$, in which the acetate ligand was thought to be derived from thermal decomposition of a β-diketonate ligand.[245] The photochemically induced rearrangement of metal alkoxide chromophores to liberate hydroxide ligands, according to the reaction of eq 66, has also been studied as an alternative to hydrolysis.[243,246] The metal-based photochemistry of Ce$_2$(O-
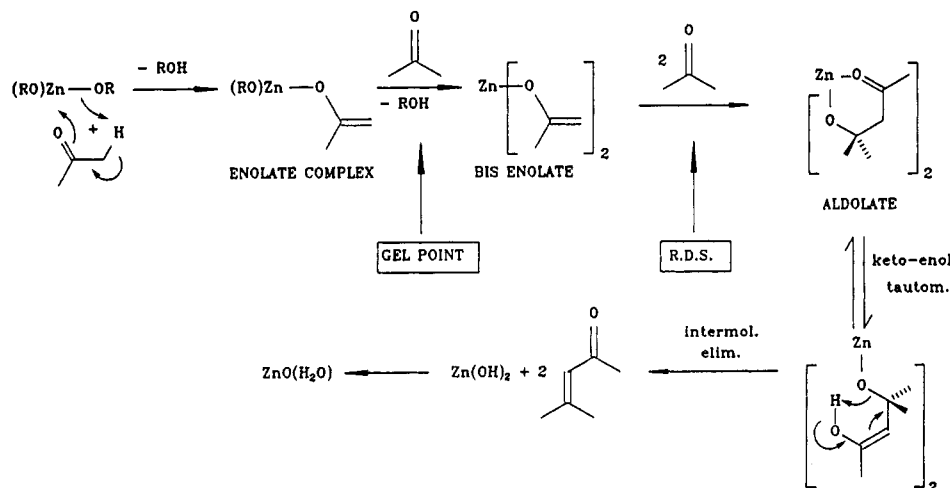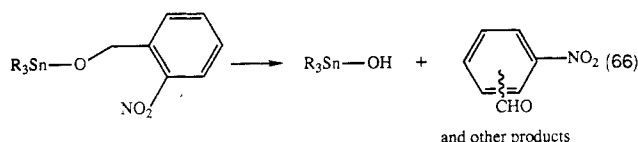
Figure 63. Proposed pathway for the acetone-induced sol–gel reaction.

and other products (66)

i-Pr)$_8$•2(HO-i-Pr) has been studied and irradiation with Indiana sunlight for 50 h gives the mixed valence species Ce$_4$O(O-i-Pr)$_{13}$(HO-i-Pr).[247]

The design aspects of a number of hydroxy carboxylate and hydroxyimino carboxylate complexes has recently been discussed.[248] In one example, zirconium bis[2-(hydroxyimino)propionate] thermally decomposed at 186 °C to give ZrO$_2$ directly, and furthermore, this species is very soluble in a number of organic solvents, which is likely to facilitate processing from these species. It was proposed that the low activation barrier to thermal decomposition might be the result of the mechanism proposed in eq 67, where rearrangement leads to the evolution of acetonitrile and CO$_2$, which were observed as volatile byproducts.

$$ZrO_2 + 2 \, MeCN + 2 \, CO_2 \qquad (67)$$
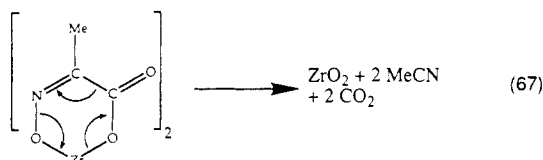
Monolithic metal oxide gels have also been formed by the nonhydrolytic reaction between metal halides and metal alkoxides according to the general reaction described by eq 68.[249] Crystalline SiO$_2$, TiO$_2$, and Al$_2$O$_3$

$$MCl_4 + M(OR)_4 \rightarrow 2MO_2 + 4RCl \qquad (68)$$

have been prepared by this method and it can be envisaged that this technique will be extended to other materials.

Inverse micelle microemulsions have been used to control the extent of hydrolysis and condensation reactions in titanium and iron alkoxide compounds. Monolithic gels were produced by this technique.[250] Ultrasound methods have also been used to generate zinc oxide colloids containing monodispersed particles from the reaction of zinc acetate with ethanol at 80 °C.[251]

In summary, further studies utilizing carefully designed experiments are required to elucidate the chemistry involved in metal–organic routes to perovskite-phase materials. Once the level of understanding of mechanistic aspects is developed to a stage where control over chemical properties such as stoichiometry and homogeneity can be exhibited, it remains to be seen whether this level of control is useful in determining the physical properties of the final material.

Acknowledgments

6. References

(1) See, for example: Frontiers in Materials Science. *Science* **1992**, *255*, 1049 and references therein.
(2) Maury, F. *Adv. Mater.* **1991**, *3*, 542.
(3) Klabunde, K. J.; Li, Y.-X.; Tan, B.-J. *Chem. Mater.* **1991**, *3*, 30.
(4) Griffiths, R. J. M. *J. Phys. iv* **1991**, *1*, 905.
(5) Gladfelter, W. L.; Simmonds, M. G. In *Chemical Aspects of Chemical Vapor Deposition for Metallization*; Hampden-Smith, M. J.; Kodas, T. T., Eds. To be published.
(6) Hampden-Smith, M. J.; Kodas, T. T. In *Chemical Aspects of Chemical Vapor Deposition for Metallization*; Hampden-Smith, M. J.; Kodas, T. T., Eds. To be published.
(7) Zinn, A.; Neimer, B.; Kaesz, H. D. *Adv. Mater.* **1992**, *4*, 375.
(8) Fix, R. M.; Gordon, R. G.; Hoffman, D. M. *Chem. Mater.* **1990**, *2*, 235.
(9) Steigerwald, M. L.; Brus, L. E. *Acc. Chem. Res.* **1990**, *23*, 183.
(10) Zanella, P.; Rossetto, G.; Brianese, N.; Ossola, F.; Porchia, M.; Williams, J. O. *Chem. Mater.* **1991**, *3*, 225.
(11) Bradley, D. C. *Chem. Rev.* **1989**, *89*, 1317.
(12) Brinker, C. J.; Scherer, G. W. *Sol-Gel Science: The Physics and Chemistry of Sol-Gel Processing*; Academic Press: Boston, 1990.
(13) Klein, L. C. *Sol-Gel Technology for Thin Films, Fibers, Preforms, Electronics and Specialty Shapes*; Noyes Publications: Park Ridge, 1988.
(14) Cousin, P.; Ross, R. A. *Mater. Sci. Eng. A* **1990**, *A130*, 119.
(15) Phule, P. P.; Risbud, S. H. *J. Mater. Sci.* **1990**, *25*, 1169.
(16) Hench, L. L.; West, J. K. *Chem. Rev.* **1990**, *90*, 33.
(17) Van Der Sluys, W. G.; Sattleberger, A. P. *Chem. Rev.* **1990**, *90*, 1027.
(18) Bradley, D. C. *Phil. Trans., R. Soc. London A* **1990**, *330*, 167.
(19) Livage, J.; Henry, M.; Jolivet, J. P.; Sanchez, C. *Mater. Res. Soc. Bull.* **1990**, *15*, 18.

(20) Hubert-Pfalzgraf, L. G. *New J. Chem.* **1987**, *11*, 663.
(21) Livage, J.; Henry, M.; Sanchez, C. *Prog. Solid State Chem.* **1988**, *18*, 259.
(22) Bradley, D. C.; Mehrotra, R. C.; Gaur, D. P. *Metal Alkoxides*; Academic Press: London, 1978.
(23) West, A. R. *Solid State Chemistry and Its Applications*; Wiley: New York, 1989.
(24) Roy, R. *Science* **1987**, *238*, 1664.
(25) Caulton, K. G.; Hubert-Pfalzgraf, L. G. *Chem. Rev.* **1990**, *90*, 969.
(26) Thomas, N. W. *Acta Crystallogr.* **1989**, *B45*, 337.
(27) Sheppard, L. M. *Am. Ceram. Soc. Bull.* **1992**, *71*, 85.
(28) Hirano, S.; Yogo, T.; Kikuta, K.; Kato, K.; Sakamoto, W.; Ogasahara, S. *Ceram. Trans.* **1992**, *25*, 19.
(29) Galasso, F. S. *Structure, Properties and Preparation of Perovskite-type Compounds*; Pergamon Press: London, 1969.
(30) Goldschmidt, V. M. *Skrifter Norske Videnskaps Akad. Oslo, I. Mater.-Naturv.* **1926**, *8*, 7.
(31) Wells, A. F. In *Structural Inorganic Chemistry*, 5th ed.; Oxford Science Publications, Clarendon Press: Oxford, 1986.
(32) Schwatrz, R. W.; Payne, D. A. *Mater. Res. Soc. Symp. Proc.* **1988**, *121*, 199.
(33) *IEEE Standard Definitions of Primary Ferroelectric Terms*, Std. 180–1986, 1986, New York.
(34) Nye, J. F. In *Physical Properties of Crystals: Their Representation by Tensors and Matrices*; Oxford Science Publications: Oxford, 1985.
(35) Newnham, R. E. In *Structure-Property Relations*; Springer-Verlag, New York, 1975.
(36) Jona, F.; Shirane, G. *Ferroelectric Crystals*; Macmillan, New York, 1962.
(37) Azaroff, L. V. *Introduction to Solids*; McGraw-Hill: New York, 1960.
(38) Brooke, R. J.; Cahn, R. W.; Bever, M. B. *Concise Encyclopedia of Advanced Ceramic Materials*; Pergamon Press: Cambridge, 1991.
(39) Morell, A.; Niepce, J.-C. *J. Mater. Educ.* **1991**, *13*, 173.
(40) Jaffe, B.; Cooke, W. R.; Jaffe, H. L. C. *Piezoelectric Ceramics*; Academic Press: New York, 1971.
(41) Tejuca, L. G.; Fierro, J. L. G.; Tascon, J. M. D. *Advances in Catalysis*; Eley, D. D.; Pines, H.; Weisz, P. B., Eds.; Academic Press: New York, 1989; Vol. 36.
(42) Teraoka, Y.; Zhang, H.-M.; Furukawa, S.; Yamazoe, N. *Chem. Lett.* **1985**, 1743.
(43) LeBlanc, O. H.; Ward, W. J., III; Matson, S. L.; Kimura, S. G. *J. Membr. Sci.* **1980**, *6*, 339.
(44) Hennings, D.; Klee, M.; Waser, R. *Adv. Mater.* **1991**, *3*, 334.
(45) Dimos, D.; Schwartz, R. W. *Mater. Res. Symp. Proc.* **1992**, *243*, 73.
(46) Dimos, D.; Land, C. E.; Schwartz, R. W. *Ceram. Trans.* **1992**, *25*, 323.
(47) Land, C. E. *Ceram. Trans.* **1990**, *11*, 343.
(48) Newnham, R. E.; Ruschau, G. R. *J. Am. Ceram. Soc.* **1991**, *74*, 463.
(49) Känzig, W. *Phys. Rev.* **1955**, *98*, 549.
(50) Arlt, G.; Hennings, D.; deWith, G. *J. Appl. Phys.* **1985**, *58*, 1619.
(51) Livage, J. In *Transformation of Organometallics into Common and Exotic Materials: Design and Activation*; NATO ASI Series E, No. 141; Laine, R. M. Ed; Martinus, Nijhoff: Dordrecht, 1988.
(52) Kodas, T. T. *Adv. Mater.* **1989**, *6*, 180.
(53) Hansen, B. N.; Hybertson, B. M.; Barkley, R. M.; Sievers, R. E. *Chem. Mater.* **1992**, *4*, 749.
(54) Beauger, A.; Mutin, J. C.; Niepce, J. C. *J. Mater. Sci.* **1983**, *18*, 3041.
(55) Enomoto, Y.; Yamaji, A. *Am. Ceram. Soc. Bull.* **1981**, *60*, 566.
(56) Bind, J. M.; Dupin, T.; Schafer, J.; Titeux, M. *J. Met.* **1987**, *39*, 60.
(57) Gopalakrishnamurthy, H. S.; Subba Rao, M.; Narayanan Kutty, T. R. *J. Inorg. Nucl. Chem.* **1975**, *37*, 891.
(58) Gopalakrishnamurthy, H. S.; Subba Rao, M.; Narayanan Kutty, T. R. *J. Inorg. Nucl. Chem.* **1975**, *37*, 1875.
(59) Rhine, W. E.; Hallock, R. B.; Davis, W. M.; Wong-Ng, W. *Chem. Mater.* **1992**, *4*, 1208.
(60) Yen, F. S.; Chang, C. T.; Chang, Y. H. *J. Am. Ceram. Soc.* **1990**, *73*, 3422.
(61) Pechard, M. E. *Compt. Rend.* **1893**, *116*, 1513.
(62) Rosenheim, A.; Schütte, O. *Z. Anorg. Chem.* **1901**, *26*, 239.
(63) Clabaugh, W. S.; Swiggard, E. M.; Gilchrist, R. *J. Res. Natl. Bur. Stand.* **1956**, *56*, 289.
(64) Kudaka, K.; Iizumi, K.; Sasaki, K. *Am. Ceram. Soc. Bull.* **1982**, *61*, 1236.
(65) Fang, T. T.; Lin, H. B. *J. Am. Ceram. Soc.* **1989**, *72*, 1899.
(66) Bhattacharjee, S.; Paria, M. K.; Maiti, H. S. *Ceram. Int.* **1990**, *16*, 211.
(67) Pechini, M. P. US patent 3, 330,697, Jul 11, 1967.
(68) Mulder, B. J. *Am. Ceram. Soc. Bull.* **1970**, *49*, 990.
(69) Salze, H.; Odier, P.; Cales, B. *J. Non Cryst. Solids* **1986**, *82*, 314.
(70) Hennings, D.; Mayr, W. *J. Solid State Chem.* **1978**, *26*, 329.
(71) Merker, L. US Patent 2964413, Dec 13, 1960.
(72) Ali, N. J.; Milne, S. J. *Br. Ceram. Trans. J.* **1987**, *86*, 113.
(73) Davis, J. A.; Dutremez, S. *J. Am. Ceram. Soc.* **1990**, *73*, 1429.
(74) Campion, J.-F.; Payne, D. A.; Chae, H. K.; Maurin, J. K.; Wilson, S. R. *Inorg. Chem.* **1991**, *30*, 3244.
(75) Xu, Z.; Chae, H. K.; Frey, M. H.; Payne, D. A. *Mater. Res. Soc. Symp. Proc.* **1992**, *271*, 339.

(76) Mazdiyasni, K. S.; Dolloff, R. T.; Smith II, J. S. *J. Am. Ceram. Soc.* **1969**, *52*, 523.
(77) Klee, M. *J. Mat. Sci. Lett.* **1989**, *8*, 985.
(78) Klee, M.; Eusemann, R.; Waser, R.; Brand, W.; van Hal, H. *J. Appl. Phys.* **1992**, *72*, 1566.
(79) Larbot, A.; Garcia, F.; Guizard, C. *Eur. J. Solid State Inorg. Chem.* **1989**, *26*, 327.
(80) Weis, R. S.; Gaylord, T. K. *Appl. Phys. A* **1985**, *37*, 191.
(81) Eichorst, D. J.; Payne, D. A. *Mater. Res. Soc. Symp. Proc.* **1988**, *121*, 773.
(82) Hirano, S.-I.; Yogo, T.; Kikuta, K.; Urahata, H.; Isobe, Y.; Morishita, T.; Ogiso, K.; Ito, Y. *Mater. Res. Soc. Symp. Proc.* **1992**, *271*, 331.
(83) Okuwada, K.; Imai, M.; Kakuno, K. *Jpn. J. Appl. Phys.* **1989**, *28*, 1271.
(84) Okuwada, K.; Nakamura, S.-I.; Imai, M.; Kakuno, K. *Jpn. J. Appl. Phys.* **1990**, *29*, 1153.
(85) Goel, S. C.; Chiang, M. Y.; Buhro, W. E. *Inorg. Chem.* **1990**, *29*, 4646.
(86) Papiernik, R.; Hubert-Pfalzgraf, L. G.; Massiani, M.-C. *Inorg. Chim. Acta* **1989**, *165*, 1.
(87) Hubert-Pfalzgraf, L. G.; Papiernik, R.; Massiani, M.-C.; Septe, B. *Mater. Res. Soc. Symp. Proc.* **1990**, *180*, 393.
(88) Govil, S.; Kapoor, P. N.; Mehrotra, R. C. *J. Inorg. Nucl. Chem.* **1976**, *38*, 172.
(89) Hubert-Pfalzgraf, L. G. *Mater. Res. Soc. Symp. Proc.* **1992**, *271*, 15.
(90) Chaput, F.; Boilot, J.-P.; Lejeune, M.; Papiernik, R.; Hubert-Pfalzgraf, L. G. *J. Am. Ceram. Soc.* **1989**, *72*, 1335.
(91) Kistler, S. S. *J. Phys. Chem.* **1932**, *36*, 52.
(92) Hallock, R. B.; Rexer, P. O.; Jolly, M. S.; Rhine, W. E.; Cima, M. J. *Mater. Res. Soc. Symp. Proc.* **1990**, *180*, 877.
(93) Laine, R. M.; Youngdahl, K. A.; Kennish, R. A.; Hoppe, M. L.; Zhang, Z.-F.; Ray, D. J. *Mater. Res. Soc. Symp. Proc.* **1990**, *180*, 865.
(94) Kemmler-Sack, S.; Kiemel, R.; Schäfer, W.; Wischert, W.; Radak, A.; Elschner, B. *J. Less-Common Met.* **1988**, *138*, L21.
(95) Zheng, H.; Mackenzie, J. D. *Mater. Lett.* **1988**, *7*, 182.
(96) Gonzalez-O, C.; Schachner, H.; Tippmann, H.; Trojer, F. *J. Physica C* **1988**, *153*, 1042.
(97) Barboux, P.; Tarascon, J. M.; Greene, L. H.; Hull Jr., G. W.; Bagley, B. G. *J. Appl. Phys.* **1988**, *63*, 2725.
(98) Zhuang, H. R.; Kozuka, H.; Sakka, S. *J. Mater. Sci.* **1990**, *25*, 4762.
(99) Katayama, S.; Sekine, M. *J. Mater. Res.* **1990**, *5*, 683.
(100) Katayama, S.; Sekine, M. *J. Mater. Chem.* **1991**, *1*, 1031.
(101) For example, see e.g. Yi, G.; Wu, Z.; Sayer, M. *J. Appl. Phys.* **1988**, *64*, 2717.
(102) Yi, G.; Sayer, M. *Am. Ceram. Soc. Bull.* **1991**, *70*, 1173.
(103) Schwartz, R. W.; Assink, R. A.; Headley, T. J. *Mater. Res. Soc. Symp. Proc.* **1992**, *243*, 245.
(104) Schwartz, R. W.; Bunker, B. C.; Dimos, D. B.; Assink, R. A.; Tuttle, B. A.; Tallant, D. R.; Weinstock, I. A. *Ferroelectrics* **1992**, *2*, 243.
(105) Yoko, T.; Kamiya, K.; Tanaka, K. *J. Mater. Sci.* **1990**, *25*, 3922.
(106) Ramamurthi, S. D.; Payne, D. A. *Mater. Res. Soc. Symp. Proc.* **1990**, *180*, 79.
(107) Ramamurthi, S. D.; Payne, D. A. *J. Am. Cer. Soc.* **1990**, *73*, 2547.
(108) Hampden-Smith, M. J.; Williams, D. S.; Rheingold, A. L. *Inorg. Chem.* **1990**, *29*, 4076.
(109) Swartz, S. L.; Ramamurthi, S. D.; Busch, J. R.; Wood, V. E. *Mater. Res. Soc. Symp. Proc.* **1992**, *243*, 533.
(110) Lakeman, C. D. E.; Campion, J.-F.; Payne, D. A. *Ceram. Trans.* **1992**, *5*, 413.
(111) Deacon, G. B.; Phillips, R. J. *Coord. Chem. Rev.* **1980**, *33*, 227.
(112) Li, S.; Condrate, R. A., Sr.; Jang, S. D.; Spriggs, R. M. *J. Mater. Sci.* **1989**, *24*, 3873.
(113) Li, S.; Condrate, R. A., Sr.; Spriggs, R. M. *Spectrosc. Lett.* **1988**, *21*, 969.
(114) Chandler, C. D.; Hampden-Smith, M. J. *Chem. Mater.* **1992**, *4*, 1137.
(115) Chandler, C. D.; Hampden-Smith, M. J.; Brinker, C. J. *Mater. Res. Soc. Symp. Proc.* **1992**, *271*, 89.
(116) Chandler, C. D.; Hampden-Smith, M. J.; Duesler, E. N. *Inorg. Chem.* **1992**, *31*, 4891.
(117) Archer, L.; Chandler, C. D.; Hampden-Smith, M. J. To be submitted for publication.
(118) Vivekanadan, R.; Philip, S.; Narayanan Kutty, T. R. *Mater. Res. Bull.* **1987**, *22*, 99.
(119) Hennings, D.; Rosenstien, G.; Schreinemacher, H. *J. Eur. Ceram. Soc.* **1991**, *8*, 107.
(120) Hennings, D.; Schreinemacher, H. *J. Eur. Ceram. Soc.* **1992**, *9*, 41.
(121) Venigella, S.; Bendale, P.; Ambrose, J. R.; Verink, E. D., Jr.; Adair, J. H. *Mater. Res. Soc. Symp. Proc.* **1992**, *243*, 309.
(122) Wang, H.-W.; Hall, D. A.; Sale, F. R. *J. Am. Ceram. Soc.* **1992**, *75*, 124.
(123) Sekar, M. M. A.; Patil, K. C. *J. Mater. Chem.* **1992**, *2*, 739.
(124) Mashina, M. *Bull. Chem. Soc. Jpn.* **1966**, *39*, 504.
(125) Livage, J.; Henry, M.; Jolivet, J. P.; Sanchez, C. *J. Mater. Educ.* **1991**, *13*, 233.
(126) Babonneau, F.; Doeuff, S.; Leaustic, A.; Sanchez, C.; Cartier, C.; Verdaguer, M. *Inorg. Chem.* **1988**, *27*, 3166.

(127) Livage, J.; Henry, M. In *Ultrastructure Processing of Advanced Ceramics*; Mackenzie, J. D., Ulrich, D. R., Eds.; Wiley: New York, 1988; p 183.

(128) Barringer, E. A.; Bowen, H. K. *J. Am. Ceram. Soc.* **1982**, 65, C199.

(129) Hartel, R. W.; Berglund, K. A. *Mater. Res. Soc. Symp. Proc.* **1986**, 73, 633.

(130) Jean, J. H.; Ring, T. A. *Langmuir* **1986**, 2, 251.

(131) Barringer, E. A.; Bowen, H. K. *Langmuir* **1985**, 1, 414.

(132) Barringer, E. A.; Bowen, H. K. *Langmuir* **1985**, 1, 420.

(133) Barringer, E. A.; Bowen, H. K. *J. Am. Ceram. Soc.* **1982**, 65, C199 and references cited therein.

(134) Fegley, B.; Barringer, E. A. *Mater. Res. Soc. Symp. Proc.* **1984**, 32, 187.

(135) Dick, S.; Suhr, C.; Rehspringer, J. L.; Daire, M. *Mater. Sci. Eng.* **1989**, A109, 227.

(136) Heisland, R. H., II; Oguri, Y.; Okamura, H.; Moffatt, W. C.; Novich, B.; Barringer, E. A.; Bowen, H. K. *Science of Ceramic Chemical Processing*; Hench, L. L., Ulrich, D. R., Eds.; Wiley: New York, 1986; p 482.

(137) Gulliver, E. A.; Wark, T. A.; Garvey, J. G.; Hampden-Smith, M. J.; Datye, A. *J. Am. Ceram. Soc.* **1991**, 74, 1091.

(138) Ogihara, T.; Ikenoto, T.; Mizutami, N.; Kato, M.; Mitarai, Y. *J. Mater. Sci.* **1986**, 21, 2771.

(139) Ogihara, T.; Mizutami, N.; Kato, N. *J. Am. Ceram. Soc.* **1989**, 72, 421.

(140) Day, V. W.; Eberspacher, T. A.; Klemperer, W. G.; Park, C. W.; Rosenberg, F. S. *J. Am. Chem. Soc.* **1991**, 113, 8190.

(141) Chen, Y. W.; Klemperer, W. G.; Park, C. W. *Mater. Res. Soc. Symp. Proc.* **1992**, 271, 57.

(142) Sinclair, R. A.; Brostrom, M. L.; Gleason, W. B.; Newmark, R. A. *Mater. Res. Soc. Symp. Proc.* **1992**, 271, 27.

(143) Yanovskii, A. I.; Turova, N. Ya.; Kozlova, N. I.; Struchkov, Yu. T. *Koord. Khim.* **1987**, 13, 242.

(144) Veith, M. *Chem. Rev.* **1990**, 90, 3.

(145) Yanovskii, A. I.; Turova, N. Ya.; Turevskaya, E. P.; Struchkov, Yu. T. *Koord. Khim.* **1982**, 8, 153; Engl. Transl. **1982**, 8, 76.

(146) Gaffney, C.; Harrison, P. G.; King, T. J. *J. Chem. Soc., Chem. Commun.* **1980**, 1251.

(147) Tulinsky, A.; Worthington, C. R.; Pignataro, E. *Acta Crystallogr.* **1959**, 12, 623.

(148) Gyani, A. K.; Khan, O. F. Z.; O'Brien, P.; Urch, D. S. *Thin Solid Films* **1989**, 182, L1.

(149) Kayama, H.; Sacto, Y. *Bull. Chem. Soc. Jpn.* **1954**, 27, 112.

(150) Harrison, P. G.; Haylett, B. J.; King, T. J. *J. Chem. Soc., Chem. Commun.* **1978**, 112.

(151) Howie, R. A.; Moser, W. *Nature* **1968**, 219, 372.

(152) Poncelet, O.; Sartain, W. J.; Hubert-Pfalzgraf, L. G.; Folting, K.; Caulton, K. G. *Inorg. Chem.* **1989**, 28, 263.

(153) Helgesson, G.; Jagner, S.; Poncelet, O.; Hubert-Pfalzgraf, L. G. *Polyhedron* **1991**, 10, 1559.

(154) Bradley, D. C.; Chudzynska, H.; Frigo, D. M.; Hursthouse, M. B.; Mazid, M. A. *J. Chem. Soc., Chem. Commun.* **1988**, 1258.

(155) Sanchez, C.; Livage, J.; Henry, M.; Babonneau, F. *J. Non-Cryst. Solids* **1988**, 100, 65.

(156) Kawaguchi, S. In *Variety in Coordination Modes of Ligands in Metal Complexes*; Springer-Verlag: Berlin, 1988.

(157) Nakamoto, K. *Infrared and Raman Spectra of Inorganic and Coordination Compounds*, 4th ed.; Wiley: New York, 1986.

(158) Sanchez, C.; Babonneau, F.; Doeuff, S.; Leaustic, A. In *Ultrastructure Processing of Advanced Ceramics*; Mackenzie, J. D., Ulrich, D. R., Eds.; Wiley: New York, 1988; p 77.

(159) Leaustic, A.; Babonneau, F.; Livage, J. *Chem. Mater.* **1989**, 1, 240.

(160) Toledano, P.; Ribot, F.; Sanchez, C. *C. R. Acad. Sci. Ser. 2* **1990**, 311, 1315.

(161) Sanchez, C.; Toledano, P.; Ribot, F. *Mater. Res. Soc. Symp. Proc.* **1990**, 180, 47.

(162) Sanchez, C.; Ribot, F.; Doeuff, S. In *Organometallic Polymers with Special Properties*; Laine, R. M., Ed.; Kluwer: Boston. In press.

(163) Toledano, P.; In, M.; Sanchez, C. *C. R. Acad. Sci. Ser. 2* **1990**, 311, 1161.

(164) Doeuff, S.; Dromzee, Y.; Sanchez, C. *C. R. Acad. Sci. Ser. 2* **1989**, 308, 1409.

(165) For a recent review, see: Mehrotra, R. C. *Mater. Res. Soc. Symp. Proc.* **1988**, 121, 81.

(166) Mehrotra, R. C.; Agarwal, M. M.; Kapoor, P. N. *J. Chem. Soc. A* **1968**, 2673.

(167) Eichorst, D. J.; Howard, K. E.; Payne, D. A. *Proceedings of the Fourth International Conference on Ultrastructure Processing of Ceramics, Glasses and Composites*; Uhlmann, D. R.; Weinberg, M. C.; Risbud, S. H.; Ulrich, D. R., Eds.; Wiley: New York. In press.

(168) Eichorst, D. J.; Payne, D. A.; Wilson, S. R.; Howard, K. E. *Inorg. Chem.* **1990**, 29, 1458.

(169) Vaarstra, B. A.; Huffman, J. C.; Streib, W. E.; Caulton, K. G. *Inorg. Chem.* **1991**, 30, 3068.

(170) Amini, M. M.; Sacks, M. D. *Mater. Res. Soc. Symp. Proc.* **1990**, 180, 675.

(171) Reference to BaTi(O-*i*-Pr)₅ was made in ref 5.

(172) Jones, K.; Davies, T. J.; Emblem, H. G.; Parkes, P. *Mater. Res. Soc. Symp. Proc.* **1986**, 73, 111.

(173) Hampden-Smith, M. J.; Wark, T. A.; Jones, L. C.; Brinker, C. J. *Ceram. Trans.* **1992**, 25, 187.

(174) Kirby, K. W. *Mater. Res. Bull.* **1988**, 23, 881.

(175) Purdy, A. P.; George, C. F.; Callahan, J. H. *Inorg. Chem.* **1991**, 30, 2812.

(176) Wark, T. A.; Gulliver, E. A.; Hampden-Smith, M. J.; Rheingold, A. L. *Inorg. Chem.* **1990**, 29, 4360.

(177) McGeary, M. J.; Coan, P. S.; Folting, K.; Streib, W. E.; Caulton, K. G. *Inorg. Chem.* **1991**, 30, 1723.

(178) Shriver, D. F.; Atkins, P. W.; Langford, C. H. *Inorganic Chemistry*; W.H. Freeman and Company: San Francisco, 1990; p 173.

(179) Veith, M.; Roesler, R. *Z. Naturforsch. B* **1986**, 41B, 1071.

(180) Vaarstra, B. A.; Streib, W. E.; Caulton, K. G. *J. Am. Chem. Soc.* **1990**, 112, 8593.

(181) Samuels, J. A.; Vaarstra, B. A.; Huffman, J. C.; Trojan, K. L.; Hatfield, W. E.; Caulton, K. G. *J. Am. Chem. Soc.* **1990**, 112, 9623.

(182) Whitmire, K. H.; Jones, C. M.; Burkart, M. D.; Hutchinson, J. C.; McKnight, A. L. *Mater. Res. Soc. Symp. Proc.* **1992**, 271, 149.

(183) Papiernik, R.; Hubert-Pfalzgraf, L. G.; Daran, J.-C.; Jeannin, Y. *J. Chem. Soc., Chem. Commun.* **1990**, 695.

(184) Bates, J.; West, B. O.; Fallon, G. D. Private communication, 1992.

(185) Francis, L. F.; Payne, D. A.; Wilson, S. R. *Chem. Mater.* **1990**, 2, 645.

(186) Francis, L. F.; Payne, D. A. *Proceedings of the 7th IEEE International Symposium on Applications of Ferroelectrics, ISAF '90*, 1990; p 263.

(187) Goel, S. C.; Kramer, K. S.; Gibbons, P. C.; Buhro, W. E. *Inorg. Chem.* **1989**, 28, 3620.

(188) Goel, S. C.; Kramer, K. S.; Chiang, M. Y.; Buhro, W. E. *Polyhedron* **1990**, 9, 611.

(189) Matchett, M. A.; Chiang, M. Y.; Buhro, W. E. *Inorg. Chem.* **1990**, 29, 358.

(190) Rees, W. S.; Moreno, D. A. *J. Chem. Soc., Chem. Commun.* **1991**, 1759.

(191) Goel, S. C.; Matchett, M. A.; Chiang, M. Y.; Buhro, W. E. *J. Am. Chem. Soc.* **1991**, 113, 1845.

(192) Poncelet, O.; Hubert-Pfalzgraf, L. G.; Daran, J.-C.; Astier, R. *J. Chem. Soc., Chem. Commun.* **1989**, 1846.

(193) Hursthouse, M. B.; Izod, K. J.; Mazid, M. A.; Thornton, P. *Polyhedron* **1990**, 9, 535.

(194) Fiedler, R.; Follner, H. *Monatsh. Chem.* **1977**, 108, 319.

(195) Follner, H. *Monatsh. Chem.* **1972**, 103, 1438.

(196) Poncelet, O.; Hubert-Pfalzgraf, L. G.; Toupet, L.; Daran, J.-C. *Polyhedron* **1991**, 10, 2045.

(197) Caulton, K. G.; Chisholm, M. H.; Drake, S. R.; Folting, K. *Inorg. Chem.* **1991**, 30, 1500.

(198) Caulton, K. G.; Chisholm, M. H.; Drake, S. R.; Folting, K. *J. Chem. Soc., Chem. Commun.* **1990**, 1349.

(199) Irwin, A.; Assink, R.; Chandler, C. D.; Hampden-Smith, M. J. To be submitted.

(200) Van der Sluis, P.; Spek, A. L.; Timmer, K.; Meinema, H. A. *Acta Crystallogr. Sect. C* **1990**, 46, 1741.

(201) Norman, J. A. T.; Pez, G. P. *J. Chem. Soc., Chem. Commun.* **1991**, 971.

(202) Shin, Y.-G.; Hampden-Smith, M. J.; Kodas, T. T.; Duesler, E. N. *Polyhedron*, in press.

(203) Bradley, D. C.; Hursthouse, M. B.; Ibrahim, A. A.; Abdul Malik, K. M.; Motevalli, M.; Möseler, R.; Powell, H.; Runnacles, J. D.; Sullivan, A. C. *Polyhedron* **1990**, 9, 2959.

(204) Rogers, R. D.; Bond, A. H.; Aguinaga, S.; Reyes, A. *J. Am. Chem. Soc.* **1992**, 114, 2967.

(205) Rogers, R. D.; Bond, A. H.; Aguinaga, S. *J. Am. Chem. Soc.* **1992**, 114, 2960.

(206) Evans, W. J.; Hain, J. H., Jr. *Mater. Res. Soc. Symp. Proc.* **1990**, 180, 39.

(207) Hubert-Pfalzgraf, L. G.; Poncelet, O.; Daran, J.-C. *Mater. Res. Soc. Symp. Proc.* **1990**, 180, 73.

(208) Sauer, N. N.; Garcia, E.; Salazar, K. V.; Ryan, R. R.; Martin, J. A. *J. Am. Chem. Soc.* **1990**, 112, 1524.

(209) Schindler, F.; Schmidbaur, H. *Angew. Chem., Int. Ed. Engl.* **1967**, 6, 683.

(210) Shiihara, I.; Schwartz, W. T., Jr.; Post, H. W. *Chem. Rev.* **1961**, 61, 1.

(211) Bradley, D. C.; Thomas, I. M. *J. Chem. Soc.* **1959**, 3404.

(212) Roger, C.; Hampden-Smith, M. J. To be published.

(213) Ouhadi, T.; Bioul, J. P.; Stevens, C.; Warin, R.; Hocks, L.; Teyssie, P. *Inorg. Chim. Acta* **1976**, 19, 203.

(214) Oudahi, T.; Hamitou, A.; Jerome, R.; Teyssie, P. *Macromolecules* **1976**, 9, 927.

(215) Ouhadi, T.; Hubert, A. J.; Teyssie, P.; Derouane, E. G. *J. Am. Chem. Soc.* **1973**, 95, 6481.

(216) Gurkovich, S. R.; Blum, J. B. *Ferroelectrics* **1985**, 62, 189.

(217) Blum, J. B.; Gurkovich, S. R. *J. Mater. Sci.* **1985**, 20, 4479.

(218) Dekleva, T. W.; Hayes, J. M.; Cross, L. E.; Geoffroy, G. L. *J. Am. Ceram. Soc.* **1988**, 71, C280.

(219) Hayashi, Y.; Blum, J. B. *J. Mater. Sci.* **1987**, 22, 2655.

(220) Ayral, A.; Phalippou, J.; Droguet, J. C. *Mater. Res. Soc. Symp. Proc.* **1988**, 121, 239.

(221) Sherif, F. G.; Herman, H. *Mater. Res. Soc. Symp. Proc.* **1990**, 180, 831.

(222) Takahashi, Y.; Wada, Y. *J. Electrochem. Soc.* **1990**, *137*, 267.
(223) Takahashi, Y.; Hayashi, H.; Ohya, Y. *Mater. Res. Soc. Symp. Proc.* **1992**, *271*, 401.
(224) Suzuki, T.; Matsuki, M.; Kobayashi, J. Jpn Kokai Tokkyo Koho JP 01,287,278, Nov 17, 1989.
(225) Makita, K.; Hattori, A.; Tanaka, K. Ger. Offen. DE 3,841,255, Jun. 22, 1989.
(226) Hills, M. M.; Parmeter, J. E.; Weinberg, W. H. *J. Am. Chem. Soc.* **1987**, *109*, 4224. This paper describes the first unambiguous characterization of surface vinylidene species on Ru(100) surfaces. Vinylidenes ligands had been previously observed in molecular chemistry 10 years earlier; see ref 210.
(227) Deeming, A. J.; Underhill, M. *J. Chem. Soc., Dalton Trans.* **1974**, 1415; Andrews, J. R.; Kettle, S. F. A.; Powell, D. B.; Sheppard, N. *Inorg. Chem.* **1982**, *21*, 2874.
(228) Hardcastle, F. D.; Wachs, I. E. *J. Raman Spectrosc.* **1990**, *21*, 683.
(229) Sanchez, C.; In, M.; Toledano, P.; Greismar, P. *Mater. Res. Soc. Symp. Proc.* **1992**, *271*, 669.
(230) Nazar, L. F.; Klein, L. C. *J. Am. Ceram. Soc.* **1988**, *71*, C85.
(231) Harris, R. K. *Nuclear Magnetic Resonance Spectroscopy*; Pitman: Boston, 1983.
(232) Harris, R. K.; Mann, B. E. *NMR and the Periodic Table*; Academic Press: New York, 1978.
(233) Laszlo, P. *NMR of Newly Accessible Nuclei*; Academic Press: New York, 1983.
(234) Wrackmeyer, B.; Horchler, K. *Ann. Rep. on NMR Spectroscopy* **1990**, *22*, 249.
(235) Maciel, G. E.; Dallas, J. L. *J. Am. Chem. Soc.* **1973**, *95*, 3039.

(236) Piette, L. H.; Weaver, H. E. *J. Chem. Phys.* **1958**, *28*, 735.
(237) Rocard, J. M.; Bloom, M.; Robinson, L. B. *Can. J. Phys.* **1959**, *37*, 522.
(238) Kennedy, J. D.; McFarlane, W.; Pyne, G. S. *J. Chem. Soc., Dalton Trans.* **1977**, 2332.
(239) Hani, R.; Geanangel, R. A. *Coord. Chem. Rev.* **1982**, *44*, 229.
(240) Hampden-Smith, M. J.; Wark, T. A.; Rheingold, A. L.; Huffman, J. C. *Can. J. Chem.* **1991**, *69*, 121.
(241) Lockhart, T. P. *Inorg. Chem.* **1989**, *28*, 4265.
(242) Lockhart, T. P.; Puff, H.; Schuh, W.; Reuter, H.; Mitchell, T. N. *J. Organomet. Chem.* **1989**, *366*, 61.
(243) Goel, S. C.; Chiang, M. Y.; Gibbons, P. C.; Buhro, W. E. *Mater. Res. Soc. Symp. Proc.* **1992**, *271*, 3.
(244) Nandi, M.; Rhubright, D.; Sen, A. *Inorg. Chem.* **1990**, *29*, 3065.
(245) Poncelet, O.; Hubert-Pfalzgraf, L. G.; Daran, J.-C. *Polyhedron* **1990**, *9*, 1305.
(246) Roger, C.; Hampden-Smith, M. J.; Brinker, C. J. American Chemical Society Meeting, San Francisco, California, Spring 1992.
(247) Yanlu, K.; Gradeff, P. S.; Edelstein, N.; Kot, W.; Shalimoff, G.; Streib, W. E.; Vaarstra, B. A.; Caulton, K. G. *Inorg. Chem.* **1991**, *30*, 2317.
(248) Apblett, A. W.; Lei, J.; Georgeva, G. D. *Mater. Res. Soc. Symp. Proc.* **1992**, *271*, 77.
(249) Corriu, R. J. P.; Leclerq, D.; Lefevre, P.; Mutin, P. H.; Vioux, A. *J. Mater. Chem.* **1992**, *2*, 673.
(250) Guizard, C.; Stitou, M.; Larbot, A.; Cot, L.; Rouviere, J. *Mater. Res. Soc. Symp. Proc.* **1988**, *121*, 115.
(251) Spanhel, L.; Anderson, M. A. *J. Am. Chem. Soc.* **1991**, *113*, 2826.